

Pacific Northwest National Laboratory

Operated by Battelle for the
U.S. Department of Energy

Electrically Switched Cesium Ion Exchange

September 1998

Prepared for
the Office of Science and Technology
U.S. Department of Energy's
Office of Environmental Management
Efficient Separations and Processing
Crosscutting Program
under Contract DE-AC06-76RLO 1830

RECEIVED

NOV 05 1998

OSTI

Pacific Northwest National Laboratory
Operated for the U.S. Department of Energy
by Battelle



DISCLAIMER

This report was prepared as an account of work sponsored by an agency of the United States Government. Neither the United States Government nor any agency thereof, nor Battelle Memorial Institute, nor any of their employees, makes any warranty, express or implied, or assumes any legal liability or responsibility for the accuracy, completeness, or usefulness of any information, apparatus, product, or process disclosed, or represents that its use would not infringe privately owned rights. Reference herein to any specific commercial product, process, or service by trade name, trademark, manufacturer, or otherwise does not necessarily constitute or imply its endorsement, recommendation, or favoring by the United States Government or any agency thereof, or Battelle Memorial Institute. The views and opinions of authors expressed herein do not necessarily state or reflect those of the United States Government or any agency thereof.

PACIFIC NORTHWEST NATIONAL LABORATORY
operated by
BATTELLE MEMORIAL INSTITUTE
for the
UNITED STATES DEPARTMENT OF ENERGY
under Contract DE-AC06-76RLO 1830

Printed in the United States of America

Available to DOE and DOE contractors from the
Office of Scientific and Technical Information, P.O. Box 62, Oak Ridge, TN 37831;
prices available from (615) 576-8401.

Available to the public from the National Technical Information Service,
U.S. Department of Commerce, 5285 Port Royal Rd., Springfield, VA 22161



This document was printed on recycled paper.

DISCLAIMER

Portions of this document may be illegible in electronic image products. Images are produced from the best available original document.

Electrically Switched Cesium Ion Exchange

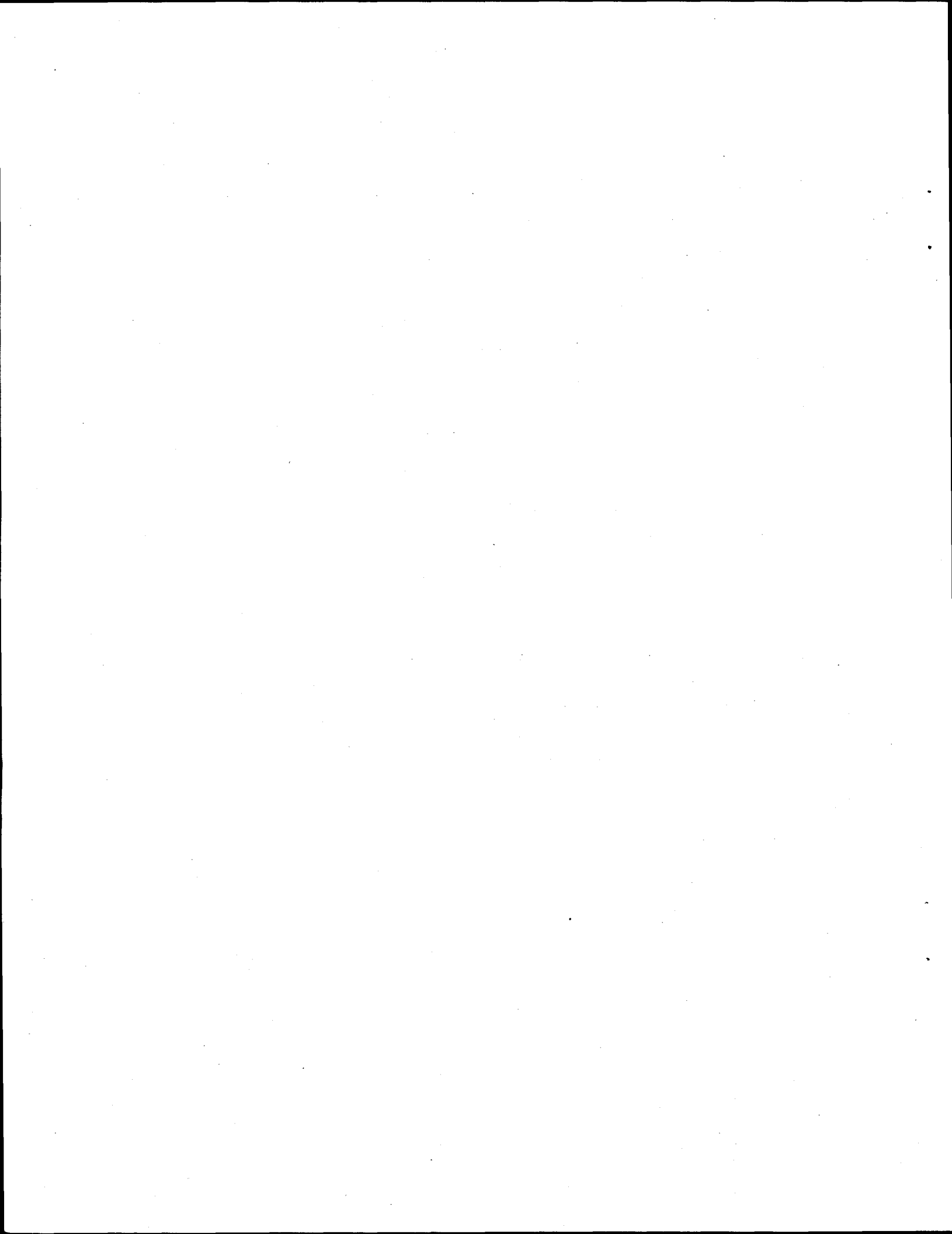
FY 1998 Final Report

Michael A. Lilga
Rick J. Orth
Johanes P. H. Sukamto
Pacific Northwest National Laboratory

September 1998

Prepared for
the Office of Science and Technology
U.S. Department of Energy Office of Environmental Management
Efficient Separations and Processing Crosscutting Program
under Contract DE-AC06-76RLO 1830

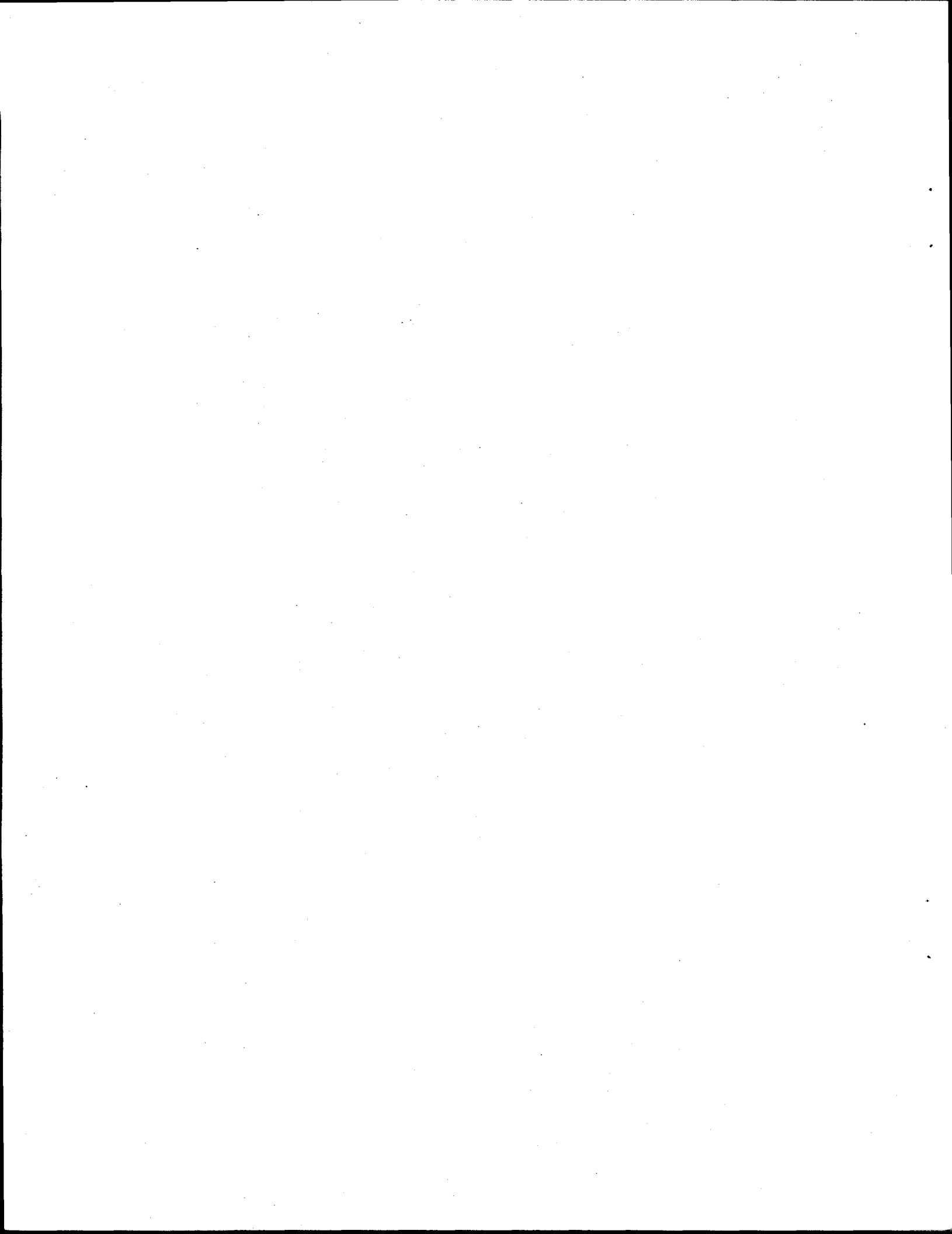
Pacific Northwest National Laboratory
Richland, Washington 99352



Summary

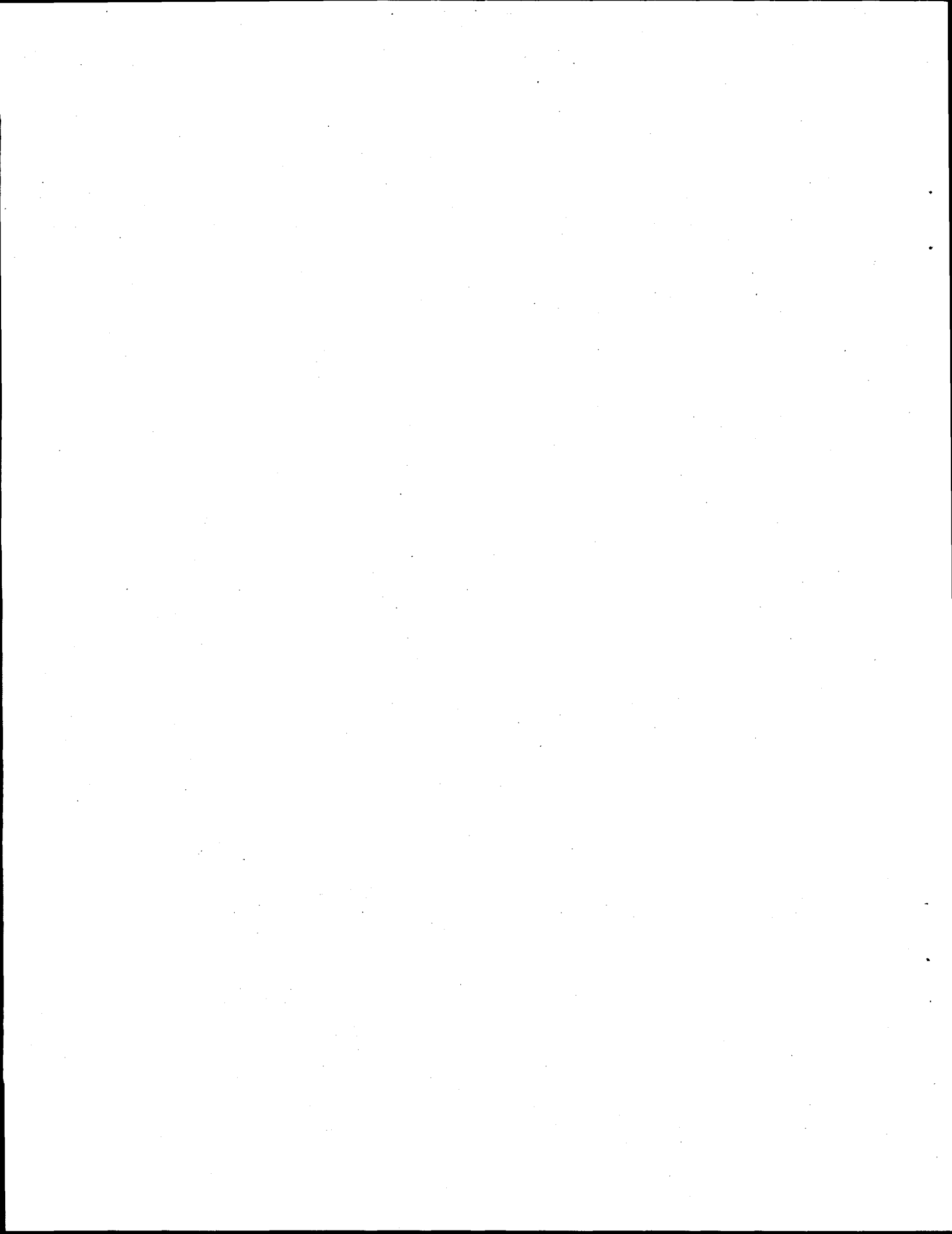
This report discusses the results of work to develop Electrically Switched Ion Exchange (ESIX) for separations of ions from waste streams relevant to DOE site clean-up. ESIX combines ion exchange and electrochemistry to provide a selective, reversible method for radionuclide separation that lowers costs and minimizes secondary waste generation typically associated with conventional ion exchange. In the ESIX process, an electroactive ion exchange film is deposited onto a high surface area electrode, and ion uptake and elution are controlled directly by modulating the potential of the film. As a result, the production of secondary waste is minimized, since the large volumes of solution associated with elution, wash, and regeneration cycles typical of standard ion exchange are not needed for the ESIX process.

The document is presented in two parts: Part I, the Summary Report, discusses the objectives of the project, describes the ESIX concept and the approach taken, and summarizes the major results; Part II, the Technology Description, provides a technical description of the experimental procedures and in-depth discussions on modeling, case studies, and cost comparisons between ESIX and currently used technologies.



Acknowledgments

This work was funded by the Office of Science and Technology within the Department of Energy's Office of Environmental Management and under the Efficient Separations and Processing Crosscutting Program. Part of the work on this project was conducted by The Electrosynthesis Company, the University of Washington, and Parsons Infrastructure and Technology Group, Inc. acting as subcontractors to the Pacific Northwest National Laboratory. Their work is summarized in appendices. Laboratory Directed Research and Development funding was received for developing the ESIX technology for other applications.



Contents

Summary	iii
---------------	-----

Acknowledgments	v
-----------------------	---

Part I. Summary Report

1.0 Objective	I-1
---------------------	-----

2.0 Approach	I-2
--------------------	-----

3.0 Results and Discussion	I-4
----------------------------------	-----

4.0 References	I-6
----------------------	-----

Part II. Technology Description

1.0 Experimental	II-1
------------------------	------

1.1 Development of Improved Films	II-1
---	------

1.2 Flow Cell Testing	II-2
-----------------------------	------

2.0 Film Preparation, Characterization, and Batch Results	II-7
---	------

2.1 Comparison of Film Preparation Methods on Flat Plates	II-7
---	------

2.2 Cesium Uptake/Elution From Flat Plate Electrodes	II-12
--	-------

2.3 Batch Results on High Surface Area Electrodes	II-15
---	-------

3.0 Flow Cell Results	II-18
-----------------------------	-------

3.1 Micro Flow Cell Results Using a Single Electrode	II-18
--	-------

3.1 Micro Flow Cell Results Using Stacked Electrodes	II-20
--	-------

3.1 MP Results Using a Single Electrode	II-26
---	-------

4.0 Modeling of Micro Flow Cell and MP Cell Data	II-29
--	-------

5.0 ESIX Case Studies and Cost Comparison	II-34
5.1 ESIX Case Study for Cesium Removal From KE Basin	II-34
5.1.1 Bases and Assumptions.....	II-34
5.1.2 Process Concept and Estimated Costs.....	II-37
5.1.3 Potential Advantages of ESIX for KE Basin Application	II-38
5.2 ESIX Case Study for Strontium Removal from Groundwater at 100N	II-39
5.2.1 Bases and Assumptions.....	II-39
5.2.2 Process Concept and Estimated Costs.....	II-39
5.2.3 Potential Advantages of ESIX for 100N Application.....	II-40
5.3 Cost Comparison With Empore™	II-41
5.3.1 ESIX System Design.....	II-42
5.3.2 Cost Comparison.....	II-43
6.0 Conclusions.....	II-45
7.0 Publications, Reports, and Patent Applications.....	II-46
8.0 References.....	II-47
Appendix A: Development of ESIX Films Selective for Peracthnetate	A-1
Appendix B: ESIX – The Electrosynthesis Co., Inc.....	B-1
Appendix C: ESIX – University of Washington	C-1
Appendix D: Column Cost Benefit Analysis – Parsons.....	D-1

Figures

Part I

1. Cation Uptake and Elution in the ESIX Process..... 2

Part II

1. Solution and Current Flow Patterns in Electrochemical Cells Used for Flow Tests..... 3
2. Micro Flow Cell Apparatus with a Single Electrode 4
3. Close-up of the Micro Flow Cell with a Single Electrode..... 4
4. Micro Flow Cell Apparatus with 5-Electrode Stack..... 5
5. Close-up of the Micro Flow Cell with 5-Electrode Stack 5
6. MP Cell Experimental Setup 6
7. Cyclic Voltammetry of a Bare Nickel Electrode in 1 M NaNO₃..... 8
8. Cyclic Voltammetry in 1 M NaNO₃ of Hexacyanoferrate Films Prepared by Three Different Methods (Cycle #2) 8
9. Charge Passed as Determined by Integration of a Single Potential Cycle (Cycle #2) for Three Film Preparations 9
10. Repeated Potential Cycling of PNNL-1 in 1 M NaNO₃ 10
11. Maximum Charge Passed as a Function of Cycle Number for Three Different Film Preparations (Cyclic Voltammetry in 1 M NaNO₃)..... 11
12. Normalized Maximum Charge as a Function of Cycle Number for Three Different Film Preparations (Cyclic Voltammetry in 1 M NaNO₃)..... 11
13. Normalized Charge as a Function of Time for Three Different Film Preparations (from Cyclic Voltammetry in 1 M NaNO₃) 12
14. Cyclic Voltammetry for a Film in the Cesium Form and After Two and 25 Potential Cycles in 1 M NaNO₃ 13
15. Cyclic Voltammetry of a Film in the Sodium Form and After Two Potential Cycles in 1 M CsNO₃..... 13

16. Long-term Cycling of a Hexacyanoferrate Film Deposited on a 20 ppi High Surface Area Nickel Electrode.....	15
17. Effect of Applied Potential on Cesium Uptake in Batch Experiments.....	17
18. Effect of Sodium on Cesium Uptake in Batch Experiments	17
19. Effect of Elution Solution on Cesium Unloading in Batch Experiments (Applied Potential = 0.8 V)	18
20. Effect of Flow Rate on Cesium Breakthrough in Flow-Through Mode ([Cs] ₀ = 0.2 ppm)	19
21. Effect of [Cs] ₀ on Cesium Breakthrough in Flow-Through Mode (Flow Rate = 8 BV/h)	20
22. Consistency of Performance for Two Separate Electrodes in Flow-Through Mode ([Cs] ₀ = 0.2 ppm; Flow Rate = 13 BV/h).....	21
23. Effect of Number of Electrodes Used in Micro-Cell Testing in Flow-Through Mode	22
24. Effect of Flow Rate on Cesium Breakthrough in a Micro Flow Cell Containing Five Stacked Electrodes Operated in Flow-Through Mode ([Cs] ₀ = 0.2 ppm).....	23
25. Effect of Filling Void Space in the 5-Electrode Micro Cell with Glass Beads as Packing	24
26. Consecutive Breakthrough Curves for the 8-Electrode Stack Eluted and Regenerated In-Line	25
27. Effect of Feed Cesium Concentration on Cesium Breakthrough in an MP Cell Containing a Single Electrode Operated in Flow-by Mode	27
28. Model Fit to Breakthrough Data for [Cs] ₀ = 0.2 ppm and Flow Rate = 10, 30, and 90 BV/h in Flow-Through Mode for 5-Electrode Stack. Model Calculated for k_a and q_M Independent of Flow Rate	31
29. Model Fit to Breakthrough Data for [Cs] ₀ = 0.2 ppm and Flow Rate = 10, 30, and 90 BV/h in Flow-Through Mode for 5-Electrode Stack. Model Calculated for $k_a \propto v^{0.39}$	32

30. Model Fit to Breakthrough Data for $[Cs]_0 = 0.2$ ppm and Flow Rate = 10, 30, and 90 BV/h in Flow-Through Mode for 5-Electrode Stack. Model Calculated for $k\alpha \propto v^{0.61}$	32
31. Model Fit to Breakthrough Data for $[Cs]_0 = 0.2$ ppm and Flow Rate = 10, 30, and 90 BV/h in Flow-Through Mode for 5-Electrode Stack. Model Calculated for $k\alpha \propto v^{0.7}$	33
32. Model Fit to Breakthrough Data for Flow Rate = 8.5 BV/h and $[Cs]_0 = 0.18, 1.03,$ and 1.35 ppm in Flow-by Mode for a Single Electrode.....	33
33. Model Fit to Breakthrough Data for $[Cs]_0 = 0.2$ ppm and Flow Rate = 10 BV/h in Flow-Through Mode for Single and Stacked Electrodes.....	35
34. Predicted Breakthrough for ESIX Treatment of KE Basin Water at 10 BV/h for Feeds of 10^{-7} and 10^{-10} M Cs	35
35. Flow Diagram for Waste Decontamination with ESIX.....	36
36. Application of ESIX for Strontium Removal from Groundwater	40
37. ESIX System Flow Schematic.....	43
38. Cost Comparison of Four Treatment Options for Clean-up of Radioactively Contaminated Water at CP-5	44

Tables

Part II

1. Actual and Theoretical Cesium Loading on 60 ppi Nickel Foam Electrodes.....	II-16
2. Summary of Results from Micro Flow Cell Tests	II-21
3. Performance of 60 ppi Nickel Foam Electrodes in Flow-by Mode as a Function of Feed Cesium Concentration	II-27
4. Reproducibility and Flow Rate Dependence of Nickel Foam Electrodes in Flow-by Mode ($[Cs]_0 = 0.2$ ppm)	II-28
5. Cases Compared for Cesium Removal from K-Basin	II-37
6. Cases Compared for Strontium Removal from 100N	II-40

Part I. Summary Report

Part I summarizes the work of developing Electrically Switched Ion Exchange (ESIX) for separation of ions from various waste streams within the U.S. Department of Energy (DOE) complex. The objectives and approach to this work are discussed in Sections 1 and 2, as well as introducing the ESIX concept. Major results are presented in Section 3. Part II of this report contains the technical presentation of the research.

1.0 Objective

Separation technologies play an important role in the clean-up and management of radioactive wastes throughout the various DOE sites. Removal of radioactive components such as cesium or strontium from fuel storage basin water or groundwater helps protect the safety of workers and the public by decreasing exposure and preventing contamination of water supplies. Separation treatment of the radioactive components also allows maintenance and clean-up activities to occur with lower risk to workers. There are economic considerations as well – the high cost of immobilization by vitrification favors the removal of radionuclides before procedures for permanent disposal can be carried out. Separating out and concentrating most of the radionuclides would allow the bulk of the waste to be disposed of less expensively as low-level waste.

Technologies used must be effective, economical, and safe. In addition, it is desirable that these technologies do not increase the volume of waste needing treatment, such as through addition of other chemicals or generation of contaminated equipment.

Currently, the most accepted option for radionuclide separation before final disposal is conventional ion exchange. Both inorganic and organic ion exchangers are under consideration. Unfortunately, for regenerable ion exchange materials, a large amount of secondary waste results from the numerous process steps required (acid elution, exchanger water rinse, and sodium loading of the exchanger). Neutralization of the acidic eluant typically adds sodium to the waste, restricting the choice of final waste form and limiting the amount of waste that can be incorporated. In the use of organic ion exchangers, it has been reported that they lose approximately 3% of their capacity per cycle (Kurath et al. 1994). Therefore, a typical organic exchanger can be used for only 20 to 30 cycles before it must also be disposed of as another form of secondary waste. Most inorganic ion exchange materials are not regenerable, adding substantial costs for ion exchange replacement and secondary waste disposal.

The objective of the work discussed in this report is to develop a separation technology that provides a more economical remediation alternative to conventional ion exchange and one that does not generate significant secondary waste. The technology developed, ESIX, has initially focussed on cesium separation; electroactive substrates for cesium removal have been prepared

and tested, and process development and optimization are well underway. In addition, materials for technetium separation have been prepared.

2.0 Approach

ESIX, developed at Pacific Northwest National Laboratory (PNNL),^(a) combines ion exchange and electrochemistry to provide a selective, reversible method for radionuclide separation that lowers costs and minimizes secondary waste generation typically associated with conventional regenerable ion exchange processes.

In the ESIX process, an electroactive ion exchange film is deposited onto a high surface area electrode, and ion uptake and elution are controlled directly by modulating the potential of the film. Figure 1 shows the concept for cation separations. Electrochemical reduction of the electroactive species X, by application of a cathodic potential to the film, forces a cation from the waste solution into the film to maintain charge neutrality (Figure 1a). Elution occurs when the potential is switched to oxidize X, forcing the cation out of the film and into an elution solution (Figure 1b).

An alternate method of cation uptake may also be used. If X⁻ has a greater selectivity for the cation of interest M₁⁺ than a second cation M₂⁺, the film may first be "activated" by reduction in the presence of a solution of M₂⁺. Introduction of the waste solution results in uptake of M₁⁺ by ion exchange for M₂⁺. M₂⁺ is displaced into the waste solution.

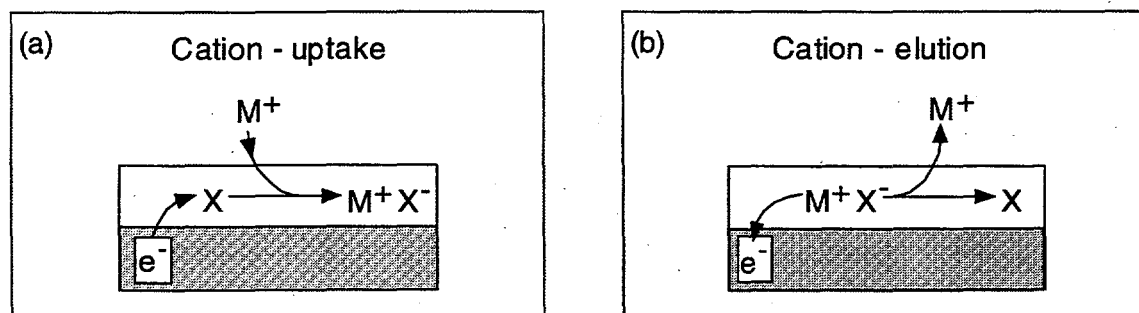


Figure 1. Cation Uptake and Elution in the ESIX Process

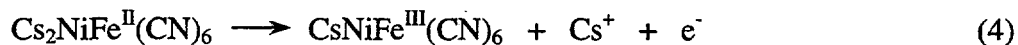
^(a) Operated for the U.S. Department of Energy by Battelle under Contract DE-AC06-76RLO 1830.

Just as in conventional ion exchange, selectivity of X^- for the metal ion of interest is important anytime the waste solution contains more than one cation. Competition for binding sites will occur and loading will be driven by thermodynamics. Therefore, to successfully remove the target cation, films must bind that ion the tightest.

For cesium, the electroactive films being tested are nickel hexacyanoferrates. As a general class, hexacyanoferrates are well-known ion exchangers (Barton et al. 1958; Harjula et al. 1994; Koukím et al. 1964; Lehto and Harjula 1987; Lehto et al. 1987; Loewenschuss 1982; Loos-Neskovic and Fedoroff 1984-1989b; Loos-Neskovic et al. 1976a, 1976b; Prout et al. 1965; Tusa et al. 1994) having high selectivities for cesium in concentrated sodium solutions (Barton et al. 1958; Harjula et al. 1994; Loos-Neskovic et al. 1976a, 1976b; Prout et al. 1965; Tusa et al. 1994). A disadvantage of hexacyanoferrates used in conventional packed column ion exchange is that they are very difficult to elute and columns are normally used once and discarded.

Modification of electrode surfaces with electroactive films has been studied extensively (Andrieux and Saveant 1980; Laviron 1980; Murray 1980, 1984). In particular, the preparation and characteristics of ferrocyanide films have been reported by several groups (Bacsikai et al. 1995; Bocarsly and Sinha 1982a, 1982b; Humphrey et al. 1984, 1987; Itaya et al. 1986; Lasky and Buttry 1988; Schneemeyer et al. 1985; Sinha et al. 1984). Prussian Blue films on a platinum electrode for metal ion separations has been reported (Ikeshoji 1986). Nickel ferrocyanide films, $M_2NiFe(CN)_6$ ($M = Na, K$), have been prepared by immersing a nickel electrode into a $Fe(CN)_6^{-3}$ solution, which oxidizes the metal electrode to precipitate the electroactive film, or more commonly by electrochemically oxidizing the nickel electrode in a $Fe(CN)_6^{-3}$ solution (Bacsikai et al. 1995; Sinha et al. 1984). Electrochemical deposition gave the most reproducible films with highly reversible behavior. Bocarsly and Sinha (1982b) found that the redox potential and electron transfer properties of the films demonstrated a dependence on the alkali metal cation present in the supporting electrolyte, with cesium ion greatly affecting the observed behavior. Films showed selectivity for metal cations in the order cesium > potassium > sodium (Sinha et al. 1984); however, the main purpose of these studies apparently was electrocatalysis (Humphrey et al. 1987), not ion separations. Selectivity is believed to be dependant on metal ion size (Schneemeyer et al. 1985) and cation loading and unloading apparently require solvent transport (Lasky and Buttry 1988).

When a cathodic potential is applied to the nickel hexacyanoferrate film, Fe^{+3} (ferricyanide) is reduced to the Fe^{+2} state (ferrocyanide), and a cation must be intercalated into the film to maintain charge neutrality. In practice, the reduction step is normally conducted in a sodium solution (Eq. 2). The film is then contacted with the waste solution containing cesium, which loads into the film by ion exchange for sodium (Eq 3.). When an anodic potential is applied, a cesium cation must be released from the film (Eq. 4). This method works well because hexacyanoferrates have very high selectivities for cesium over sodium and the electrochemistry is highly reversible.



ESIX is a regenerable ion exchange process that has great potential to minimize secondary waste and produce a low-sodium, cesium-rich waste stream. An important advantage of the ESIX process is that cesium can be eluted into the same elution solution over several load cycles, because the unload step is conducted electrochemically without added chemicals and is independent of the soluble cesium concentration. This improved process would result in the generation of a waste stream with a very low sodium concentration and a cesium concentration that is limited only by solubility, radiation, and/or heat generation. Such a concentrated cesium waste product allows for a broader range of final waste forms, including those that cannot tolerate sodium. The production of secondary waste would be minimized, since the large volumes of solution associated with elution, wash, and regeneration cycles typical of standard ion exchange are not needed for the ESIX process. A small amount of wash solution may be necessary after the unload cycle, but this solution could be used in subsequent cycles for unloading the exchanger. Ratios of the volume of generated secondary waste to the volume of processed waste are estimated to be as low as 0.0006 for the ESIX process, or about two orders of magnitude lower than for a typical regenerable process using commercially available CS-100 ion exchange resin.

The combination of ion exchange and electrochemistry has been attempted previously. The most successful attempt has been the electrochemical ion exchange (EIX) technology developed by AEA Technology, United Kingdom (Bridger et al. 1991; Jones et al. 1992). In EIX, the ion exchange properties of an exchanger/electrode are controlled by generating acid and base locally by water electrolysis. ESIX is significantly different because the uptake and elution of ionic species in a modified electrode or ion exchange film are controlled by modulating the potential of the film directly without changing the local interfacial pH. Furthermore, the potentials used in this method do not result in the electrolysis of water, leading to more efficient use of electrical energy and eliminating the safety issues associated with hydrogen evolution.

3.0 Results and Discussion

Research was conducted to establish the viability of ESIX for cesium separations by increasing the stability and capacity of electroactive nickel hexacyanoferrate films, depositing these films on high surface area supports, and determining uptake and elution parameters of the process under flow conditions. Early work focused on deposition of films with higher capacities and stabilities than for previously reported films (Bocarsly and Sinha 1982). Successful results from this testing led to procedures for deposition on high surface area electrodes and bench-scale flow

studies. A conceptual process was devised for cesium separation based on a case study of the Hanford KE Basin.

Deposition procedures were developed (Lilga et al. 1996) for nickel ferrocyanide films, $M_2NiFe(CN)_6$ ($M = Na, K$), on flat-plate or high surface area nickel foam electrodes. These films are prepared by electrochemically oxidizing the nickel electrode in a $Fe(CN)_6^{3-}$ solution, precipitating the active film on the electrode surface. Electrochemical deposition gives reproducible films with reversible behavior; i.e., metal ions are loaded and unloaded reversibly by switching the electrode potential. Films prepared by modified literature procedures have higher capacity and stability than those previously reported in the literature, and retain the high selectivity for cesium that ferrocyanide materials are known to possess.

Improved capacity and durability are illustrated, for example, by films prepared on flat-plate electrodes, which have almost twice the capacity of previously reported films and lose less than 20% of their capacity after 2000 load/unload cycles. In contrast, a literature film on a flat plate lost 50% of its capacity after the same cycling. Furthermore, films on 20 pores per inch (ppi) ($13 \text{ cm}^2/\text{cm}^3$), high surface area nickel foam electrodes lost only about 20% of their capacity after 1500 load/unload cycles.

The use of metal hexacyanoferrates, which are known cesium ion exchange materials (Lehto and Harjula 1987), gives high selectivity for cesium over sodium as shown by cyclic voltammetry and in batch experiments. In the batch experiments, cesium uptake was unaffected by Na/Cs molar ratios of up to 2×10^4 . Cesium uptake reached equilibrium within 18 h in the batch experiments.

Flow cell testing was conducted with use of high surface area ESIX electrodes. Comparison of results for a stacked 5-electrode cell versus a single electrode cell in the flow cell showed enhanced breakthrough performance. In the stacked configuration, breakthrough began at about 95 bed volumes (BV) for a feed containing 0.2 ppm cesium at a flow rate of 10 BV/h. Breakthrough at 90 BV/h in this cell started at about 40 BV, which is adequate performance on which to base a separation process. Flow cell experiments showed that films on 60 ppi electrodes were stable at least up to 113 BV/h, the maximum flow rate tested in single electrode experiments.

In-line elution of a single electrode in the cell was found to be quick and complete under potential control. Application of 0.8 V with 1 M $NaNO_3$ in batch recycle operation resulted in 88% elution within 2 min and 100% elution after 5 min. Preliminary results with an 8-electrode stack, however, indicated that elution was not complete after 20 min. The in-line elution method will require optimization; but, even with the current system performance, a viable system can be designed for many applications, such as the maintenance of KE Basin water.

A case study for the KE Basin on the Hanford Site was conducted based on the results of the experimental testing and modeling efforts. Engineering design baseline parameters for film deposition, film regeneration, cesium loading, and cesium elution were used to develop a conceptual system. Order of magnitude cost estimates were computed to compare with conventional ion exchange. This case study demonstrated that KE Basin wastewater could be processed continuously at 90 BV/h with minimal secondary waste and reduced associated disposal costs, as well as lower capital and labor expenditures. The ESIX system generated about 100 times less waste than the currently used conventional ion exchange system.

A conceptual case study was also conducted for strontium removal at Hanford's 100 N area. Although ESIX materials have not been prepared for strontium, the case study was conducted to determine the advantages of using ESIX over conventional ion exchange if materials of equal selectivity were used. The results demonstrate that at least an order of magnitude less waste would be generated and higher process flow rates could be used.

A cost comparison conducted by Parsons Infrastructure and Technology Group, Inc. found that ESIX was competitive with an Empore™ system field-tested at Chicago Pile 5 (CP-5). For a 0.5 gpm system treating 24,000 gal of wastewater at CP-5, ESIX was projected to save approximately 40% over the Empore™ system, 43% over a mobile ion exchange system, and 71% over an evaporation system. In the specific application to CP-5, where the volume of waste water to be treated is relatively small, the ESIX System produces slightly more waste than the Empore™ system. However, as concentrations of cesium increase and the volume of liquid processed increases, it is anticipated that the ESIX system would produce less waste because of its ability to reuse the elution solution.

In further work at PNNL, a different proprietary film selective for ReO_4^- (a pertechnetate surrogate) has also been developed (see Part II, Appendix A). In ReO_4^- (i.e., TcO_4^-) separation, loading occurs when the film is oxidized and unloading occurs upon film reduction.

4.0 References

Andrieux, C. P. and J. M. Saveant. 1980. "Electron Transfer Through Redox Polymer Films." *Journal of Electroanalytical Chemistry* 111:377.

Bacsikai, J., K. Martinusz, E. Czirok, G. Inzelt, P. J. Kulesza, and M. A. Malik. 1995. "Polynuclear Nickel Hexacyanoferrates: Monitoring of Film Growth and Hydrated Counter-cation Flux/Storage during Redox Reactions." *Journal of Electroanalytical Chemistry* 385:241.

- Barton, G. B., J. L. Hepworth, J. E. D. McClanahan, R. L. Moore, and H. H. van Tuyl. 1958. "Chemical Processing Wastes - Recovering Fission Products." *Industrial and Engineering Chemistry* 102:212.
- Bocarsly, A. B. and S. Sinha. 1982a. "Chemically Derivatized Nickel Surfaces: Synthesis of a New Class of Stable Electrode Interfaces." *Journal of the Electroanalytical Chemistry and Interfacial Electrochemistry* 137:157.
- Bocarsly, A. B. and S. Sinha. 1982b. "Effects of Surface Structure on Electrode Charge Transfer Properties. Induction of Ion Selectivity at the Chemically Derivatized Interface." *Journal of the Electroanalytical Chemistry and Interfacial Electrochemistry* 140:167.
- Bridger, N. J., C. P. Jones, and M. D. Neville. 1991. "Electrochemical Ion Exchange." *Journal of Chemical Technology and Biotechnology* 50:469.
- Harjula, R., J. Lehto, E. H. Tusa, and A. Paavola. 1994. "Industrial Scale Removal of Cesium with Hexacyanoferrate Exchanger - Process Development." *Nuclear Technology* 107:272.
- Humphrey, B. D., S. Sinha, and A. B. Bocarsly. 1984. "Diffuse Reflectance Spectroelectrochemistry as a Probe of the Chemically Derivatized Electrode Interface. The Derivatized Nickel Electrode." *Journal of Physical Chemistry* 88:736.
- Humphrey, B. D., S. Sinha, and A. B. Bocarsly. 1987. "Mechanisms of Charge Transfer at the Chemically Derivatized Interface: The $\text{Ni}/[\text{Ni}^{\text{II}}(\text{CN})\text{Fe}^{\text{III}}(\text{CN})_5]^{2-/1-}$ System as an Electrocatalyst." *Journal of Physical Chemistry* 91:586.
- Ikeshoji, T. 1986. "Separation of Alkali Metal Ions by Intercalation into a Prussian Blue Electrode." *Journal of the Electrochemical Society* 133:2108.
- Itaya, K, I. Uchida, and V. D. Neff. 1986. "Electrochemistry of Polynuclear Transition Metal Cyanides: Prussian Blue and Its Analogues." *Accounts of Chemical Research* 19:162.
- Jones, C. P., M. D. Neville, and A. D. Turner. 1992. "Electrochemical Ion Exchange" in *Electrochemistry for a Cleaner Environment*, D. Genders and N. Weinberg, Eds., The Electrosynthesis Company Inc., East Amherst, New York, p. 207.
- Koukím, V., J. Rais, and B. Million. 1964. "Exchange Properties of Complex Cyanides - I. Ion Exchange of Caesium on Ferrocyanides." *Journal of Inorganic and Nuclear Chemistry* 26:1111.

Kurath, D. E., L. A. Bray, K. P. Brooks, G. N. Brown, S. A. Bryan, C. D. Carlson, K. J. Carson, J. R. DesChane, R. J. Elovich, and A. Y. Kim. 1994. *Experimental Data and Analysis to Support the Design of an Ion-Exchange Process for the Treatment of Hanford Tank Waste Supernatant Liquids*, PNNL-10187, Pacific Northwest National Laboratory, Richland, Washington.

Lasky, S. J. and D. A. Buttry. 1988. "Mass Measurements Using Isotopically Labeled Solvents Reveal the Extent of Solvent Transport during Redox in Thin Films on Electrodes." *Journal of the American Chemical Society* 110:6258.

Laviron, E. 1980. "A Multilayer Model for the Study of Space Distributed Redox Modified Electrodes." *Journal of Electroanalytical Chemistry* 112:1.

Lehto J. and R. Harjula. 1987. "Separation of Cesium from Nuclear Waste Solutions with Hexacyanoferrate(II)s and Ammonium Phosphomolybdate." *Solvent Extraction and Ion Exchange* 5:343.

Lehto, J., R. Harjula, and J. Wallace. 1987. "Absorption of Cesium on Potassium Cobalt Hexacyanoferrate(II)" *Journal of Radioanalytical and Nuclear Chemistry* 111:297.

Lilga, M. A., R. T. Hallen, E. V. Alderson, M. O. Hogan, T. L. Hubler, G. L. Jones, D. J. Kowalski, M. R. Lumetta, W. F. Riemath, R. A. Romine, G. F. Schiefelbein, and M. R. Telander. 1996. Ferrocyanide Safety Project. Ferrocyanide Aging Studies Final Report, PNNL-11211, Pacific Northwest National Laboratory, Richland, Washington.

Loewenschuss, H. 1982. "Metal-Ferrocyanide Complexes for the Decontamination of Cesium from Aqueous Radioactive Waste." *Radioactive Waste Management* 2:327.

Loos-Neskovic, C. and M. Fedoroff. 1984. "Recovery of Silver from Solutions by Fixation on Insoluble Ferrocyanides." *Annales de Chimie Science des Matériaux* 9:609.

Loos-Neskovic, C. and M. Fedoroff. 1987. "Exchange Mechanisms of Silver on Nickel and Zinc Ferrocyanides." *Solvent Extraction and Ion Exchange* 5:757.

Loos-Neskovic, C. and M. Fedoroff. 1988. "Exchange Mechanisms of Alkali Ions on Zinc Ferrocyanides." *Reactive Polymers* 7:173.

Loos-Neskovic, C. and M. Fedoroff. 1989a. "Fixation Mechanisms of Cesium on Nickel and Zinc Ferrocyanides." *Solvent Extraction and Ion Exchange* 7:131.

Loos-Neskovic, C. and M. Fedoroff. 1989b. "Decontamination of Liquid Nuclear Wastes by Fixation of Radioactive Elements on Nickel and Zinc Ferrocyanides." *Radioactive Waste Management and the Nuclear Fuel Cycle* 11:347.

Loos-Neskovic, C., M. Fedoroff, E. Garnier, and P. Gravereau. 1984. "Zinc and Nickel Ferrocyanides: Preparation, Composition, and Structure." *Talanta* 31:1133.

Loos-Neskovic, C., M. Fedoroff, and G. Revel. 1976b. "Influence of Sodium Content of Nickel Ferrocyanides on the Retention of Alkaline Ions." *Radiochemistry and Radioanalytical Letters* 26(1):17-26.

Murray, R. W. 1980. "Chemically Modified Electrodes." *Accounts of Chemical Research* 13:135.

Murray, R. W. 1984. "Chemically Modified Electrodes." in *Electroanalytical Chemistry*, Vol. 13, A. J. Bard, Ed., Marcel Dekker, Inc., New York.

Prout, W. E., E. R. Russell, and H. J. Groh. 1965. "Ion Exchange Absorption of Cesium by Potassium Hexacyanocobalt(II)Ferrate(II)." *Journal of Inorganic and Nuclear Chemistry* 27:473.

Schneemeyer, L. F., S. E. Spengler, and D. W. Murphy. 1985. "Ion Selectivity in Nickel Hexacyanoferrate Films on Electrode Surfaces." *Inorganic Chemistry* 24:3044.

Sinha, S., B. D. Humphrey, and A. B. Bocarsly. 1984. "Reaction of Nickel Electrode Surfaces with Anionic Metal-Cyanide Complexes: Formation of Precipitated Surfaces." *Inorganic Chemistry* 23:203.

Tusa, E. H., A. Paavola, R. Harjula, and J. Lehto. 1994. "Industrial Scale Removal of Cesium with Hexacyanoferrate Exchanger - Process Realization and Test Run." *Nuclear Technology* 107:279.

Part II. Technology Description

Part I of this document presented the objectives of this work, described the ESIX technology, and summarized the major results. In Part II, experimental details (Section 1) and a more in-depth discussion of the results of the research are presented. Research initially focused on the preparation of electroactive hexacyanoferrate films having improved capacity and stability. Films were prepared using modifications to the published procedures (Section 2). Research then entailed batch studies of cesium loading and unloading (Section 2) and flow cell testing of hexacyanoferrate-coated high surface area nickel foam electrodes for cesium separation (Section 3). Modeling (Section 4) and case studies (Section 5) were performed for cesium separation from KE Basin water at the Hanford Site and a conceptual system for strontium separation from ground water at 100N to obtain preliminary estimates of the required equipment sizes and capital costs. A cost comparison between ESIX and the Empore™ technology was conducted for cesium separation from storage basins and canals (Section 5.3). Conclusions are drawn (Section 6) and patent applications, publications, and reports are listed (Section 7).

1.0 Experimental

Experimental procedures for development of films with improved stability and capacity are presented in this section. Procedures for flow cell testing are also described.

1.1 Development of Improved Films

A PAR 273A potentiostat/galvanostat was used to deposit and characterize films. Potentials were recorded versus a saturated calomel electrode (SCE). In basic solutions, a Zitex filter membrane made of TFE was used in the SCE for improved stability. Experiments were controlled and data collected with a Dell 466/MX computer via a GPIB card using LabView™ software.

A 99.98% pure nickel substrate (Goodfellow) was used as the electrode. In one experimental setup, disks of 1.27-cm-diameter (1.27 cm^2) were embedded in epoxy, polished, and suspended in the test solution. In another apparatus, a nickel plate was sealed to a specially built electrochemical cell with an o-ring and clamp. The exposed portion of the electrode had a diameter of 1.90 cm (2.84 cm^2). Prior to each film deposition, the substrate was abraded using a 600-grit sandpaper and then thoroughly rinsed. Three different deposition procedures were used. One procedure was similar to that of Bocarsly and Sinha (1982a, 1982b), where the nickel surface was exposed to a solution of 5 mM $\text{K}_3\text{Fe}(\text{CN})_6$ and 0.1 M KNO_3 and a 1.0 V (SCE) potential was applied to the nickel electrode for 300 s. This method is designated the "literature" procedure. One variant of this method, entailing application of 0.65 V for 10 min followed by

1 V for 30 min, was used to prepare films for chronocoulometry experiments. The other procedures were PNNL proprietary methods designated as PNNL-1 and PNNL-2. All chemicals were A.C.S. reagent grade and solutions were prepared with 18.2 M Ω -cm water.

A nickel sponge electrode (Electrosynthesis Co., Inc.) with a nominal surface area per volume of 13 cm²/cm³ (20 pores per inch, ppi) was also coated with a nickel hexacyanoferrate film using the literature procedure and tested.

The characteristics of the films were determined by use of cyclic voltammetry and chronocoulometry. Cyclic voltammetry was typically conducted in 1 M NaNO₃ or 1 M CsNO₃ solutions starting from an applied potential of 0.25 V, scanning anodically to 0.8 V, then cathodically to -0.1 V, returning to 0.25 V (SCE) at a scan rate of 50 mV/s. Chronocoulometry was conducted by stepping to 0.25 V (SCE) to load the film and to 0.5 V (SCE) to unload the film, typically in 0.5 M Na₂SO₄.

1.2 Flow Cell Testing

Flow cell tests were conducted with derivatized Ni foam electrodes in two types of electrochemical cells, a Teflon Micro Flow cell (ElectroCell AB) and an MP cell (ElectroCell AB). Each cell had a different flow pattern (Figure 1). The Micro Flow cell was used in PNNL tests in which solution passed through the face of a square 0.64-cm-thick ESIX electrode. This type of flow is called flow-through mode and, for the electrodes used, the bed depth was 0.64 cm (0.25") per electrode in the cell. The performance of a single electrode (cell and experimental apparatus shown in Figures 2 and 3) and stacks of 5 (Figures 4 and 5) and 8 electrodes in series were tested in this cell. The dimensions of the electrode in single electrode tests were 3.0 x 2.5 x 0.64 cm. Each electrode in the 5 and 8 electrode stacks had dimensions of 3.2 x 3.1 x 0.64 cm. Before flow testing began, batch tests were conducted to study film capacity and regeneration.

The MP cell was modified to house the nickel foam electrode (Figure 6). Solution flow in this cell (flow-by) passed through the length of a 10 cm x 10 cm x 0.64 cm electrode (bed depth of 10 cm). The Electrosynthesis Co., Inc., performed MP cell tests; their findings are summarized in Section 1.5.3 and reported in Appendix B.

In both cell designs, cesium ion exchange was conducted on open circuit; i.e., the cesium feed solution passed through regenerated electrodes without the application of an electrochemical potential or current. After a cesium ion exchange experiment, electrodes were regenerated either *in situ* or *ex situ* (after cell disassembly) by applying either a controlled current or controlled potential. A Masterflex pump was used to control liquid flow through the cells at the desired rate (5 to 45 mL/min in Micro Flow cell tests; 8 to 24 mL/min in MP cell tests). Effluent samples were collected at predetermined intervals for cesium analysis. Cesium analyses were conducted by flame emission or graphite furnace atomic absorption (AA) spectro-

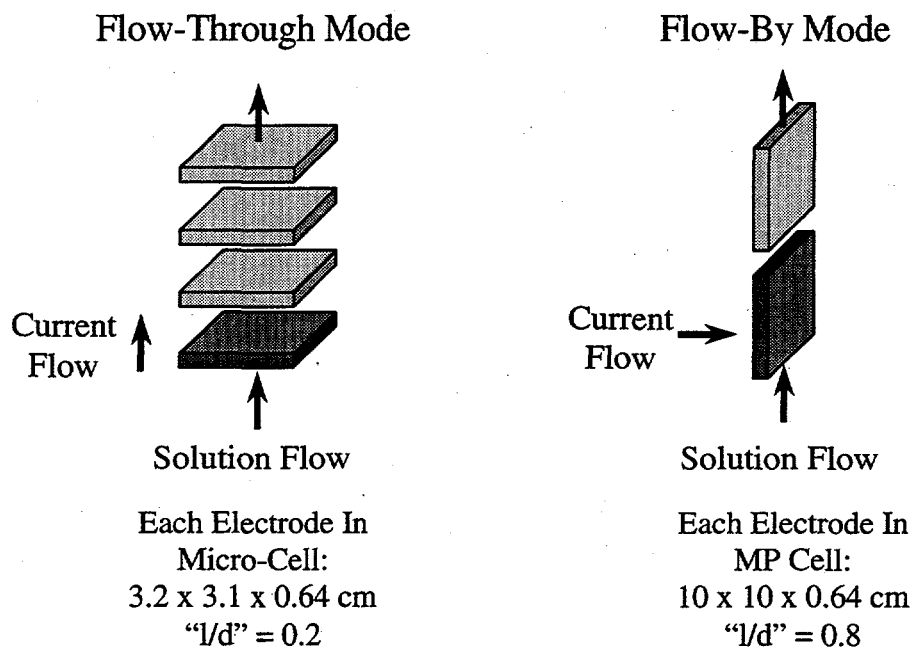


Figure 1. Solution and Current Flow Patterns in Electrochemical Cells Used for Flow Tests

photometry. Samples analyzed by flame emission AA were diluted with an aqueous potassium solution for increased sensitivity for cesium ion.

During testing at PNNL, a PAR 273A potentiostat/galvanostat (Princeton Applied Research) was used to deposit and characterize films. Potentials were recorded versus a saturated calomel electrode (SCE). Experiments were controlled and data collected with a Dell 466/MX computer via a GPIB card using LabView™ software.

Nickel foam electrodes (supplied by The Electrosynthesis Co., Inc.) with a nominal surface area per volume of $40 \text{ cm}^2/\text{cm}^3$ (60 ppi) coated with nickel hexacyanoferrate films were used in most of the PNNL batch and all of the Micro Flow cell experiments. Films were deposited using a PNNL-proprietary method (PNNL-2) similar to that of Bocarsly and Sinha (1982), where the nickel surface was exposed to a solution of $5 \text{ mM K}_3\text{Fe}(\text{CN})_6$ and 0.1 M KNO_3 , and a 1.0 V (SCE) potential was applied to the nickel electrode for 300 s. All chemicals were A.C.S. reagent grade, and solutions were prepared with $18.2 \text{ M}\Omega\text{-cm}$ water.

Cyclic voltammetry and chronocoulometry were used to characterize and, in many experiments, regenerate films on the high surface area electrodes. Cyclic voltammetry was typically conducted in 1 M NaNO_3 solutions starting from an applied potential of 0.25 V , scanning

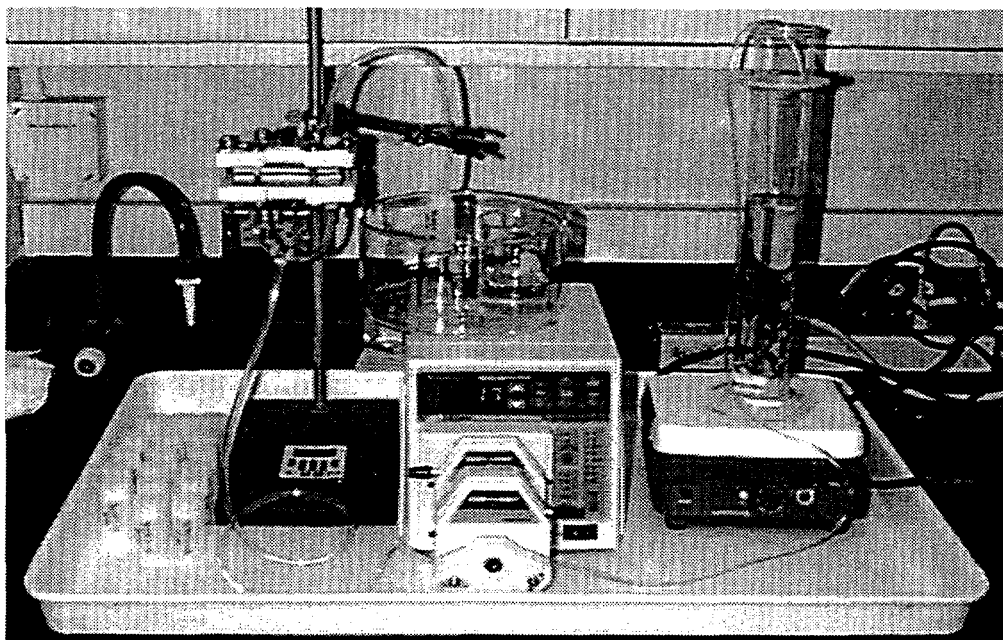


Figure 2. Micro Flow Cell Apparatus with a Single Electrode

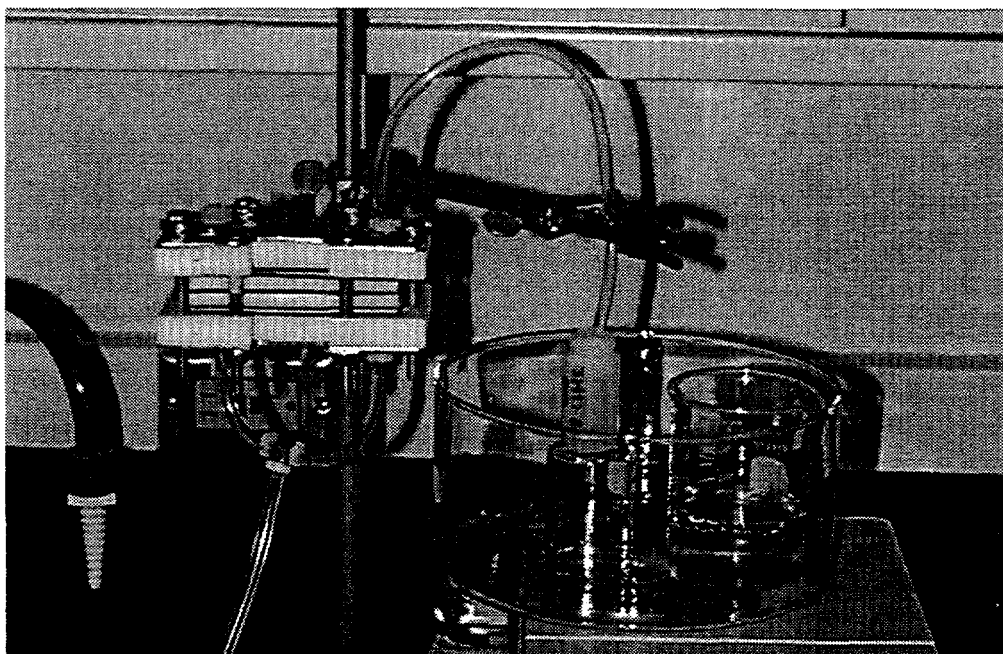


Figure 3. Close-up of the Micro Flow Cell with a Single Electrode

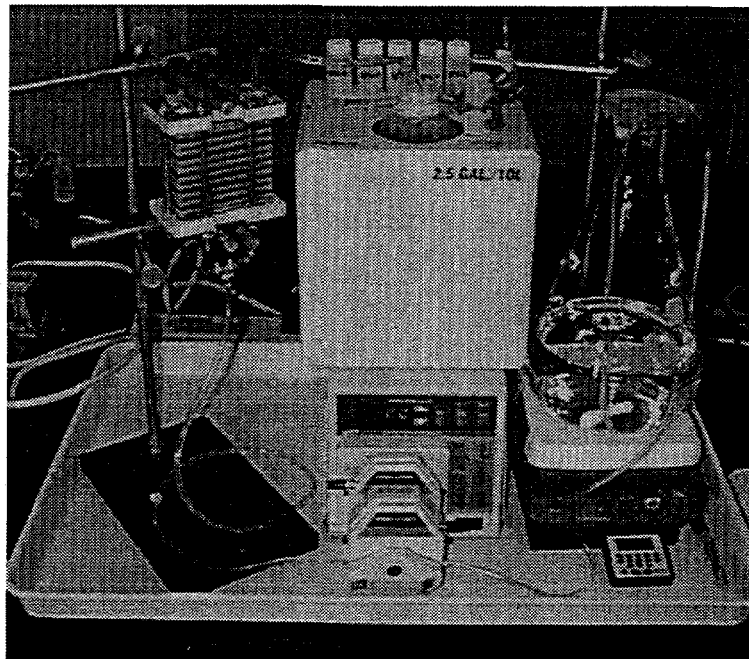


Figure 4. Micro Flow Cell Apparatus with 5-Electrode Stack

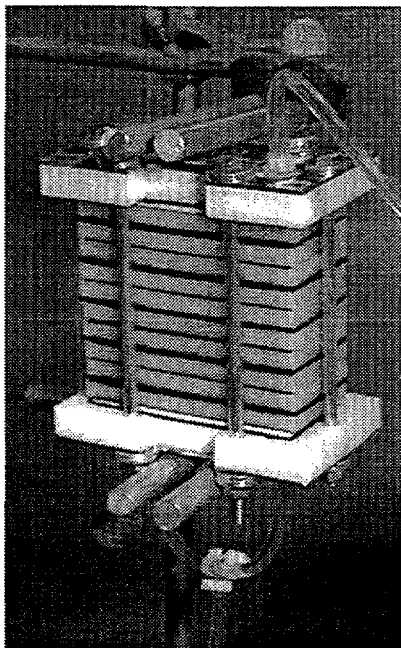


Figure 5. Close-up of the Micro Flow Cell with 5-Electrode Stack

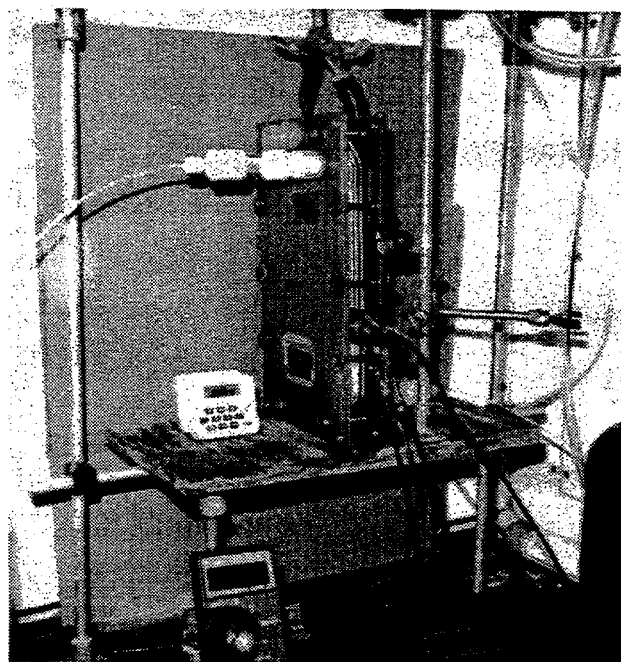


Figure 6. MP Cell Experimental Setup

anodically to 0.8 V, then cathodically to -0.1 V, returning to 0.25 V (SCE) at a scan rate of 50 mV/s. Chronocoulometry was conducted by stepping to 0.25 V (SCE) to load the film and to 0.5 V (SCE) to unload the film, also in 1.0 M NaNO₃.

In situ elution of high surface area electrodes was carried out at PNNL by recirculating a 1 M NaNO₃ solution through the cell while applying a constant potential of 0.8 V. Initial testing with a single electrode was conducted at a solution flow of 150 BV/h (20 mL/min) and elution lasted 5 min. An 8-electrode stack was in-line eluted at a flow rate of 30 BV/h (24 mL/min) by application of 0.8 V for 20 min.

In experiments conducted at The Electrosynthesis Co., Inc., porous nickel foams of porosity 60 and 80 ppi were used. The same PNNL method for film preparation was used except the electrolyte for film deposition was a solution containing 0.1 M KNO₃ and 10 mM K₃Fe(CN)₆, and a PAR 273 potentiostat was used to control the potential. All voltammograms were conducted at a scan rate of 50 mV/s between -0.25 and 1.05 V vs. Ag/AgCl. The oxidation and reduction waves were integrated to obtain the film loading or capacity of the film. Chronocoulometric experiments were also performed to determine the film capacity. The areas under the current decay curves at 0.8 V and 0.2 V (potentials vs. Ag/AgCl) for 30 s each were used to measure film capacities.

Regeneration of films *in situ* involved passing a solution of 0.1 M NaNO₃ through the cell while maintaining a low constant current (5 mA). A low current was used in these initial tests to

demonstrate the viability of the *in situ* method, but a higher current would give faster regeneration. Passage of about 300 mL of 0.1 M NaNO₃ solution for about 2 to 3 h was sufficient to elute 70% to 75% of the cesium exchanged on the film.

2.0 Film Preparation, Characterization, and Batch Results

This section presents results of work to prepare electroactive hexacyanoferrate films with increased capacity and stability. Performance of the films on high surface area electrodes in batch cesium uptake experiments is also discussed.

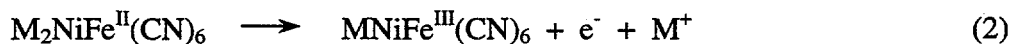
2.1 Comparison of Film Preparation Methods on Flat Plates

Films were prepared on a nickel substrate by applying an anodic potential in a solution containing K₃Fe(CN)₆. The film is formed when Ni⁺² ion generated at the electrode surface reacts with the ferricyanide anion to precipitate the insoluble nickel hexacyanoferrate material on the electrode surface (Eq. 1). Once the electrode has been coated, it displays the properties of the



nickel hexacyanoferrate, rather than the substrate on which it was deposited. For example, Figure 7 shows a cyclic voltammogram of a bare nickel electrode in 1 M CsNO₃ electrolyte. Within the potential range studied, only a small amount of current is passed associated with oxidation of the nickel surface. The current on the 5th cycle is larger than that on the 15th cycle because the electrode surface passivates as an oxide coating forms. Figure 8 shows cyclic voltammetry in 1 M NaNO₃ electrolyte of films prepared by three different deposition protocols. The redox behavior of the surface-bound hexacyanoferrate is readily apparent.

Cyclic voltammetry shows that the ferrocyanide film may be oxidized to the ferricyanide form, which may in turn be reduced back to the ferrocyanide form. Eqs. 2 and 3, respectively, illustrate these reactions for any alkali metal counterion (M⁺). Note that reduction requires uptake of a metal ion, M⁺, and oxidation requires release of the ion to retain charge neutrality in the film.



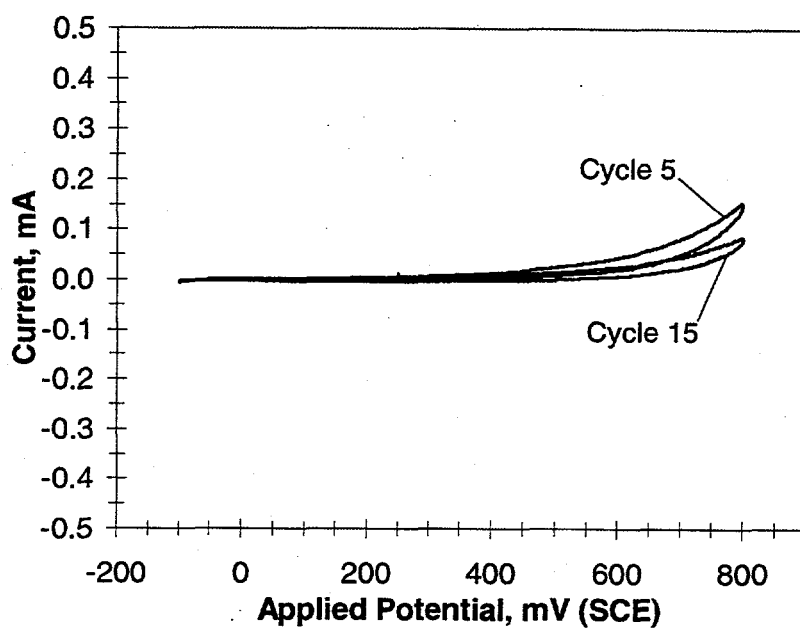


Figure 7. Cyclic Voltammetry of a Bare Nickel Electrode in 1 M NaNO₃

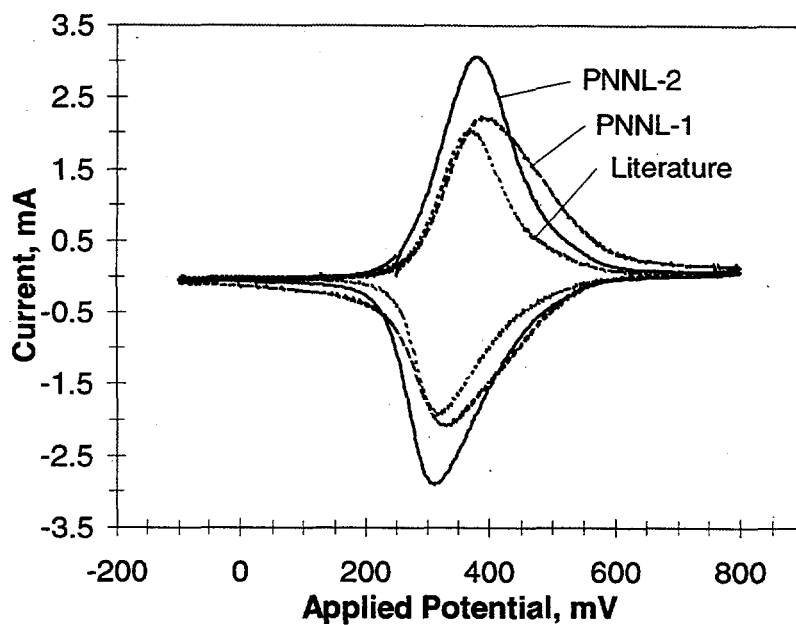


Figure 8. Cyclic Voltammetry in 1 M NaNO₃ of Hexacyanoferrate Films Prepared by Three Different Methods (Cycle #2)

Cyclic voltammograms in Figure 8 show that the processes in Eqs. 2 and 3 are chemically reversible and that metal ion loading and unloading can be controlled by modulating the electrode potential. Films in Figure 8 are initially in the reduced state (the films are loaded). During unloading of sodium from the films, the peak current in the cyclic voltammogram occurs at about 400 mV (SCE) and the current approaches zero at 800 mV as oxidation of ferrocyanide to ferricyanide nears completion. Potential scan reversal results in sodium ion uptake as ferricyanide is reduced; the peak current occurs at about 350 mV.

Figure 8 also shows that different deposition protocols give films with different capacities, as estimated by the charge passed, i.e., the area under the curve for each potential scan. The capacity of each preparation is illustrated more clearly in Figure 9, which is an integration of current passed over the course of an entire cyclic voltammetric sweep. The PNNL-prepared films using modified deposition procedures have greater capacity than the films prepared using the standard literature procedure. The maximum capacity of literature, PNNL-1, and PNNL-2 films is $2.1 \times 10^{-3} \text{ C/cm}^2$, $3.3 \times 10^{-3} \text{ C/cm}^2$, and $3.5 \times 10^{-3} \text{ C/cm}^2$, respectively. These capacities correspond to surface coverages of $2.2 \times 10^{-8} \text{ moles/cm}^2$, $3.4 \times 10^{-8} \text{ moles/cm}^2$, and $3.6 \times 10^{-8} \text{ moles/cm}^2$, respectively, for the literature, PNNL-1, and PNNL-2 films. The thickness of

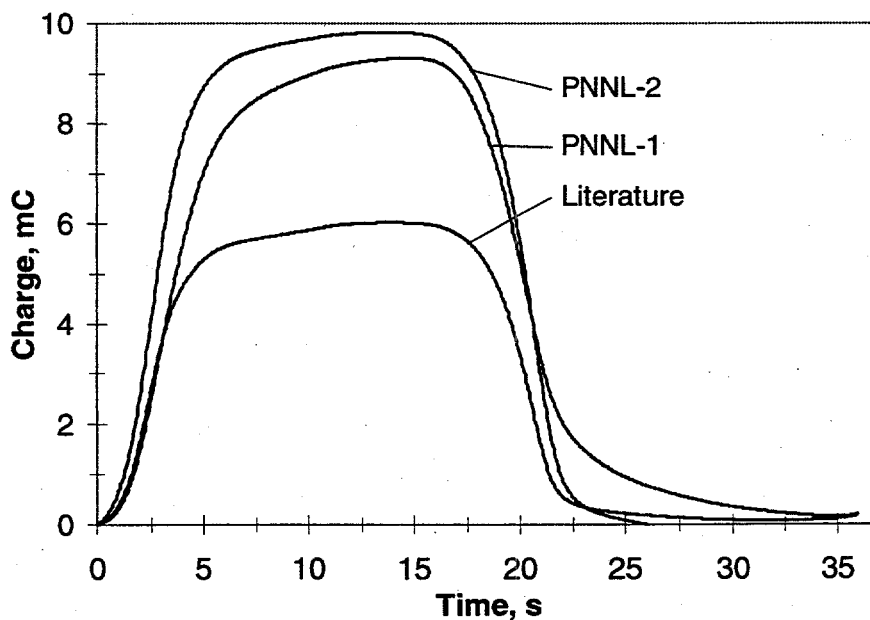


Figure 9. Charge Passed as Determined by Integration of a Single Potential Cycle (Cycle #2) for Three Film Preparations

PNNL-2 is approximately 540Å, or about 54 unit cells deep (Loos-Neskovic et al. 1984), assuming that all sites are electrochemically active (Bocarsly and Sinha 1982a; Sinha et al. 1984) and that the film is uniform.

Some loss of activity occurs on repeated cycling (Figure 10). The stability of the films can be improved, however, by modifying the deposition procedure. Figure 11 compares the maximum charge passed for several different film preparations on 1.9-cm-diameter electrodes as a function of cycle number. The normalized data showing fraction of charge passed as a function of cycle number is shown in Figure 12. PNNL-2 demonstrates a loss of about 20% of its capacity after 2000 cycles. The literature film, in contrast, lost 50% of its capacity after 2000 cycles.

Rates of sodium ion loading and unloading can be estimated from the normalized data of Figure 9. In Figure 13, fractional charge passed for each film is plotted as a function of time. The data show that for the literature film, 7.8 s were required to unload 95% of the film and 9.7 s were required to load 95% of the film. For PNNL-1, the unload and load times were 9.3 s and 13.9 s, respectively; for PNNL-2, these times were 6.5 s and 8.9 s. Therefore, while PNNL-1 had a higher capacity than the literature film, the rate of unloading was slower. The PNNL-2 film had superior capacity and similar rates of unloading and loading as the literature film.

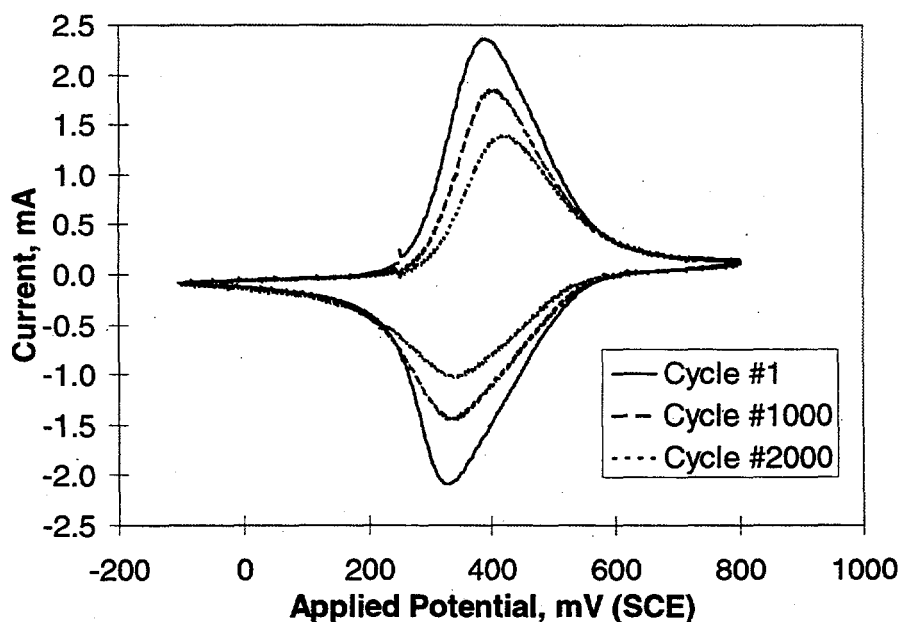


Figure 10. Repeated Potential Cycling of PNNL-1 in 1 M NaNO₃

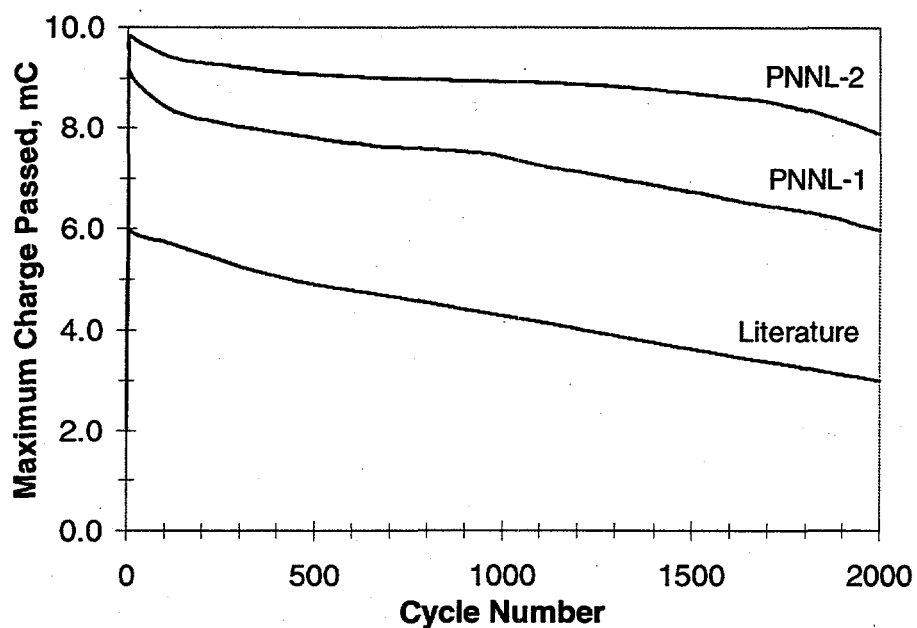


Figure 11. Maximum Charge Passed as a Function of Cycle Number for Three Different Film Preparations (Cyclic Voltammetry in 1 M NaNO₃).

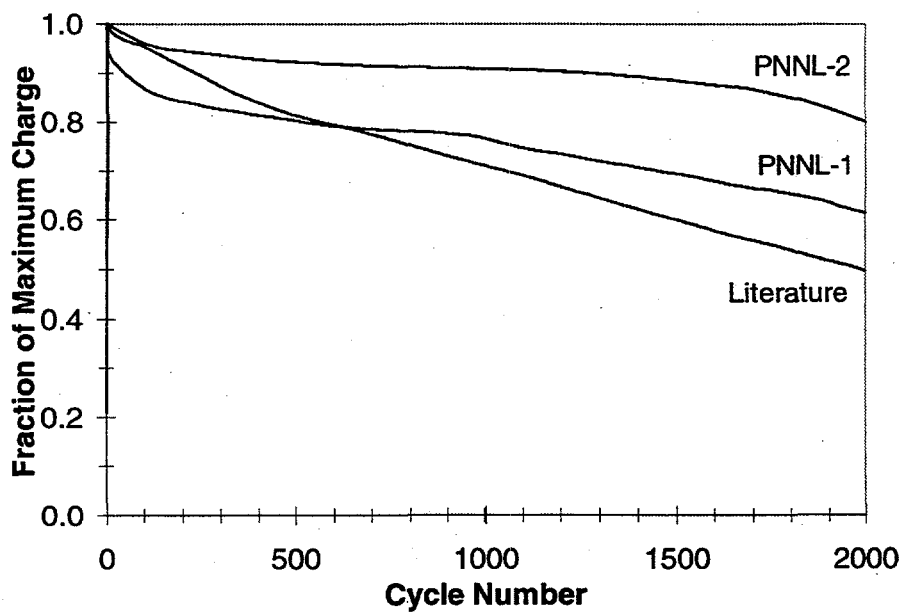


Figure 12. Normalized Maximum Charge as a Function of Cycle Number for Three Different Film Preparations (Cyclic Voltammetry in 1 M NaNO₃).

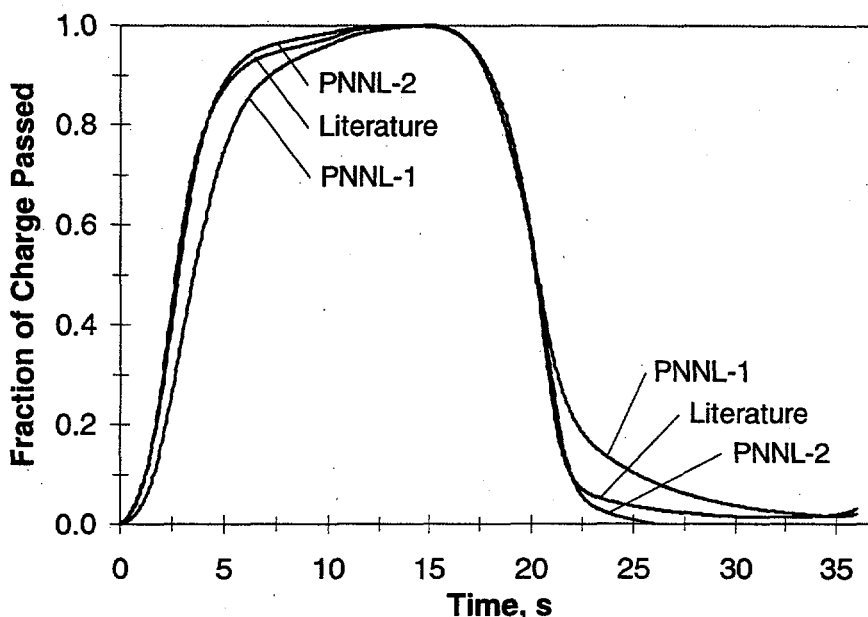


Figure 13. Normalized Charge as a Function of Time for Three Different Film Preparations (from Cyclic Voltammetry in 1 M NaNO₃)

2.2 Cesium Uptake/Elution From Flat Plate Electrodes

The high affinity of hexacyanoferrates in the film for cesium is demonstrated by cyclic voltammetry. Conversion of the cesium form to the sodium form requires repeated cycling in 1 M NaNO₃. Figure 14 shows this transformation. After two potential cycles in the unstirred solution, only about half of the film is in the sodium form. The peak for the sodium form increases upon cycling, but the affinity of the film for cesium is large enough that even after 25 cycles in initially pure 1 M NaNO₃, a peak associated with cesium uptake is still observed. The only cesium in this experiment is that initially in the film, estimated to be about 1.6×10^{-8} moles for a 1.27-cm-diameter electrode with a surface coverage of 6.5×10^{-9} moles/cm². These results show that low cesium concentrations compete with high sodium concentrations for ion exchange sites in the film.

A film initially in the sodium form converts readily to the cesium form before the second potential cycle in 1 M CsNO₃ (Figure 15). Displacement of sodium by cesium occurs during electrochemical cycling as well as by chemical ion exchange, as in a conventional ion exchange column. In other testing, it has been shown that as little as 5 mM cesium added to a 1 M NaNO₃ solution converts much of the sodium form to the cesium form. Similar results were obtained by chemical analyses of films purposely dissolved. For example, films on a 1.27-cm-diameter

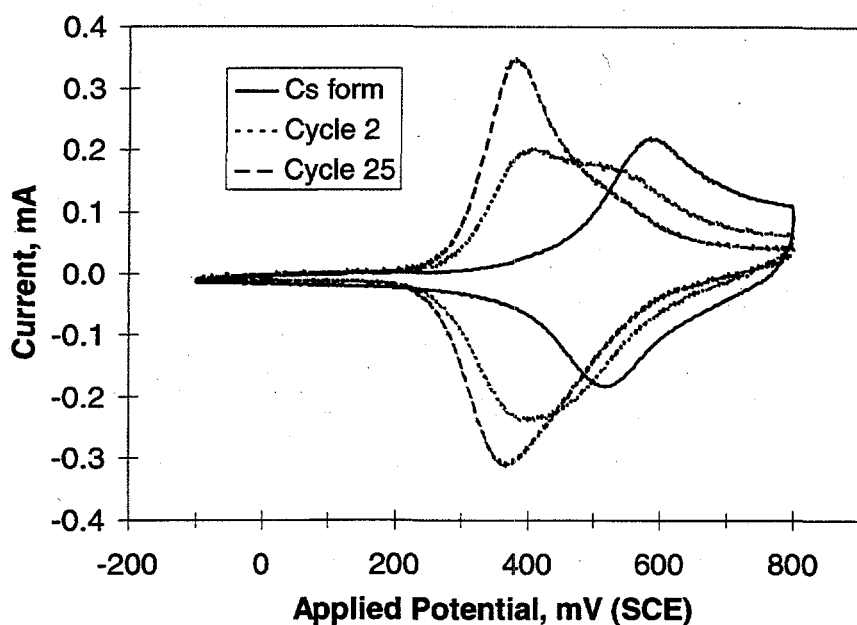


Figure 14. Cyclic Voltammetry for a Film in the Cesium Form and After Two and 25 Potential Cycles in 1 M NaNO_3

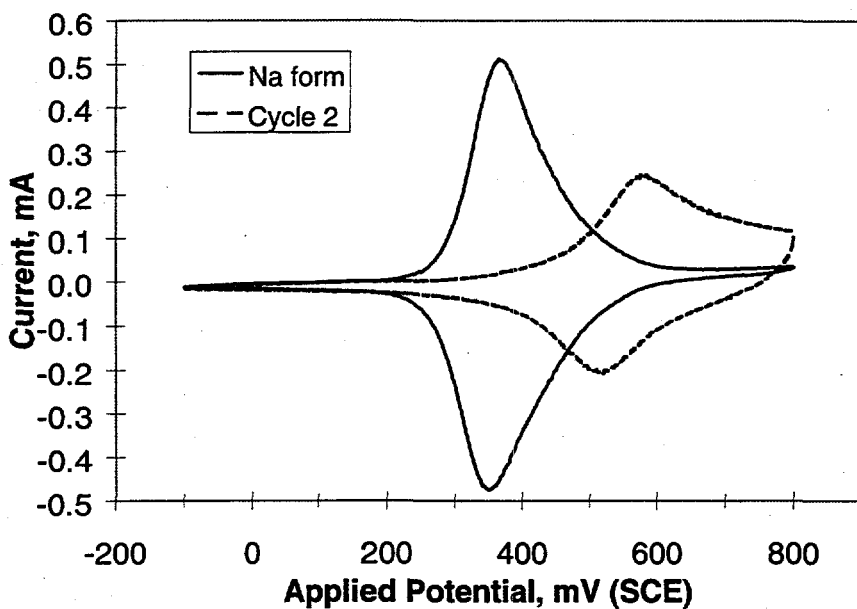


Figure 15. Cyclic Voltammetry of a Film in the Sodium Form and After Two Potential Cycles in 1 M CsNO_3

electrode were exposed to 5mM CsNO₃ in 1M KNO₃. Dissolution of the films and analysis by atomic absorption showed significant selectivity for cesium over potassium, but the small amount of material on the electrode precluded accurate quantification.

Figures 14 and 15 show that, like sodium ion, cesium ion uptake and release is also chemically reversible. However, cesium peaks are much broader and shifted anodically. The practical consequence is that in a process for cesium separation, loading of the film with cesium requires an applied potential of about 0.55 V or less and unloading must be conducted at 0.60 V or greater. Because sodium loading occurs at about 0.40 V, it is possible that selectivity for cesium over sodium could be enhanced by applying the appropriate potential. The applied potential is an additional driving force to increase the Cs/Na separation factor.

The broad anodic peak with a smaller peak current for cesium compared to sodium suggests that unloading of cesium is slower than sodium unloading. The cation dependence of the cyclic voltammetry, which has been seen before (Bocarsly and Sinha 1982b, Humphrey et al. 1984), suggests that ion diffusion through the film is the rate-limiting process, consistent with the known high affinity of metal hexacyanoferrates for cesium. This high affinity forms the basis for the use of these materials as ion exchangers for the removal of cesium from nuclear waste (Barton et al. 1958; Harjula et al. 1994; Lehto and Harjula 1987; Loewenschuss 1982; Loos-Neskovic and Fedoroff 1989b; Tusa et al. 1994). The high current after the anodic cesium peak in Figures 14 and 15 indicates that cesium was still being unloaded from the film when the potential was reversed. On the time scale of the experiment, the cesium film used about 73% of the capacity displayed by the sodium film.

Nickel hexacyanoferrate films are not applicable for cesium removal directly from tank wastes because stability in highly basic media is required. Metal hexacyanoferrates are well known to dissolve in strongly basic solutions (Bocarsly and Sinha 1982a, Lilga et al. 1996) to form nickel hydroxide and soluble hexacyanoferrate. However, nickel hexacyanoferrates containing cesium, such as Cs₂NiFe(CN)₆, are insoluble in up to 4 M NaOH solutions (Lilga et al. 1996). Electroactive nickel hexacyanoferrate films containing cesium ion are stable for over two months in 1 M NaOH solutions containing 5 mM cesium ion. Application of a cathodic potential in the caustic solution results in ion uptake without significant film loss. However, without cesium in solution, the films degrade within two weeks. Apparently, the small amount of cesium in the solution sufficiently shifts the equilibrium to the insoluble cesium phases and away from the more soluble sodium phases. These results suggest that ESIX using nickel hexacyanoferrate films for cesium removal from highly basic tank wastes would most likely have to be combined with processes that reduce the pH of the solution (e.g., a salt-splitting process).

2.3 Batch Results on High Surface Area Electrodes

A film was deposited on a 20 ppi ($13 \text{ cm}^2/\text{cm}^3$) high surface area nickel electrode using the literature procedure. In characterization tests using 1 M sodium nitrate as the test solution, the film on this electrode had a surface coverage of $2.0 \times 10^{-8} \text{ moles}/\text{cm}^2$, which was the same as that obtained using the 1.9-cm-diameter flat plates. These results indicate that the two electrode geometries have similar film deposition properties. The film on the 20 ppi electrode retained 81% of its capacity after 1500 cycles, as determined by integration of the curves shown in Figure 16.

Batch testing was conducted to study cesium loading and regeneration of 60 ppi high surface area nickel foam electrodes. Cesium uptake was monitored with time and compared with the theoretical capacity based on integration of cyclic voltammograms in a sodium solution. Table 1 shows the results for cesium uptake by films initially in the reduced state, $[\text{Na}_2\text{NiFe}^{\text{II}}(\text{CN})_6]$, from solutions initially containing 6 ppm and 8 ppm cesium. Cesium uptake was 70% to 80% complete after 1 h and reached equilibrium within 18 h. Under the conditions of the experiment, cesium loading reached 22% of the theoretical ion exchange capacity based on voltammetry. Similarly, experimental cesium capacities for nickel hexacyanoferrate powders are reported to be in the range of 23% to 46% of theoretical (Streat and Jacobi 1995).

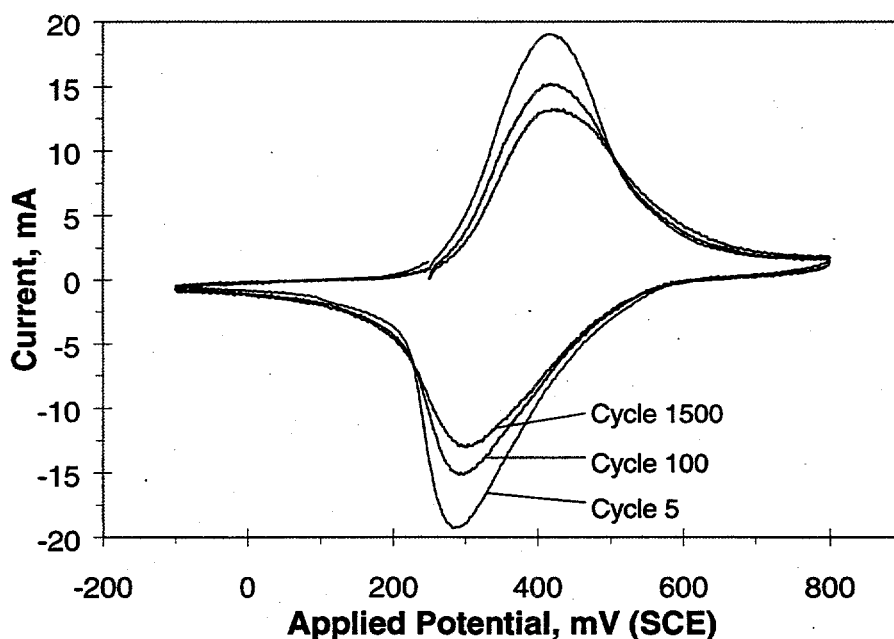


Figure 16. Long-term Cycling of a Hexacyanoferrate Film Deposited on a 20 ppi High Surface Area Nickel Electrode

Table 1. Actual and Theoretical Cesium Loading on 60 ppi Nickel Foam Electrodes. Theoretical Capacity Based on Integration of Cyclic Voltammograms in Sodium-Containing Solutions

$[\text{Cs}]_0$	Time (h)	Actual Cs Loaded (moles/cm ²)	Theoretical Cs Loaded (moles/cm ²)	Actual/Theoretical (%)
6 ppm	1	5.6×10^{-9}	3.4×10^{-8}	16
	16	7.6×10^{-9}	3.4×10^{-8}	22
	24	7.1×10^{-9}	3.4×10^{-8}	21
8 ppm	1	5.7×10^{-9}	3.3×10^{-8}	17
	16	7.0×10^{-9}	3.3×10^{-8}	21
	24	7.2×10^{-9}	3.3×10^{-8}	22

Figure 17 shows cesium loading data for the 6 ppm and 8 ppm solutions with reduced films, as well as loading by an oxidized film and by an initially oxidized film with a cathodic (reducing) potential of 0.1 V (SCE) applied during uptake. The oxidized film $[\text{NaNiFe}^{\text{III}}(\text{CN})_6]$ without applied potential loaded roughly half as much cesium as the reduced films. This is expected since the oxidized film contains half the number of exchangeable sodium atoms as the reduced film. However, application of 0.1 V (SCE) to an initially oxidized film results in loading to 90% of the level obtained for the reduced films within 1 h. Application of the potential accelerates cesium loading as the film is reduced (1 h data), but apparently does not affect the overall capacity of the film.

Batch tests were also conducted to determine the influence of sodium on cesium uptake. Figure 18 compares data for sodium-free cesium solutions with solutions containing Na/Cs molar ratios of 190 (0.01 M Na^+) and 17,000 (1 M Na^+). Sodium ion might slow the kinetics of cesium binding slightly since less was loaded after 1 h. However, after 24 h, very nearly the same loading was observed as when sodium was not present, with some depression by 1 M Na^+ possibly indicated. The films on the high surface area electrodes appear to have the same high selectivity for cesium as films previously prepared on flat electrodes and the same as nickel hexacyanoferrate powders or packed beds.

The effect of elution solution conductivity on unloading the films was investigated in batch tests. Conductive solutions appear to be best for unloading at an applied potential of 0.8 V (SCE), as shown in Figure 19. In an elution solution containing 1 M NaNO_3 , the cesium in the film was

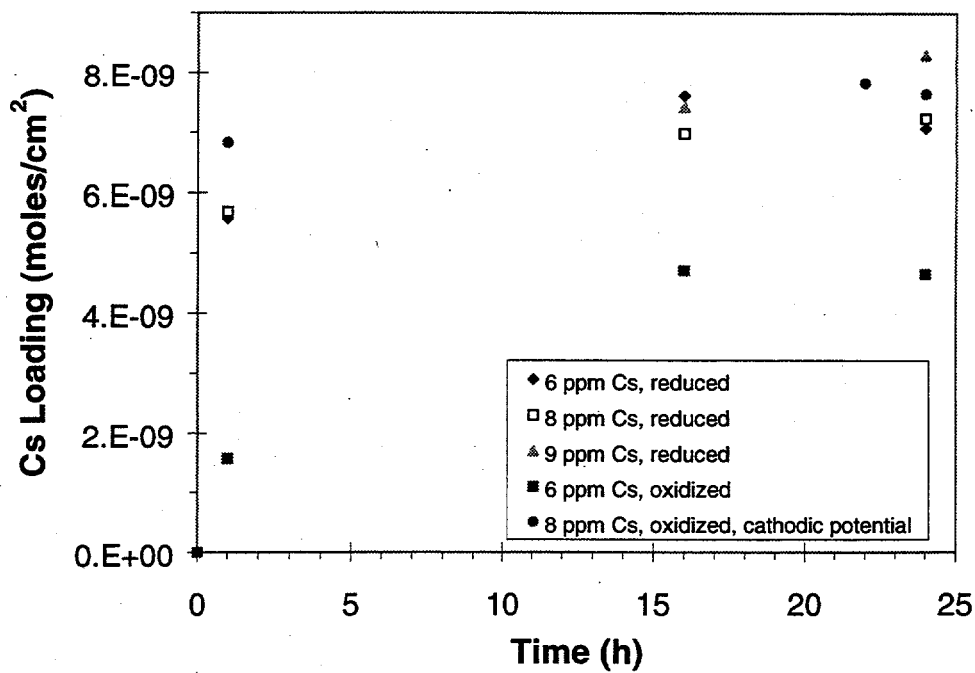


Figure 17. Effect of Applied Potential on Cesium Uptake in Batch Experiments

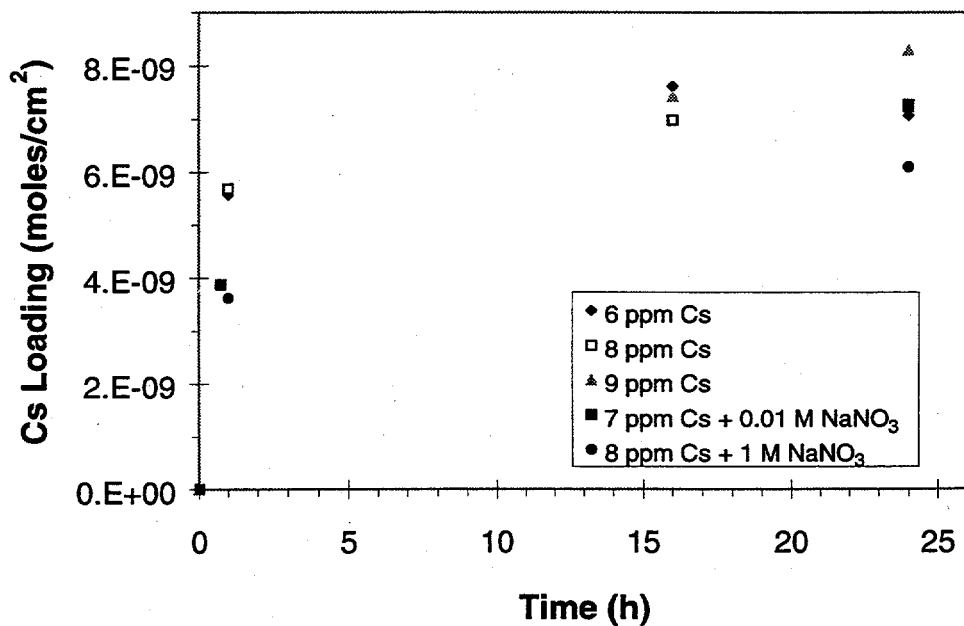


Figure 18. Effect of Sodium on Cesium Uptake in Batch Experiments

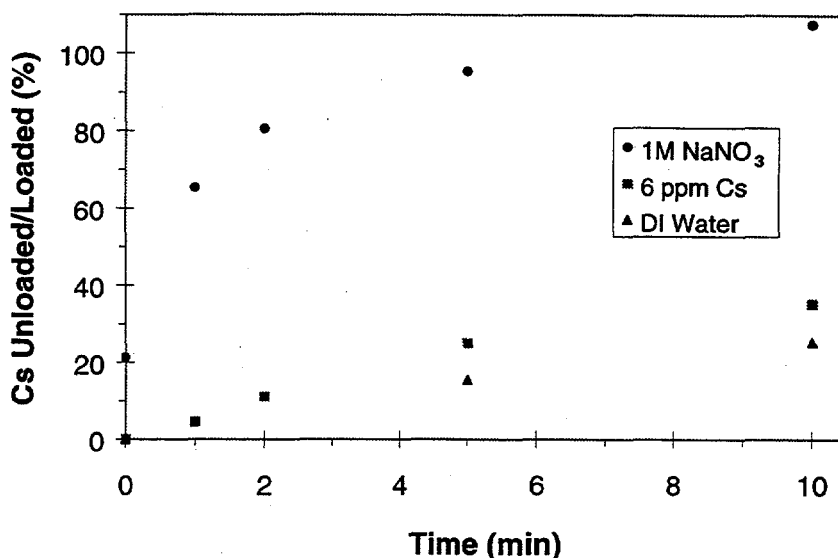


Figure 19. Effect of Elution Solution on Cesium Unloading in Batch Experiments (Applied Potential = 0.8 V)

fully unloaded after 10 min at this potential. However, films were only about 35% unloaded in 6 ppm cesium and about 25% unloaded in distilled water after 10 min. After 60 min in distilled water, films were 45% unloaded (not shown).

3.0 Flow Cell Results

This section presents the results of studies to determine the performance of hexacyanoferrate-modified nickel electrodes for the removal of cesium under flow conditions. Micro Flow cell tests (conducted by PNNL) of single- and multiple-stacked electrodes operated in flow-through mode are described here. An initial engineering evaluation is presented for an application at Hanford's KE Basin, based on the test results. Results of tests with an MP cell (conducted by The Electrosynthesis Co., Inc.) containing a single electrode operated in flow-by mode are also discussed in this section.

3.1 Micro Flow Cell Results Using a Single Electrode

Bench-scale flow experiments were conducted in which cesium uptake was measured as a function of flow rate and initial cesium concentration, $[Cs]_0$, for solutions passed through a single 60 ppi nickel foam electrode upon which the electroactive film was deposited using the PNNL-2 method. Experiments reported here were conducted without applying a potential and in flow-through mode, in which solution was forced through the 3.0 x 2.54 cm face of the high surface

area electrode, passing through the electrode thickness of 0.64 cm ("length/diameter," or l/d , = 0.2). Figure 20 shows breakthrough curves for a feed containing 0.2 ppm Cs as a function of flow rate. In nonradioactive testing, 0.2 ppm Cs was the lowest concentration that could be used due to cesium detection limits of approximately 0.02 ppm for atomic absorption analyses. At 13 BV/h, no breakthrough was observed until about 22 BV; 50% breakthrough occurred at 50 BV. Similar behavior was observed at slower flow rates, but breakthrough occurred immediately at the faster flow rates tested.

The breakthrough curves were well defined, even though the l/d was relatively low for the single electrode flow-through setup. The low l/d does not allow for fully developed flow, and some channeling and significant dispersion are expected.

Initial cesium concentration did not greatly affect breakthrough for $[Cs]_0$ of 0.12 and 0.18 ppm at 8 BV/h (Figure 21). Breakthrough occurred rapidly at a feed concentration of 0.38 ppm.

The flow studies show that films are stable up to the maximum flow rate tested of 113 BV/h. No significant decline in capacity or performance was observed throughout experimentation. Table 2 summarizes results of all Micro Flow cell testing, in the order experiments were conducted. While a slight drop is seen in the theoretical loading based on cyclic voltammetry in sodium solutions, the amount of cesium loaded remains about constant. The drop in theoretical loading results from the normal loss in capacity after the film has been subjected to the numerous redox cycles during the course of experimentation. Over the course of experimentation, the film maintained about a 10% efficiency in site utilization. This efficiency is about half that obtained

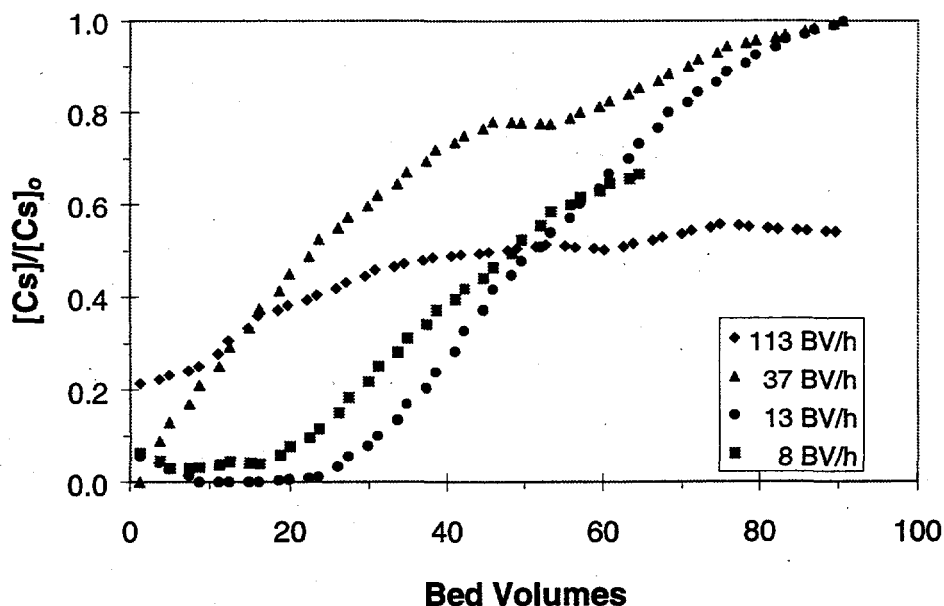


Figure 20. Effect of Flow Rate on Cesium Breakthrough in Flow-Through Mode ($[Cs]_0 = 0.2$ ppm)

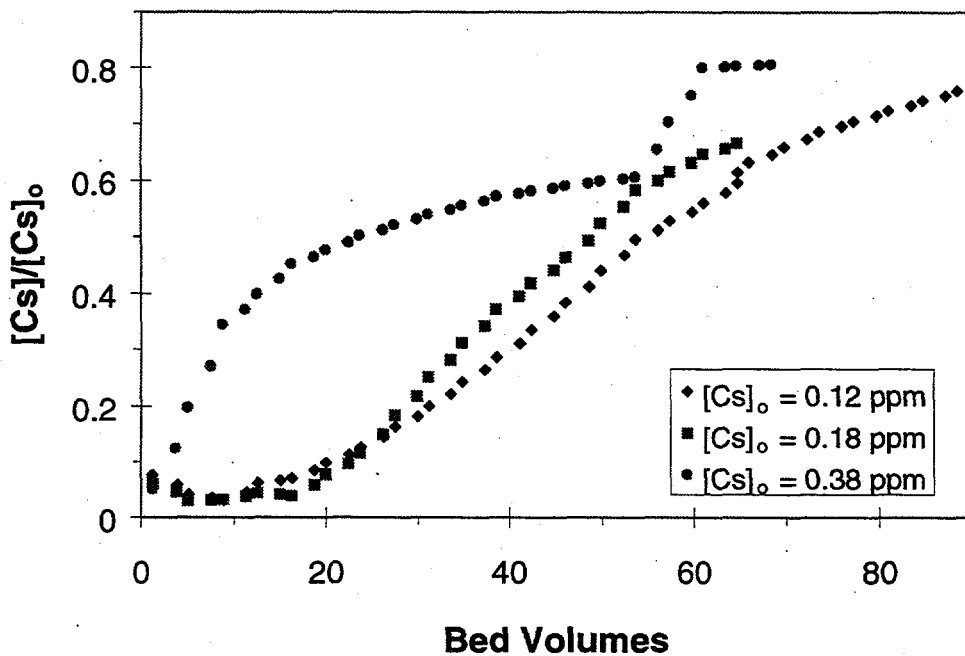


Figure 21. Effect of $[Cs]_0$ on Cesium Breakthrough in Flow-Through Mode (Flow Rate = 8 BV/h)

in batch testing, which suggests that stacking the electrodes to give a longer bed depth may lead to improved performance and better utilization of film capacity. (Stacked electrode results are discussed in the following section.) Films were unloaded quantitatively, as indicated both by the amount of cesium unloaded compared with the amount loaded and by the consistency of the amount of cesium loaded from one run to the next.

Table 2 also shows that Electrode 2, a new electrode with a fresh film, performs the same as Electrode 1. The similarity in cesium breakthrough for these two electrodes is shown in Figure 22. These results are another indication of the consistency from one film deposition to the next.

3.2 Micro Flow Cell Results Using Stacked Electrodes

A stacked electrode configuration was used in the Micro Flow cell to increase the effective bed depth of the cell. Stacks of 5 and 8 electrodes were tested. In 5-electrode stack experiments, two sets of five 60 ppi electrodes were coated with a hexacyanoferrate film (PNNL-2 method). One set of 5 electrodes was assembled in the cell such that solution flowed from the bottom of the cell up through the large face of each electrode in series (Figures 4 and 5). The bed depth, therefore, was five times that used in the single electrode experiments, or 3.18 cm (1.25 in), giving an l/d of about 1.0. As a result, the bed volume was also about five times greater and the volumetric flow rates (mL/min) in the stacked cell were approximately five times those used in the single

Table 2. Summary of Results from Micro Flow Cell Tests

$[Cs]_0$	BV/h	Cs Loaded (moles/cm ²)	Cs Unloaded (moles/cm ²)	Theoretical [ⓐ] (moles/cm ²)	Loaded/ Theoretical
[ⓐ] 0.18	112	1.6×10^{-9}	2.0×10^{-9}	1.8×10^{-8}	9 %
0.18	13	1.7×10^{-9}	2.6×10^{-9}	1.8×10^{-8}	9 %
0.20	37	1.1×10^{-9}	2.1×10^{-9}	1.7×10^{-8}	6 %
0.38	8	2.2×10^{-9}	2.2×10^{-9}	1.4×10^{-8}	16 %
0.17	8	1.4×10^{-9}	1.3×10^{-9}	1.4×10^{-8}	10 %
0.12	8	1.2×10^{-9}	1.2×10^{-9}	1.3×10^{-8}	9 %
[ⓐ] 0.20	13	1.9×10^{-9}	NA	2.2×10^{-8}	9 %

① Electrode #1, in order of testing

② Na charge basis

③ Electrode #2

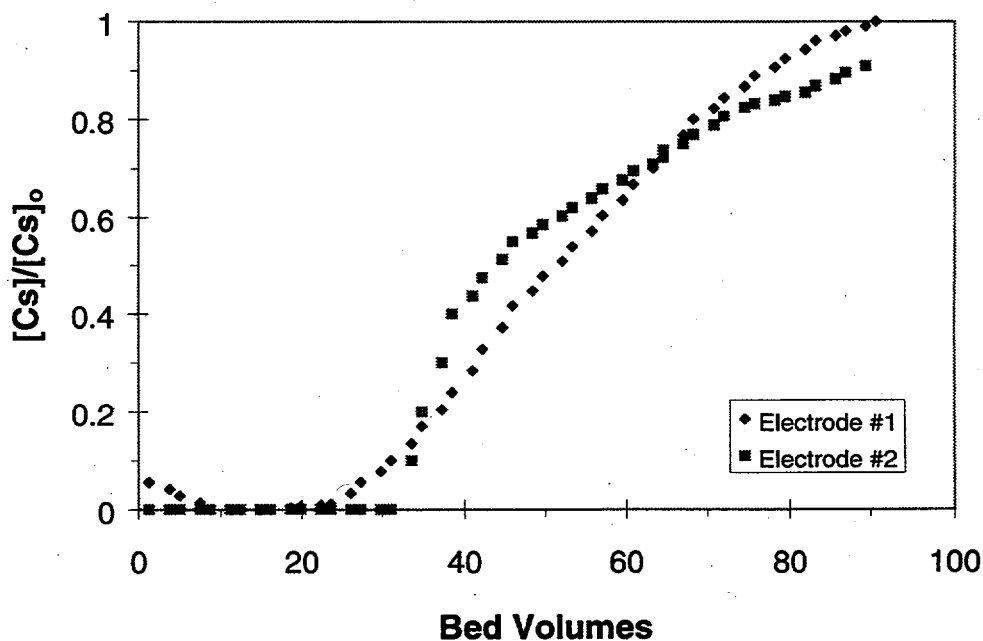


Figure 22. Consistency of Performance for Two Separate Electrodes in Flow-Through Mode ($[Cs]_0 = 0.2$ ppm; Flow Rate = 13 BV/h)

electrode experiments at the same BV/h flow rates. In the 8-electrode stack, the bed depth was 5.08 cm (2.0 in) and the l/d was 1.6. Ion exchange experiments were conducted with regenerated films $[\text{Na}_2\text{NiFe}^{\text{II}}(\text{CN})_6]$ without application of a potential. The concentration of cesium in the feed, $[\text{Cs}]_0$, was 0.2 ppm in all tests. Due to analytical detection limits, this was the lowest Cs feed concentration evaluated.

Figure 23 shows the effect of the number of electrodes in a stack in flow-through mode. The performance of the 5- and 8-electrode stacks was much better than that seen for a single electrode at about the same BV/h flow rates. For example, the best onset of breakthrough for a single electrode was 22 BV obtained at a flow rate of 13 BV/h; 50% breakthrough occurred at 50 BV under these conditions. The 5-electrode stack at a flow rate of 10 BV/h operated about four times more efficiently than the single electrode cell, with onset of breakthrough at 95 BV and 50% breakthrough at about 145 BV. Although the data are scattered, the 8-electrode stack performed the same as the 5-electrode stack; the performance of the 5-electrode cell should be representative of performance in larger cells. The longer cells presumably allow for more fully developed flow, minimizing channeling and dispersion.

The effect of flow rate on cell performance in the 5-electrode stack was determined. Figure 24 shows breakthrough as a function of flow rate. The results of two initial experiments at 10 BV/h and 30 BV/h are not shown because the experiments were only run for 76 BV and collected samples contained no detectable cesium; i.e., breakthrough was not observed. In subsequent

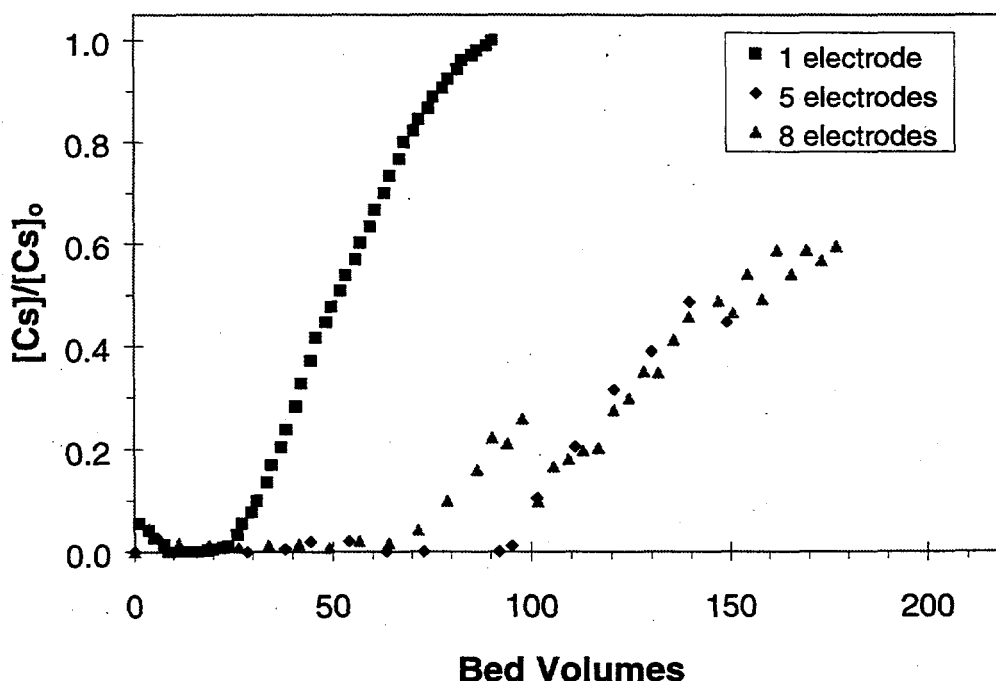


Figure 23. Effect of Number of Electrodes Used in Micro-Cell Testing in Flow-Through Mode

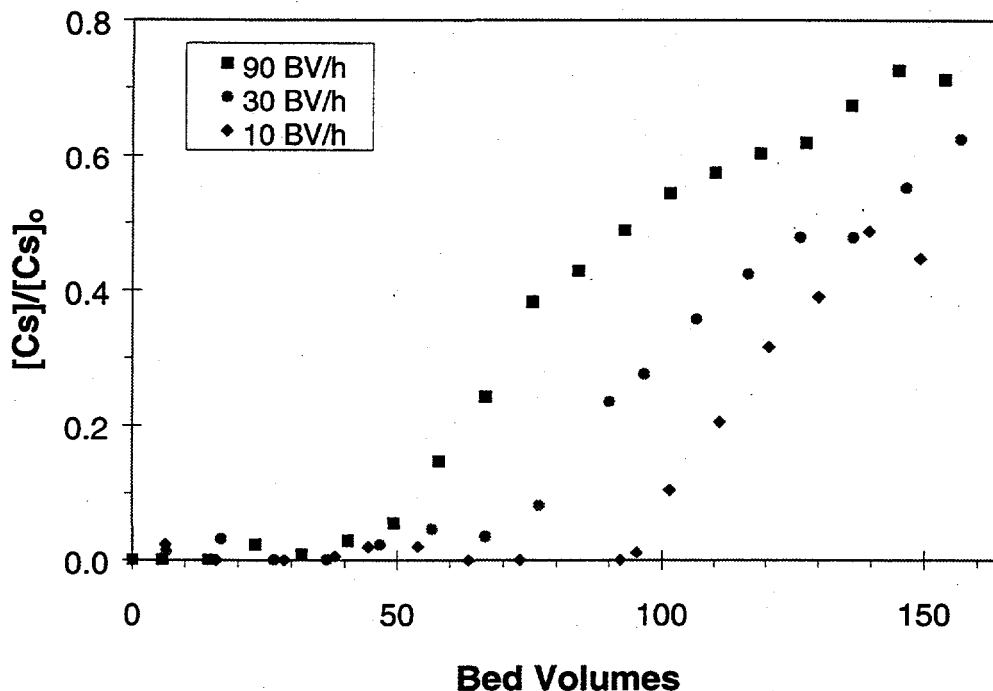


Figure 24. Effect of Flow Rate on Cesium Breakthrough in a Micro Flow Cell Containing Five Stacked Electrodes Operated in Flow-Through Mode ($[Cs]_0 = 0.2$ ppm)

experiments conducted for about 150 BV, a flow rate dependence was observed that was similar to that obtained in single-electrode experiments; higher flow rates gave faster breakthrough. At 90 BV/h (electrode Set 1), 30 BV/h (Set 2), and 10 BV/h (Set 2), onset of breakthrough occurred at about 50 BV, 70 BV, and 95 BV, respectively. Fifty percent breakthrough for 30 and 10 BV/h occurred at about 145 BV; for 90 BV/h, 50% breakthrough was at about 90 BV.

In optimization testing, a 5-electrode stack was run with packing in the void space between the electrodes to improve fluid flow through the cell. Decreased mixing should sharpen breakthrough curves, allowing more BV's of feed to be processed before the onset of breakthrough. Glass beads 4.8 mm (0.19 in) in diameter were used as packing. The gap between the electrodes was 6.4 mm (0.25 in). The void volume of the beads was 40% and the effective gap between the electrodes with packing present was 2.5 mm (0.1 in). The results of experiments conducted at a flow rate of 90 BV/h and a feed cesium concentration of 0.2 ppm are shown in Figure 25. Breakthrough with packing was the same as that without packing. The results indicate either that back-mixing with and without packing was the same or that there was no back-mixing in the cell.

In-line (continuous flow) elution of a single electrode was conducted. An electrode that had been previously loaded with cesium during an in-line flow test to remove cesium from solution

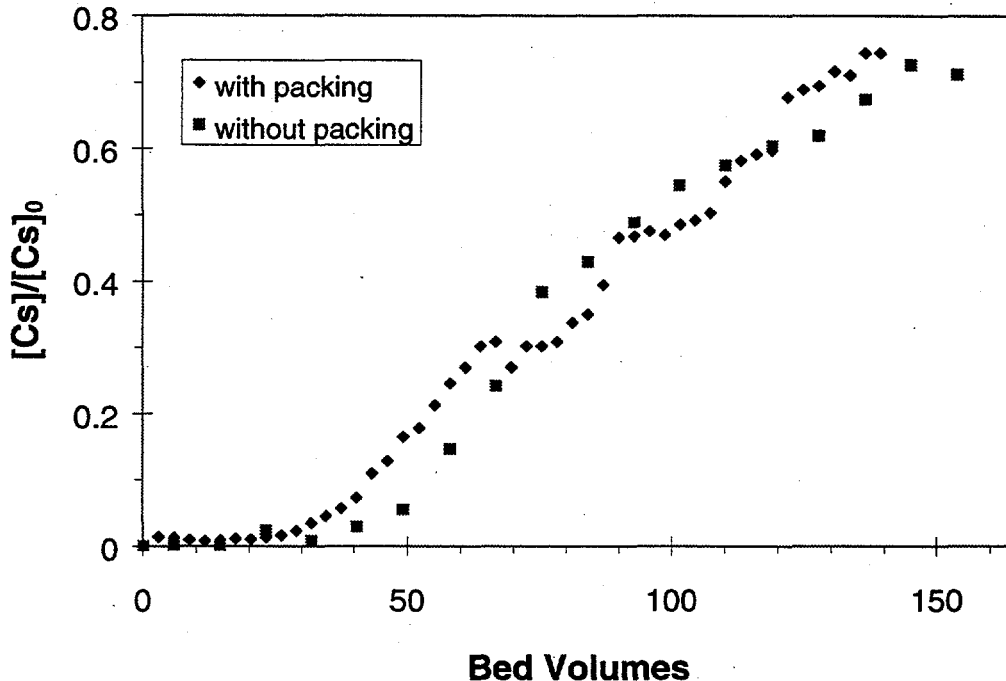


Figure 25. Effect of Filling Void Space in the 5-Electrode Micro Cell with Glass Beads as Packing

was used. The in-line elution was conducted under constant potential control with 1 M NaNO₃ in batch recycle operation. Samples were taken from the feed/product tank after 2, 5, and 10 minutes of operation at an applied potential of 0.8V (vs SCE). The tests show that cesium elution is fast via the in-line method, being essentially complete within the first 2 minutes of operation. The 2, 5, and 10 minute samples contained 0.22, 0.25, and 0.25 mg/L of cesium, respectively, by flame atomic absorption. At the completion of the in-line elution testing, the electrode was taken out of the flow cell and batch elution was conducted. No additional cesium was eluted from the electrode during the batch elution testing, indicating that all of the cesium was eluted during the in-line testing. Therefore, during in-line elution, the electrode was 88% eluted after 2 min and 100% eluted after 5 min. Comparison of previous batch elution testing of this same electrode after it had been loaded with cesium indicated that the in-line elution method was just as effective as the batch method, i.e., comparable amounts of cesium were eluted in both cases.

A stacked, integrated, ESIX system was constructed to test the efficiency of several uptake and in-line elution sequences. The system was comprised of eight ESIX electrodes and eight platinum mesh counter electrodes, stacked alternately and connected in parallel by platinum wire electrical leads. The arrangement, therefore, was an interdigitated array of high surface area

ESIX electrodes and platinum mesh electrodes. As usual, flow was bottom-up through the cell and the feed was 0.2 ppm Cs as the nitrate salt. Generally, elution was conducted under potential control by applying a potential of 0.8 V to the entire stack for 20 min while the elution solution (1 M NaNO₃) was passed through the cell in batch recycle mode. The reference electrode (SCE) was placed in the solution reservoir, at the exit (top) of the cell. Both feed and elution solutions flowed at 30 BV/h. In some cases, cyclic voltammetry (typically cycling between 0.1 and 0.8 V) was conducted on the entire stack or on individual electrodes during elution. The stack was regenerated by applying 0.1 V for 10 min while fresh 1 M NaNO₃ was recirculated through the cell. Before the stack was assembled (before Run 1), each electrode had been individually batch eluted by controlled potential coulometry and cyclic voltammetry, then regenerated in 1 M NaNO₃.

Sequential breakthrough curves for three uptake experiments are shown in Figure 26. The first uptake run started to brake through after about 30 BV. After Run 1, the entire stack was eluted by application of 0.8 V for 20 min and regenerated in 1 M NaNO₃. Breakthrough during the second run started at about 7 BV. After Run 2, both controlled potential elution and cyclic voltammetry (7 cycles) on the entire stack were conducted. Performance improved slightly in Run 3 with onset of breakthrough occurring at about 15 BV.

Better performance in Run 1 likely occurs because the film is in the fully reduced and sodium-exchanged state, i.e., the film consists of Na₂NiFe(CN)₆. In this state, it is possible to bind two cesium ions for each active site in the film. The decrease in performance for Runs 2 and 3 is consistent with several scenarios. In the first, the potential distribution in the cell is poor and

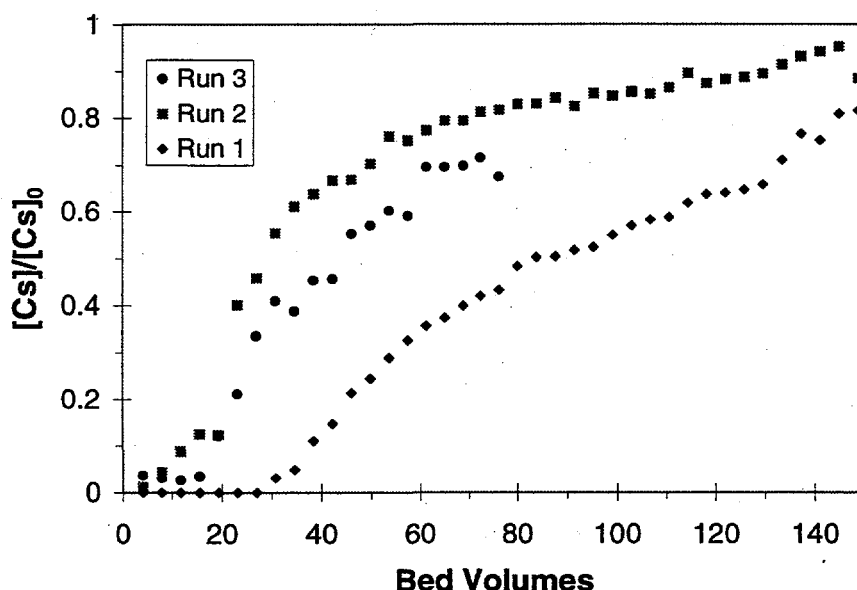


Figure 26. Consecutive Breakthrough Curves for the 8-Electrode Stack Eluted and Regenerated In-Line

only certain electrodes are properly eluted and regenerated. Capacity would decrease because only some of the electrodes participate in ion exchange. In the second scenario, the potential distribution is good and the entire stack is regenerated, but only one cesium per active site is removed. Regeneration would form $\text{NaCsNiFe}(\text{CN})_6$, which can only remove one cesium in the subsequent uptake. A third possibility is that cesium eluted from one electrode is absorbed by other downstream electrodes.

Further work is needed to determine which scenario is correct. In-line elution of the single electrode, in the same configuration as the electrode stack, eluted completely and quickly, suggesting there may be potential control problems. However, the measured potential drop across the stack was only on the order of 0.002 V, suggesting that uncompensated resistance in the cell was very small. On the other hand, after the first elution, the capacity dropped to about half, possibly consistent with the presence of $\text{NaCsNiFe}(\text{CN})_6$ in the film. Seven cyclic voltammetric cycles in addition to the potential step elution improved performance, suggesting that more cesium was replaced by sodium during cycling.

The in-line elution method needs to be optimized. However, the performance of the cell is still adequate for most applications, such as KE Basin water maintenance. Further discussion of system performance and impacts on costs and waste generation for a KE Basin application are presented in Section 5.1.

3.3 MP Results Using a Single Electrode

Experiments were conducted to investigate the performance of hexacyanoferrate-coated nickel foam electrodes in flow-by mode. The Electrosynthesis Co., Inc., conducted these experiments in a commercial MP cell, using a 10 cm x 10 cm x 0.64 cm electrode, and investigated the effects of cesium concentration and flow rate on cesium uptake. *In situ* regeneration of the ESIX electrode was also studied. Their results are summarized here and reported in Appendix B.

Figure 27 shows plots of $[\text{Cs}]/[\text{Cs}]_0$ versus bed volumes of feed cesium solution for four cesium concentrations; Table 3 summarizes these data. All of these experiments were carried out using foams with similar loadings of $\text{Na}_2\text{NiFe}(\text{CN})_6$ (equivalent to 10 to 15 mg cesium per electrode) as determined voltammetrically. In all cases, breakthrough occurred when approximately 10% of the cations in the film had been exchanged. The foam continued to exchange cesium after breakthrough, but the observed $[\text{Cs}]/[\text{Cs}]_0$ increased rapidly; typically, the exchange reached 20% to 30% before experiments were discontinued. It can be seen that, in this situation, the performance is very dependent on cesium concentration and the foam performance improves substantially as the concentration is decreased.

Several experiments were carried out with a cesium concentration of 0.2 ppm to study the effects of flow rate and film reproducibility. The results are summarized in Table 4. The effect of flow

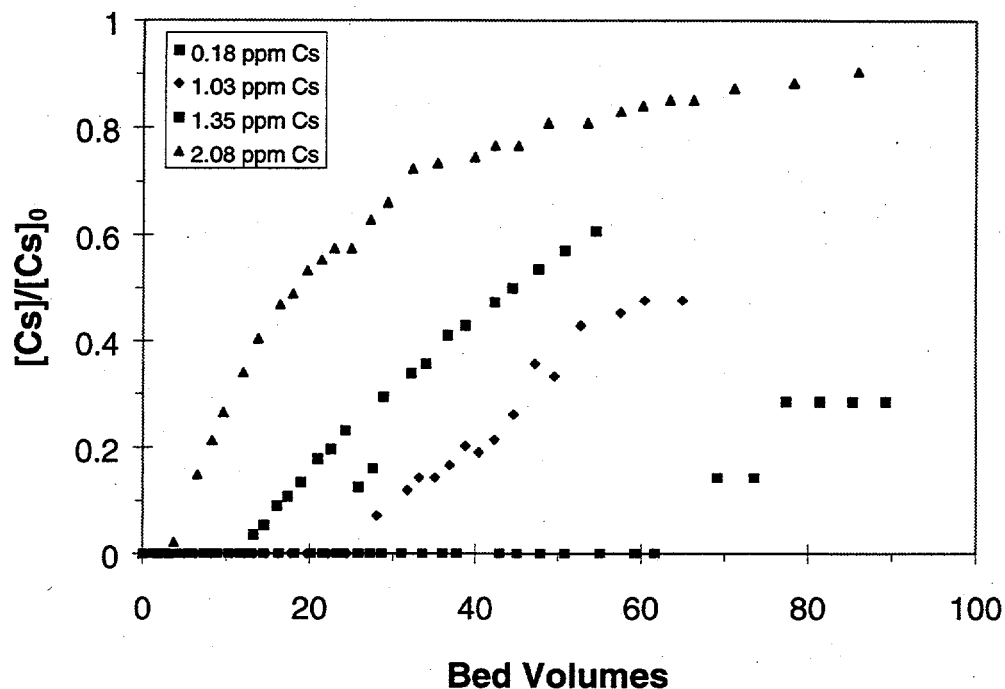


Figure 27. Effect of Feed Cesium Concentration on Cesium Breakthrough in an MP Cell Containing a Single Electrode Operated in Flow-by Mode

Table 3. Performance of 60 ppi Nickel Foam Electrodes in Flow-by Mode as a Function of Feed Cesium Concentration

$[Cs]_0$ (ppm)	Capacity [ⓐ] (mg Cs)	Flow Rate (BV/h)	Bed volumes to $[Cs]/[Cs]_0 = 0.1$	Fractional loading at $[Cs]/[Cs]_0 = 0.1$
2.0	10	11.3	6	0.08
1.35	14.4	8.6	17	0.10
1.03	15	8.2	27	0.12
0.18	13.8	8.5	65	0.06

ⓐ Maximum film capacity based on voltammetry.

Table 4. Reproducibility and Flow Rate Dependence of Nickel Foam Electrodes in Flow-by Mode ($[Cs]_0 = 0.2$ ppm)

<u>Porosity (ppi)</u>	<u>Capacity^① (mg Cs)</u>	<u>Flow Rate (BV/h)</u>	<u>Bed Volumes to [Cs]/[Cs]₀ = 0.1</u>	<u>Fractional Loading at [Cs]/[Cs]₀ = 0.1</u>
60	13.8	8.5	65	0.06
	11.6	14.9	90	0.09
	13.8	18	110	0.10
	13.8	22.7	100	0.09
80	4.4	8.5	38	0.09
	16.7	8.2	100	0.07
	^② 16.7	8.7	80	0.07
	^② 16.7	8.7	120	0.10
	^② 16.7	22.6	80	0.06
	^② 16.7	8.8	80	0.06

① Maximum film capacity based on voltammetry.

② Capacity of original film; capacity not measured after *in situ* regeneration.

rate in the MP cell is not obvious from these experiments (60 ppi electrode). No clear trend relating flow rate and breakthrough was observed.

Generally, the experiments conducted with the 80-ppi electrode were carried out under similar conditions, and results show good reproducibility. It is clear, however, that a large change in film capacity does influence electrode performance. In the experiment with a thin film equivalent to only 4.4 mg of cesium, breakthrough occurred at a much lower solution volume compared with films of higher capacity (Table 4). Regardless of total capacity, breakthrough occurred at very similar values of fractional ion exchange.

The *in situ* elution of cesium from films on the nickel foam electrode by anodic oxidation was studied (Eq. 2). Since the thermodynamics of binding of the cesium within the layer are more favorable than those for sodium, removal of the cesium by application of a potential step (as opposed to repeated potential cycling) is most likely to occur locally, within the layer, where the fraction of cesium is high. As noted earlier, this will be the case close to the inlet to the foam and through the foam as more complete exchange is carried out during loading. During removal,

some of the cesium could exchange back onto the film as the elution solution passes further down the foam toward the exit.

Four experiments were carried out where an 80-ppi nickel foam ESIX electrode (initial cesium capacity equivalent to 16.7 mg) was loaded to an extent of 15% to 20% with cesium, using a solution containing 0.2 ppm cesium. These experiments correspond to the last four shown in Table 4. The cesium-loaded foam was then oxidized using a constant current of 5 mA while passing a solution of 0.1 M NaNO₃ (300 mL) through the foam at a flow rate of 1 mL/s. The eluant was about 3 ppm in cesium, and the total recoveries of cesium were between 60% and 80%. The bed performance for cesium uptake was not greatly altered after each regeneration cycle, as indicated by the consistent breakthrough and fractional loading data in Table 4.

These experiments were all conducted with a current of 5 mA, a very low current density. The low current was employed in these preliminary experiments to avoid possible competing electrode reactions such as oxygen evolution. However, the voltammetric response suggests it would be possible to discharge most of the cesium at a much higher rate, speeding regeneration, giving a higher cesium concentration in the eluant, and affording a higher concentration factor.

4.0 Modeling of Micro Flow Cell and MP Cell Data

With the Micro Flow cell and MP cell data presented above as a basis, the expected performance of ESIX to treat wastes can be estimated using the following expression developed for conventional ion exchange (Hiester and Vermeulen 1952; Thomas 1944).

$$\frac{c}{c_0} = \frac{J(RS, T)}{J(RS, T) + e^{(R-1)(T-S)} [1 - J(S, RT)]} \quad (4)$$

where $S = \frac{\kappa a V \epsilon}{Q}$ is the column capacity parameter, $T = \frac{\kappa a (Qt - V \epsilon)}{D_G Q}$ is the solution capacity parameter, $D_G = \frac{q_M}{c_0 \epsilon}$ is the column distribution ratio, $R = \frac{1}{K}$ and $K = \frac{(c_0 - c)q}{c(q_M - q)}$ is the

equilibrium constant, c_0 is the Cs concentration at the inlet, q_M is the maximum concentration of exchangeable ions in the solid matrix, c is the Cs concentration in solution, q is the concentration of Cs in the solid matrix, ϵ is the porosity of the solid matrix, κa is the overall mass transfer coefficient, V is the reactor volume, t is time, and Q is the solution flow rate. The function J is the zeroth order Bessel function for a purely imaginary argument,

$$J(x, y) = 1 - \int_0^x e^{-y-\xi} I_0(2\sqrt{y\xi}) d\xi \quad (5)$$

For the limiting condition where the film is very selective for Cs (or equivalently, $K \rightarrow \infty$), which is the case here as shown earlier with the batch results, the expression above simplifies to Eq. 6:

$$\frac{c}{c_0} = \frac{1}{1 + e^{S-T} (1 - e^{-S})} \quad (6)$$

From the definitions of S and T above, the only free parameters are κa and q_M . V , ε , Q , and c_0 are all fixed at the outset. To verify the applicability of the expression above in describing the ESIX system, two sets of comparisons were carried out: 1) verify that velocity scales appropriately and 2) verify that concentration scales correctly.

To verify the velocity scaling, experimental data for the three flow rates collected using the 5-stack configuration were used. The results from the 5-stack configuration are preferred over the results obtained using the single-stack configuration since the 5-stack configuration resembles conventional ion exchange systems more closely and entrance effects and dispersion are less pronounced for the longer bed depth.

The two free parameters, κa and q_M , were determined by fitting Eq. 6 to one experimental set. Once these parameters were determined, Eq. 6 was used to predict the breakthrough curves for conditions used in the other experimental sets. The results are shown in Figure 28, where the data obtained at 10 BV/h were used to determine the parameters. The results clearly show that the model does not describe the experimental data very well; specifically, the model predicts immediate breakthrough for both 30 and 90 BV/h flow rates. It should be noted, however, that in using the parameters obtained from fitting the data at 10 BV/h to estimate the breakthrough curves for flow rates of 30 BV/h and 90 BV/h, both κa and q_M were assumed to be independent of the flow rate. While q_M is not expected to depend on the flow rate, κa contains the mass transfer coefficient of the liquid side, which depends on the flow rate. In particular, the mass transfer coefficient in the liquid side has been reported to scale with the superficial velocity (v) raised to the power of 0.39, 0.61 (Montillet et al. 1994), and 0.7 (Brown et al. 1994). Mass transport coefficients calculated in this work were found to scale with superficial velocity raised to the power of 0.58, which is in good agreement with the literature.

Scaling the mass transfer coefficient with the superficial velocity yielded slightly better agreement between the model and the experimental results, as shown in Figures 29 ($\kappa a \propto v^{0.39}$), 30 ($\kappa a \propto v^{0.61}$), and 31 ($\kappa a \propto v^{0.70}$). The two main conclusions are 1) a conventional ion exchange model describes the process reasonably well, and 2) mass transfer resistance in the liquid side cannot be dismissed *a priori*. The agreement is still not completely accurate for all flow rates, possibly because q_M was assumed to be constant in the modeling, but appears to vary

in the experimental data. The discrepancies seen between the model and the experimental results are also likely due at least in part to using a second set of electrodes at the fastest flow rate, as well as to dispersion and channeling effects. While channeling and dispersion effects seem to play a role in the 5-electrode stack, the effects were apparently larger in the single electrode stack since modeling results could not be extrapolated as accurately to other flow rates. We are currently studying these effects further. (It should be noted that the choice of which data set is used to determine the parameters is arbitrary, and if another data set is chosen, the results are qualitatively similar to those shown in Figures 28 through 31.)

To investigate the scaling of inlet concentration, three sets of concentration dependence data from MP cell testing were used (Table 3, $[Cs]_0 = 0.18, 1.03, \text{ and } 1.35 \text{ ppm}$). These sets were chosen simply because they had similar experimental conditions with the exception of the inlet concentration. The 1.03 ppm data were used to determine the parameters as before, and they, in turn, were used to calculate the expected breakthrough curves for the other two data sets. The results are shown in Figure 32. It can be seen that the model predicts the inlet concentration effects qualitatively.

These initial modeling efforts provide a basis for system scale-up and extrapolation of ESIX performance in treating wastes, including KE Basin water, which is discussed in Section 5.1. Additional model development and experimental testing to eliminate dispersion and channeling effects are necessary to fully understand the ESIX system.

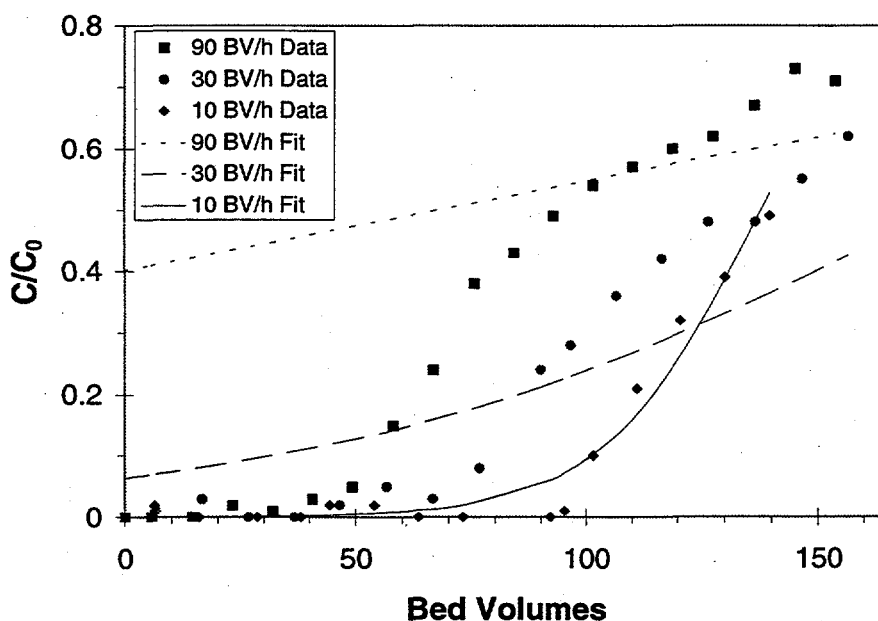


Figure 28. Model Fit to Breakthrough Data for $[Cs]_0 = 0.2 \text{ ppm}$ and Flow Rate = 10, 30, and 90 BV/h in Flow-Through Mode for 5-Electrode Stack. Model Calculated for κa and q_M Independent of Flow Rate

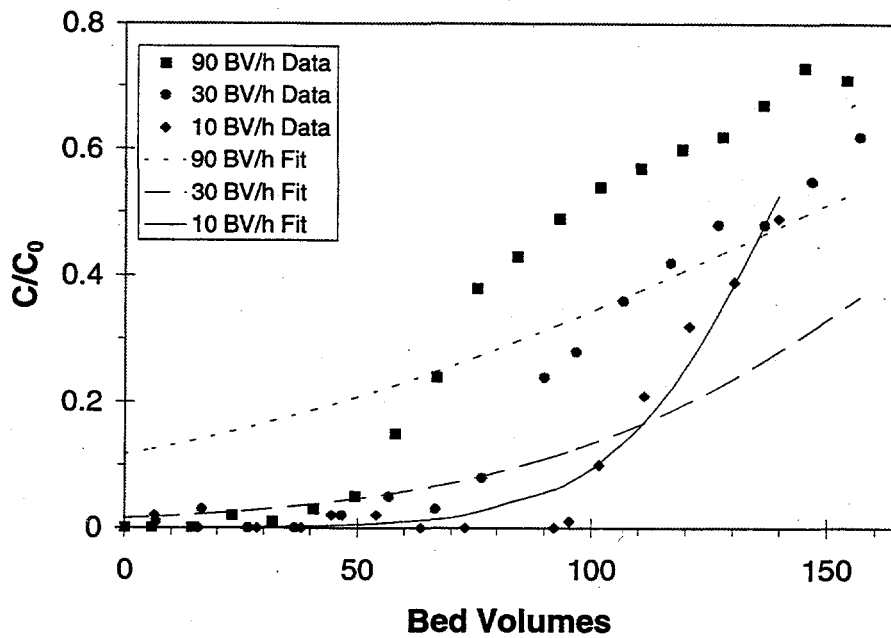


Figure 29. Model Fit to Breakthrough Data for $[Cs]_0 = 0.2$ ppm and Flow Rate = 10, 30, and 90 BV/h in Flow-Through Mode for 5-Electrode Stack. Model Calculated for $\kappa a \propto v^{0.39}$

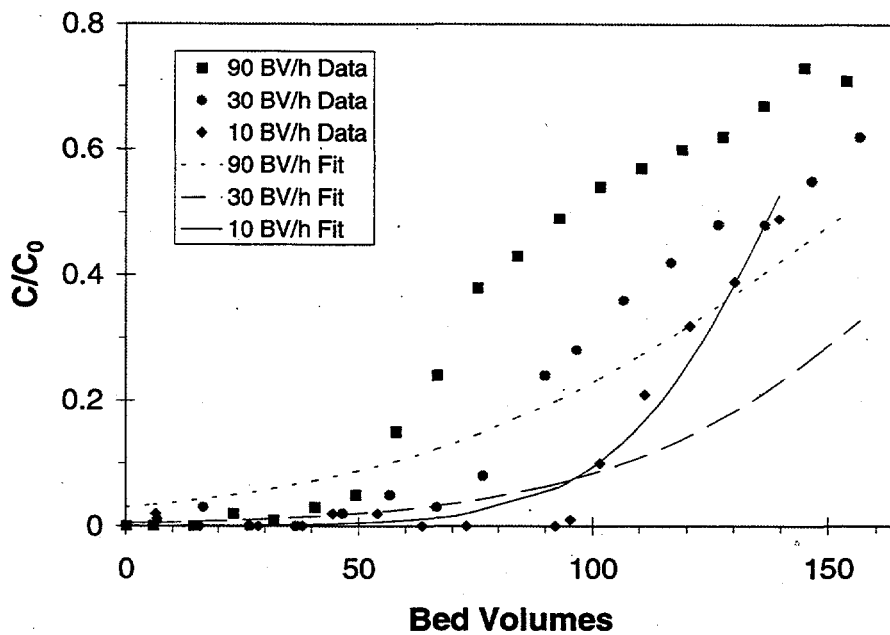


Figure 30. Model Fit to Breakthrough Data for $[Cs]_0 = 0.2$ ppm and Flow Rate = 10, 30, and 90 BV/h in Flow-Through Mode for 5-Electrode Stack. Model Calculated for $\kappa a \propto v^{0.61}$

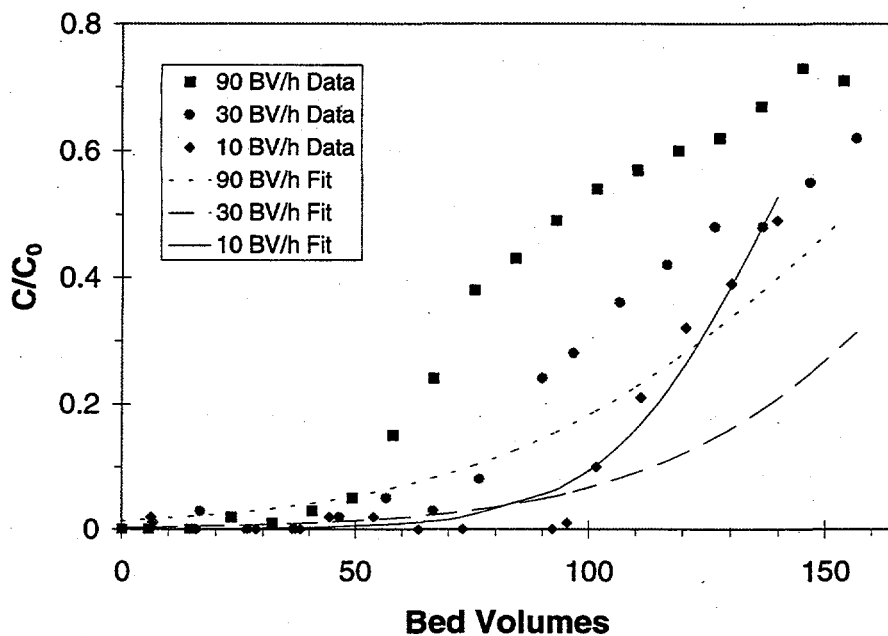


Figure 31. Model Fit to Breakthrough Data for $[Cs]_0 = 0.2$ ppm and Flow Rate = 10, 30, and 90 BV/h in Flow-Through Mode for 5-Electrode Stack. Model Calculated for $Ka \propto v^{0.7}$

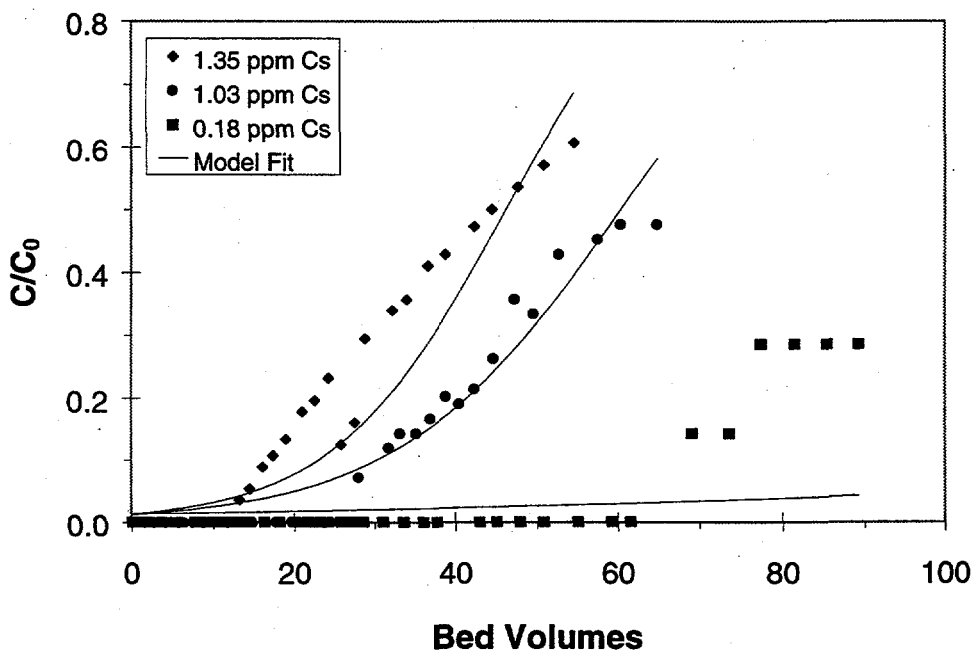


Figure 32. Model Fit to Breakthrough Data for Flow Rate = 8.5 BV/h and $[Cs]_0 = 0.18, 1.03,$ and 1.35 ppm in Flow-by Mode for a Single Electrode

5.0 ESIX Case Studies and Cost Comparison

Case studies for cesium removal from spent fuel storage basins, such as Hanford's K Basin, and for strontium removal from ground water, such as at Hanford's 100N area, are presented. In addition, a cost comparison of ESIX and Empore™ is conducted for remediation of a Chicago Pile 5 storage basin.

5.1 ESIX Case Study for Cesium Removal From KE Basin

Results are presented here for a case study for cesium removal from KE Basin. The case study shows considerable savings in capital expenditures, as well as decreased costs for secondary waste disposal. While estimates are based on KE Basin, results are expected to also be comparable to the cost savings and reduced secondary waste volumes attainable for other waste feeds when conventional ion exchange is used to remove cesium.

5.1.1 Bases and Assumptions

Experimental data from the Micro Flow cell tests, conducted by PNNL, were used to predict the breakthrough characteristics for KE Basin feeds. A model was used to fit breakthrough data obtained during the Micro Flow cell testing in both the single and stacked electrode configurations. The results are plotted in Figure 33. Model parameters were then applied to the range of concentrations of cesium encountered in KE Basin ($10^{-7} M$ near the bottom, and $10^{-10} M$ near the top), assuming the same flow rate (BV/h) would be used in the scaled-up system. Figure 34 shows the predicted column performance using both the single and stacked electrode data as a basis. For the 5-electrode stack configuration, 50% breakthrough is expected to occur after 3×10^3 to 3×10^6 BV for the highest and lowest concentrations, respectively. Since the 5-electrode stack testing showed marked improvement over the single electrode testing, and since the stacked electrode configuration is more representative of the configuration of a scaled-up system, the modeling results obtained from the 5-electrode stacked testing were used to predict the performance of a scaled-up system.

The modeling results obtained from the Micro Flow stacked cell tests were combined with conservative (worst-case) design baseline parameters for film deposition, film regeneration, cesium loading, and cesium elution, most of which were based on experimental results. The engineering bases were that the electroactive film would be deposited after every 1500 load/unload cycles; film regeneration would take 10 min (or less) with an applied potential of 0.1 V (SCE); the nominal film capacity is 1.7×10^{-9} moles Cs/cm² electrode surface area; loading would be carried out by ion exchange without application of a potential; elution would take 10 min at an applied potential of 0.8 V; the average concentration of the waste stream is $1 \times 10^{-9} M$ Cs (slightly higher than the cesium concentration currently being processed); a flow

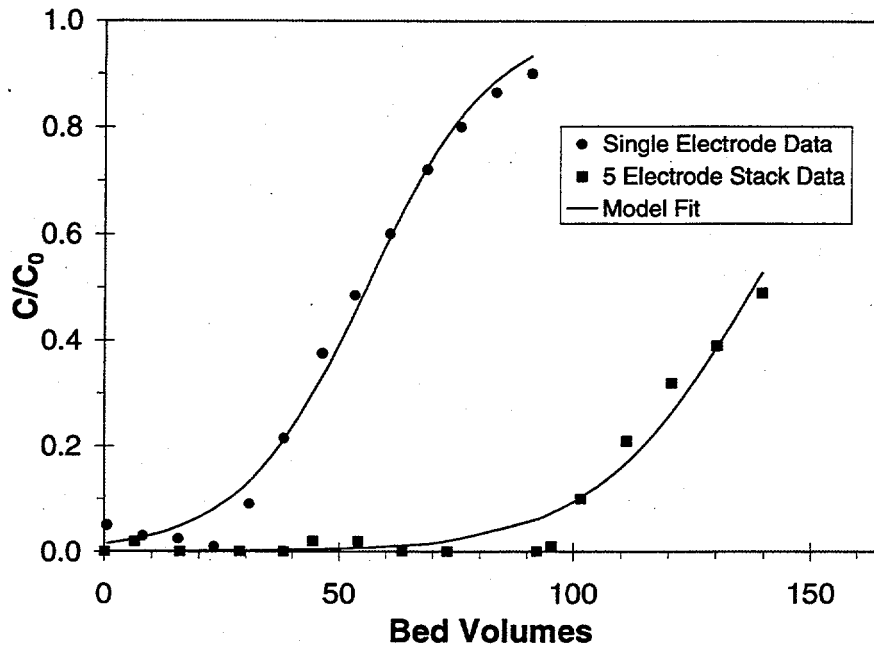


Figure 33. Model Fit to Breakthrough Data for $[Cs]_0 = 0.2$ ppm and Flow Rate = 10 BV/h in Flow-Through Mode for Single and Stacked Electrodes

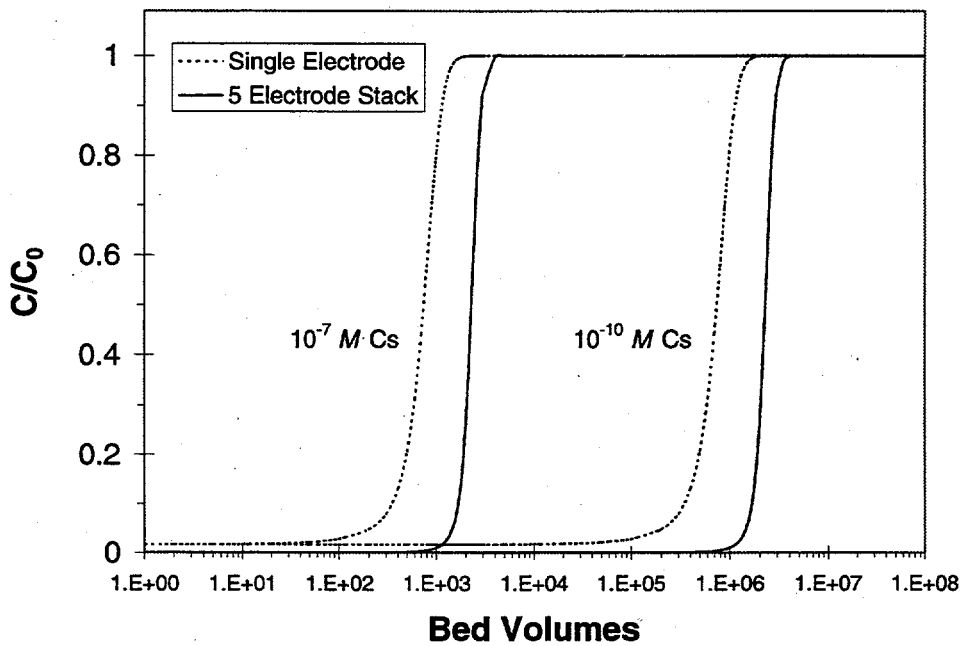


Figure 34. Predicted Breakthrough for ESIX Treatment of KE Basin Water at 10 BV/h for Feeds of 10^{-7} and 10^{-10} M Cs

rate of 400 L/min is required; cesium would be eluted just before the predicted onset of breakthrough rather than 50% breakthrough, and the solution used to rinse after each elution would be reused 10 times before disposal.

For this case study of KE Basin processing, the ESIX system would be used in semi-continuous batch recycle mode, as shown in Figure 35. This same mode of operation is currently conducted via conventional ion exchange to minimize worker exposure to cesium by maintaining a low "steady state" cesium concentration in the basin. Basin water would be passed through the ESIX column until the onset of breakthrough. When the column reaches capacity, the feed to the system is stopped. Cesium is then eluted into an elution solution, which is pumped through the system from a holding tank. For this analysis, it was assumed that the elution solution would be reused for 10 elution cycles before disposal. A wash solution, needed to remove residual cesium for improved process efficiency, would be reused 10 times before disposal. The elution solution is periodically transferred from the holding tank to the final waste form.

There are several modifications that could be made for the KE Basin or other related applications, but these were not explored in this case study. For example, the system could also be used in single-pass operation for final water decontamination or in applications in which batch recycle is not desired or feasible. A second ESIX column could be installed to allow for continuous operation by appropriate switching of valves. One column would undergo regeneration while the other would continue to take up cesium. In the case study it is assumed that the elution solution will be used 10 times before disposal, but the number of times it is reused in practice depends on the final desired concentration. The elution solution could be reused less often or until a limiting (i.e., heat load, radiation constraints, solubility, etc.) final cesium concentration is reached. The wash solution could be used once, then disposed, or it could be kept separate, reused until a

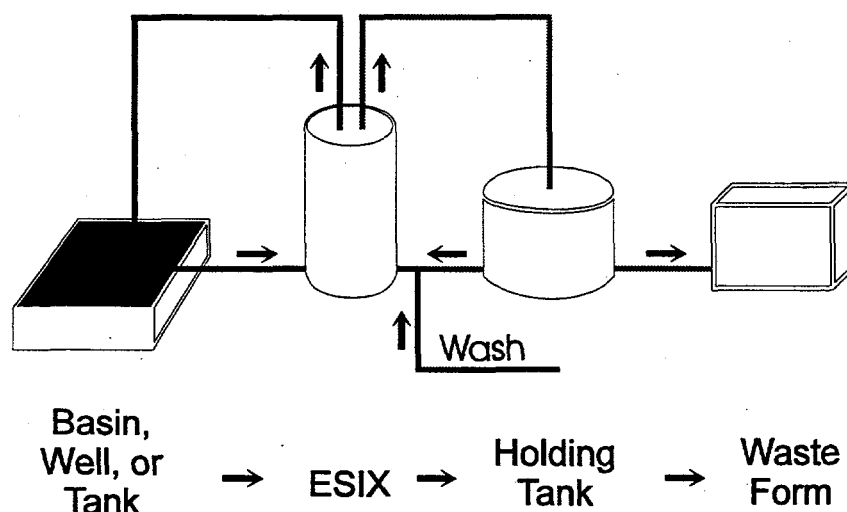


Figure 35. Flow Diagram for Waste Decontamination with ESIX

threshold concentration is reached, and used later as the next elution solution. This last option would further reduce the amount of waste generated.

5.1.2 Process Concept and Estimated Costs

Configurations for three different process flow rates (BV/h) were evaluated given the above bases and flow diagram. Flow rates up to 90 BV/h can be used without detrimental impact on system performance because regeneration is fast and easy. Faster breakthrough at the higher flow rates can be tolerated because the system is easily regenerated and eluted into a single column volume. In general, faster process flow rates allow for construction of smaller systems with investment of less capital. For this evaluation, it is assumed that commercially available electrochemical cells will be used to construct the system. However, in Section 1.9 it is shown that capital costs can be significantly decreased further by constructing purpose-built cells.

Results of the evaluation are summarized in Table 5. Cases Prod Cell A and Prod Cell B show that increasing the flow rate from 10 to 60 BV/h reduces the size of the system and decreases the capital cost by a factor of about 6. The dimensions of Prod Cell B (3.3 x 2.1 ft) give a low l/d of 1.6 that would be considered non-standard for ion exchange applications, but the design is well supported by the experimental results. For the three cases, the amount of waste generated increases with increasing flow rate because column regeneration becomes more frequent, but the amount of waste generated for each ESIX system evaluated is still about two orders of magnitude less than that generated by the current system used at K Basin.

Table 5. Cases Compared for Cesium Removal from K-Basin

Case	Flow Rate (BV/h)	Waste Generated (m ³ /yr)	Capital Cost (\$MM)	Disposal Costs (\$MM/yr)	Column Payback (yr) ^①	Dimensions (l x w, ft)
K Basin	4 ^②	84	8.4 ^③	0.3	---	(250 ft ³) ^④
Prod Cell A	10	0.53	2.3	0.002	1.6	10 x 2 ^⑤
Prod Cell B	60	0.88	0.4	0.003	0.3	3.3 x 2.1
E-Syn Cell	90	1.1	0.67	0.004	0.5	11 x 0.7 ^⑤

① ESIX Capital Cost/(Disposal Cost Savings + IX annual cost of \$1.2MM).

② Estimated, based on 7m³ IX and 400 L/min flow rate.

③ Based on replacement of IX on monthly basis for 7 years, at a cost of \$100,000/IX).

④ Includes shielding.

⑤ Two columns, each with given dimensions.

The E-Syn Cell design is considered the preferred ESIX system of those evaluated because of the larger l/d. This system would consist of 52 Electrosyn modules, each containing 20 ESIX electrodes (60 ppi nickel foam) with an associated mesh counter electrode. Electrosyn modules would be arranged in two parallel series of 26 each with an l/d of 16. The electrode volume in each Electrosyn module would be approximately 0.005 m^3 , and the surface area would be 20 m^2 . The total ESIX system working electrode volume would be approximately 0.3 m^3 .

With the E-Syn Cell design, 40,000 BV of waste would be processed before elution of the ESIX system is required. This corresponds to approximately 1×10^7 liters of waste processed and 19 days processing time for each load cycle. Over 7 years of continuous operation (assumed KE Basin baseline), approximately 140 load/elution cycles would be required; thus, film redeposition would not be required.

An "order of magnitude" capital cost of \$0.67 MM is estimated for the 52 Electrosyn modules. Each module (containing the 20 ESIX electrodes and mesh counter electrodes) would cost on the order of \$13,000 each. This estimate only includes the Electrosyn modules and electrodes, which are anticipated to be the major equipment costs associated with the system. Costs associated with radiological applications are not included in this "order of magnitude" estimate.

In-line elution results suggest the possibility that the effective capacity of the column may be about half that seen previously and used in the above analysis. The size of the system, capital costs, and payback remain the same, but the main effect would be a doubling the amount of waste produced and the waste disposal costs. However, ESIX still offers significant waste reduction because the amount of waste produced by ESIX would be about 50 times less than that produced by the current system. The time before elution would be cut in half, elution being required about every 9 days. Therefore, while higher capacity is desirable, the lower effective capacity obtained in preliminary in-line elution testing has a minor effect on system viability and waste generation.

5.1.3 Potential Advantages of ESIX for KE Basin Application

The ESIX system could have several significant advantages over current operations. Secondary waste would be reduced at least by a factor of 76. Current processing requires disposal of ion exchangers every month. Waste from this source totals approximately 80 m^3 with a disposal cost of \$300 K/year (assuming disposal costs of $\$3600/\text{m}^3$ for LLW). Reusing the elution and rinse solutions 10 times, the ESIX system is estimated to generate 1.1 m^3 of secondary waste, costing just \$16 K/year for the same LLW disposal. Costs for ESIX could be even lower if the elution solution is used more than 10 times and if the rinse solution is reused as the next elution solution. Replacement costs of exchangers in the current system are estimated to be \$1.2 M/year. The ESIX system requires a one-time capital outlay of on the order of \$0.67 M, having a payback period of approximately 0.5 years. Labor costs and worker exposure might also be less since the

current monthly column changeout is not needed for the ESIX system. Worker exposure could also be lower with ESIX because automated or remote operations may be possible.

Another potential advantage of ESIX is that loading with TRU is not expected to be a problem. Unlike the deep-bed filtration of colloidal TRU, which plagues standard ion exchange columns, TRU is less likely to accumulate on the open pore structure of the ESIX electrodes. If a small amount of TRU hangs up on the ESIX column during loading, it still may not contaminate the cesium product during elution. Elimination of TRU in the final waste allows higher cesium loading and less waste volume.

5.2 ESIX Case Study for Strontium Removal from Groundwater at 100N

Strontium in the groundwater is a critical problem in the 100N area at Hanford. The current treatment method is pump and treat using clinoptilolite as the IX material. There are several problems with this treatment, including the low selectivity of clinoptilolite for strontium and the slow release rate of strontium from soil, which necessitates a long treatment time and the pumping of large volumes of groundwater. Suggested improvements include soil flushing and electrokinetic remediation, both of which require IX concentration of strontium. Although an ESIX material for strontium has not actually been prepared, a case study for application of ESIX to these three treatments by replacement of standard IX was investigated.

5.2.1 Bases and Assumptions

Current pump and treat conditions were used as a basis for this case study. It was assumed that an ESIX material could be prepared with at least as good a selectivity for strontium over calcium as clinoptilolite. The waste stream was assumed to contain $2 \times 10^{-13} M$ Sr-90 and that a volumetric flow rate of 230 L/min was required. For this study, a 1 year operation was assumed. As in the KE Basin case study, it was estimated that the ESIX elution and rinse solutions could be reused 10 times before disposal.

The mode of operation assumed for this case study would likely be used for pump and treat, soil flushing, and electrokinetic remediation. Water would be pumped out of the ground, processed, and reinjected as illustrated in Figure 36.

5.2.2 Process Concept and Estimated Costs

The case study investigated systems operating at 100 BV/h. Each system is viable and would produce an order of magnitude less waste than the current IX system (Table 6). Elution would be required every two days after processing 5×10^5 L of groundwater. The Prod Cell and Electrosyn Cell have the lower capital costs, but the Electrosyn Cell would likely be preferred since it has a preferable 1/d (15).

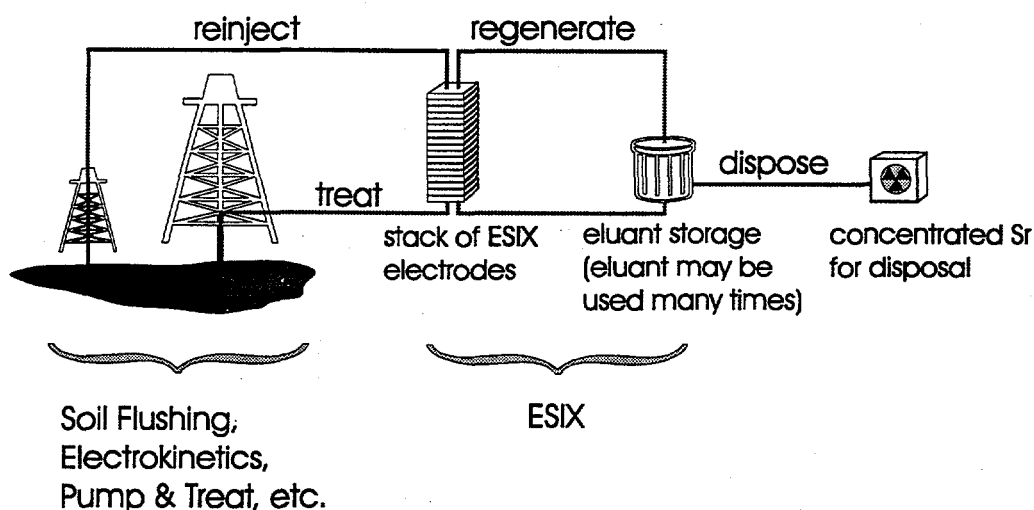


Figure 36. Application of ESIX for Strontium Removal from Groundwater

Table 6. Cases Compared for Strontium Removal from 100N

Case	Flow Rate (BV/h)	Waste Generated (m ³ /yr)	Capital Cost (\$K)	Disposal Costs (\$K/yr)	Column Payback (yr)	Dimensions (l x w, ft)
Current	2	41	---	120	---	(200 ft ³)
Prod Cell	100	6.6	128	12	1.2	1.1 x 2.1
E-Syn Cell	100	6.6	342	12	3.2	11 x 0.7
MP Cell	100	6.6	610	12	5.7	11 x 0.3 [ⓐ]

ⓐ Four columns, each 11 ft (l) x 0.3 ft (w).

5.2.3 Potential Advantages of ESIX for 100N Application

In addition to the advantages of ESIX previously discussed (Section 1.7.3), this case study points out that for ion exchange materials of equal selectivity, the ESIX system generates much less waste and allows higher BV/h flow rates than conventional ion exchange. ESIX materials with higher selectivity should be possible since regeneration is conducted electrochemically rather

than by shifting chemical equilibria with added reagents. With this stronger driving force for elution, materials with higher binding constants can be tolerated without sacrificing regenerability. As a result, materials with greater selectivity can be designed.

In the 100N application, materials that have higher selectivity or that can be regenerated easily without generation of secondary waste than clinoptilolite will be needed. ESIX has the potential to fulfill both of these requirements, allowing for the development of an improved pump and treat system or for the development of a soil flushing method. In soil flushing, a waste stream with a high calcium/strontium ratio will be generated, requiring higher selectivity for strontium than currently available. Development of ESIX materials for this application is underway.

5.3 Cost Comparison With Empore™

In September 1996, Argonne National Laboratories (ANL) provided a Large-Scale Demonstration Project (LSDP) using a 3M technology called Empore™. The LSDP objective was to select and demonstrate potentially beneficial technologies. This demonstration was completed at the ANL-East, Chicago Pile-5 research reactor (CP-5). The specific work entailed treating radioactive contaminated water, which, when treated, met regulatory criteria for the release of wastewater. The guidelines and treatment levels were derived from DOE Order 5400.5 (USDOE 1997a). The water was contaminated with radioactive isotopes consisting of cesium-137 (Cs-137) and small amounts of cobalt-60 (Co-60).

After completion of the LSDP project, a report was written and issued to the DOE in October 1997. The report, titled Empore™ Membrane Separation Technology, Innovative Technology Summary Report (USDOE 1997b), discussed the benefits of using technologies consisting of Empore™ membranes, evaporation systems, and mobile ion exchange columns. It also provided extensive detail showing that the Empore™ technology was more cost effective, while allowing for improved waste minimization.

A cost comparison of the ESIX technology and the Empore™ technology was conducted using the same criteria as defined in the Innovative Technology Summary Report for the CP-5 scenario. To provide this comparison, an ESIX system was designed to treat 24,000 gal of radioactivity-contaminated liquid containing 0.60 pCi/mL Cs-137 and 0.20 pCi/mL Co-60 at a flow rate of 0.5 gpm according to the CP-5 system requirements. The Empore™ system design and costs used in the comparison are the same as detailed in the Innovative Technology Summary Report. This study did not evaluate in detail the mobile ion exchange and evaporation technologies described within the Innovative Technology Summary Report because it has already been shown that the Empore™ technology is more applicable than these systems (USDOE 1997b). The complete cost comparison is found in Appendix D.

5.3.1 ESIX System Design

The ESIX system uses cells consisting of high surface area electrodes, derivatized with the electroactive ion exchange material, and wire mesh counter electrodes, separated and sealed with gasket material. Cells are fabricated and stacked to allow for the desired flow rates. Two standard unit sizes are anticipated for manufacturing, each handling a range of different flow rates. After the units are manufactured, they will be mounted in stacks, placed into housings, and attached together using standard pipe connections. When the system is anticipated to be used as a portable unit, it would be mounted with quick disconnects to provide for ease of installation and removal. A potentiostat controller on the side of the system would provide the necessary electrical voltage for the electrochemical process. The potentiostat is set up either for hardwiring or a receptacle plug when a portable unit is desired and could be mounted remotely when radiation levels are a factor.

The system layout used for the CP-5 scenario was based on the 0.5-gpm flow rate used by the Empore™ system. The unit size for the system was chosen to be the smaller of the two types available. Twenty units were needed to provide the required bed volume to attain the 0.5-gpm flow rate. The units would be mounted, stacked in placed within the housing, and because this application would be used only for a short duration (37 days), quick disconnects would be installed to allow for the ease of removal from the CP-5 reactor basin. On the outside face of the housing, a potentiostat would be mounted to provide the proper electrical control and wired with a standard 110-V receptacle plug.

The complete system would include a pump, two 10-gal tanks, and an ESIX system including its controller, associated piping, and valves (Figure 37). Facility modifications would include adding piping connections, installing a pump to provide the required flow, adding two small 10-gal tanks that are used for elution solution and sodium regeneration solution storage, and providing power for the system. Specifically, the intention would be to mount the system with quick disconnects and an electrical receptacle that would allow the CP-5 facility the ability to readily install and remove the system from operation. Since no mention was made in regard to radiological shielding within the Innovative Technology Summary Report (USDOE 1997b), it is assumed that no shielding is required. However, if shielding would be needed, it is assumed that temporary shielding would be used due to the small duration of treatment. The final assembly of the ESIX system would weigh approximately 75 lbs and would have a 2-ft x 2-ft x 2-ft-high footprint. The only modifications the facility would require are the installation of a pump and piping with quick disconnects, and the mounting of the 10-gal storage tanks.

Pool water would be drawn from the pool via a small proportional pump, passed through the ESIX system, and passed back to the pool to provide a recirculating action. To facilitate use, the liquid being transferred from the pump to the ESIX system and from the ESIX system to the pool could be routed with flexible hose. The ESIX system would be mounted on grating directly over

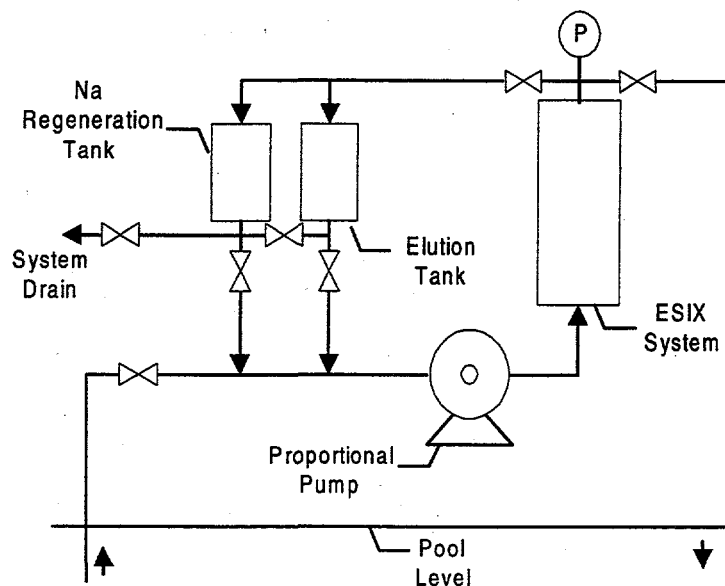


Figure 37. ESIX System Flow Schematic

the pool similar to the Empore™ system. This would allow any leaks generated from pipe connections to fall onto the grating and then back into the pool.

Based on the Cs-137 concentrations (0.60 pCi/ml), flow rates (0.5 gpm), and volume of liquid (24,000 gal) to be processed, the ESIX system would require less than two elution cycles. Currently, the ESIX elution solution can be reused up to 10 times (based on cesium concentrations) before it must be replaced. This is contingent upon Cs-137 concentrations and facility-specific dose-rate criteria. However, based on the information provided, it is anticipated that the one batch of elution solution could be used through the entire processing of the 24,000 gal. This overall elution solution would provide less than 5 gal of liquid waste at the completion of the process. Similarly, at the completion of elution, a Na regeneration would be completed, which would provide less than 5 gal of liquid waste at the completion of the process.

5.3.2 Cost Comparison

Figure 38 shows the cost comparison between the ESIX, Empore™, evaporator, and mobile ion exchange systems. The costs for the operation of the evaporator and mobile treatment systems were taken directly from the Innovative Technology Summary Report. As shown, the ESIX system is cost competitive with the Empore™ system for processing the wastewater. ESIX is projected to save approximately 40% over the Empore™ system, 43% over the mobile ion exchange system, and 71% over the evaporation system.

The procurement costs for a fully functional 0.5-gpm ESIX system is approximately \$12,477 (\$8,477 for the ESIX system and \$4,000 for a Co-60 system), while Empore™ costs are approximately \$15,772 (\$9,308 cartridge housing installation and \$6,464 cartridge costs). The cost for the ESIX system includes material procurement and assembly (costs for utility hookup are not included). This was the case because the unit is fully enclosed and mobile. The procurement costs for the Empore™ system consists of the cartridge housing purchase and installation, along with the required cartridges to complete treatment activities. The costs listed herein do not reflect the \$5,692 for three days of craft time and miscellaneous parts to provide pipe connections and power. Both systems are fully mobile units.

As indicated in Figure 38, the ESIX system is a cost-effective remediation alternative. It also reduces worker exposure while providing a wider range of flow potential. In the specific application to CP-5, the ESIX System produces slightly more waste than the Empore™ system. However, as concentrations of cesium increase and the volume of liquid processed increases, it is anticipated that the ESIX system would produce less waste because of its ability to reuse the

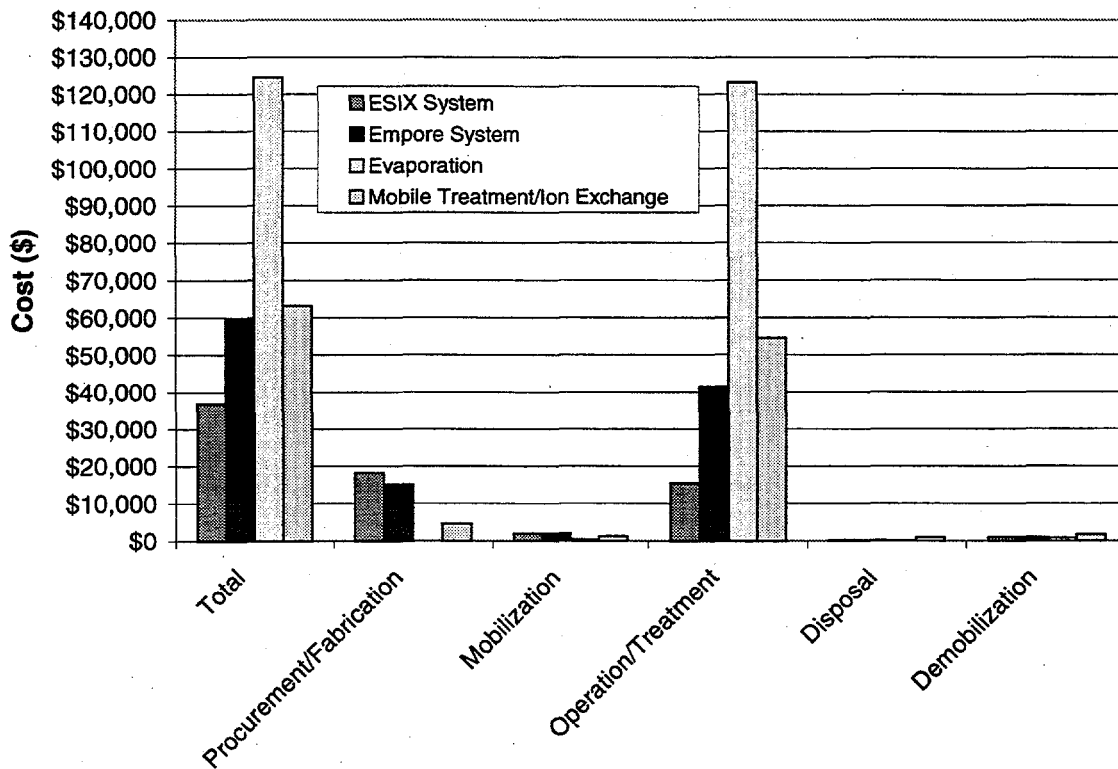


Figure 38. Cost Comparison of Four Treatment Options for Clean-up of Radioactively Contaminated Water at CP-5

elution solution. At this time, the Empore™ system is more flexible in the respect that it can be fabricated to allow for removal of more than just cesium from waste streams. Empore™ systems would likely be more cost effective when waste streams contain multiple types of radionuclides requiring removal. Development of new ESIX films for other ions would expand the applicability of the ESIX technology. However, when used specifically for cesium removal, ESIX provides a more flexible and cost-competitive system, while reducing worker exposure and secondary waste generation.

6.0 Conclusions

This research has demonstrated the viability of ESIX for metal ion separations. Ion loading and unloading are easily controlled by modulating the electrode potential and bench-scale testing has shown that cycle time and throughput are sufficient to allow ESIX to exceed the performance of standard technologies, such as conventional ion exchange. As a result, use of a regenerable material and the minimization of secondary waste are significant advantages in favor of the ESIX process.

Metal hexacyanoferrate films are relatively easy to prepare, but modifications to the reported procedures can generate films with significantly improved capacity and stability. The best films prepared to date have almost twice the capacity of previously reported films and they are durable. High surface area electrodes lose less than 20% of their capacity after 1500 cycles. Experimental results support the viability of once-through or batch recycle waste processing with ESIX for cesium removal. Electroactive films on high surface area electrodes are stable to solution flow; have high selectivity for cesium in the presence of at least 2×10^4 molar excess of sodium ion; can be efficiently eluted in-line; and have sufficient capacity to support a cesium separation process. Results from bench-scale experiments for single electrodes ($l/d = 0.3$) and 5-electrode stacks in the flow-through configuration ($l/d = 1.0$) show that the stacked configuration has significantly improved breakthrough characteristics. This is presumably because the larger l/d values allow for more fully developed flow, minimizing channeling and dispersion.

A concept for an economical remediation system has been devised and presented using design baseline parameters derived from current processing knowledge and experimental results. A case study for continuous processing of KE Basin wastewater shows the potential for significant reduction of secondary wastes and associated disposal costs, and decreased capital and labor expenditures. Other processing improvements with ESIX include less likelihood of TRU contamination; decreased worker exposure because of less contact with exchangers and process hardware; and production of a concentrated cesium product containing a minimal amount of sodium, which would be compatible with a wider variety of final waste forms.

A cost comparison conducted by Parsons Infrastructure and Technology Group, Inc. found that ESIX was competitive with an Empore™ system field-tested at Chicago Pile 5 (CP-5). For a

0.5-gpm system treating 24,000 gal of wastewater at CP-5, ESIX was projected to save approximately 40% over the Empore™ system, 43% over a mobile ion exchange system, and 71% over an evaporation system. In the specific application to CP-5, where the volume of waste water to be treated is relatively small, the ESIX System produces slightly more waste than the Empore™ system. However, as concentrations of cesium increase and the volume of liquid processed increases, it is anticipated that the ESIX system would produce less waste because of its ability to reuse the elution solution.

7.0 Publications, Reports, and Patent Applications

Publications

S. D. Rassat, R. J. Orth, J. P. H. Sukamto, M. A. Lilga, and R. T. Hallen. "Development of an Electrically Switched Ion Exchange Process for Selective Ion Separations," *Separations and Purification Technology*, accepted for publication.

N. J. Hess, J. P. H. Sukamto, S. D. Rassat, R. T. Hallen, R. J. Orth, M. A. Lilga, and W. E. Lawrence. 1997. "Characterization of Electroactive Cs Ion-Exchange Materials using XAS," *Mat. Res. Soc. Symp. Proc.*, 465, 813-818.

M. A. Lilga, R. J. Orth, J.P.H. Sukamto, S. M. Haight, and D. T. Schwartz. 1997. "Metal Ion Separations Using Electrically Switched Ion Exchange," *Separations and Purification Technology*, 11, 147-158.

S. M. Haight, D. T. Schwartz, and M. A. Lilga. "In Situ Oxidation State Profiling of Nickel Hexacyanoferrate Derivatized Electrodes using Line-Imaging Raman Spectroscopy: I. Multivariate Calibration," in preparation.

S.M. Haight, J.A. Bowman, D.T. Schwartz, and M.A. Lilga. "In Situ Oxidation State Profiling of Nickel Hexacyanoferrate Derivatized Electrodes using Line-Imaging Raman Spectroscopy: II. Cycle Life Degradation," in preparation.

Reports

Lilga, M. A., R. J. Orth, J. P. H. Sukamto, S. D. Rassat, J. D. Genders, and R. Gopal. 1997. "Electrically Switched Cesium Ion Exchange. FY 1997 Final Report," PNL-11766, Pacific Northwest Laboratory, Richland, Washington.

M. A. Lilga, R. J. Orth, J.P.H. Sukamto, D. T. Schwartz, S. M. Haight, and J. D. Genders. 1997. "Electrically Switched Cesium Ion Exchange. Target Performance, Applications, and Progress," PNNL-11567, Pacific Northwest National Laboratory, Richland, Washington.

M. A. Lilga, R. J. Orth, J.P.H. Sukamto, S. M. Haight, D. T. Schwartz, and J. D. Genders. 1996. "Electrically Switched Cesium Ion Exchange. FY 1996 Annual Report," PNNL-11441, Pacific Northwest National Laboratory, Richland, Washington.

Patent Applications

Sukamto, J. P. H. , S. D. Rassat, R. T. Hallen, R. J. Orth, and M. A. Lilga. "An Electroactive Film on a Substrate and Method of Making," patent application filed.

Sukamto, J. P. H. , S. D. Rassat, R. T. Hallen, R. J. Orth, and M. A. Lilga. "An Electroactive Film on a Porous Substrate and Method of Making," patent application filed.

8.0 References

Barton, G. B., J. L. Hepworth, Jr. E. D. McClanahan, R. L. Moore, and H. H. van Tuyl. 1958. "Chemical Processing Wastes - Recovering Fission Products." *Industrial and Engineering Chemistry* 102:212.

Bocarsly, A. B. and S. Sinha. 1982a. "Chemically Derivatized Nickel Surfaces: Synthesis of a New Class of Stable Electrode Interfaces." *Journal of the Electroanalytical Chemistry and Interfacial Electrochemistry* 137:157.

Bocarsly, A. B. and S. Sinha. 1982b. "Effects of Surface Structure on Electrode Charge Transfer Properties. Induction of Ion Selectivity at the Chemically Derivatized Interface." *Journal of the Electroanalytical Chemistry and Interfacial Electrochemistry* 140:167.

Brown, C. J., D. Pletcher, F. C. Walsh, J. K. Hammond, D. Robinson. 1994. "Studies of Three-dimensional Electrodes in the FM01-LC Laboratory Electrolyzer." *J. Applied Electrochem.* 24:95.

Haight, S. M. and D. T. Schwartz. 1995. "In situ Imaging Raman Spectroscopy of Electrochemically-deposited CuSCN." *Journal of the Electrochemical Society* 142:L156.

Harjula, R., J. Lehto, E. H. Tusa, and A. Paavola. 1994. "Industrial Scale Removal of Cesium with Hexacyanoferrate Exchanger - Process Development." *Nuclear Technology* 107:272.

Hiester, N. K., and T. Vermeulen. 1952. "Saturation Performance of Ion-Exchange and Adsorption Columns." *Chemical Engineering Progress* 48:505.

- Humphrey, B. D., S. Sinha, and A. B. Bocarsly. 1984. "Diffuse Reflectance Spectroelectrochemistry as a Probe of the Chemically Derivatized Electrode Interface. The Derivatized Nickel Electrode." *Journal of Physical Chemistry* 88:736.
- Lehto J. and R. Harjula. 1987. "Separation of Cesium from Nuclear Waste Solutions with Hexacyanoferrate(II)s and Ammonium Phosphomolybdate." *Solvent Extraction and Ion Exchange* 5:343.
- Lilga, M. A., R. T. Hallen, E. V. Alderson, M. O. Hogan, T. L. Hubler, G. L. Jones, D. J. Kowalski, M. R. Lumetta, W. F. Riernath, R. A. Romine, G. F. Schiefelbein, and M. R. Telander. 1996. Ferrocyanide Safety Project. Ferrocyanide Aging Studies Final Report, PNNL-11211, Pacific Northwest National Laboratory, Richland, Washington.
- Loewenschuss, H. 1982. "Metal-Ferrocyanide Complexes for the Decontamination of Cesium from Aqueous Radioactive Waste." *Radioactive Waste Management* 2:327.
- Loos-Neskovic, C. and M. Fedoroff. 1989. "Decontamination of Liquid Nuclear Wastes by Fixation of Radioactive Elements on Nickel and Zinc Ferrocyanides." *Radioactive Waste Management and the Nuclear Fuel Cycle* 11:347.
- Loos-Neskovic, C., M. Fedoroff, E. Garnier, and P. Gravereau. 1984. "Zinc and Nickel Ferrocyanides: Preparation, Composition, and Structure." *Talanta* 31:1133.
- Montillet, A., J. Legrand, J. Comiti, M. M. Letord, and J. M. Jud. 1994. "Using of Metallic Foams in Electrochemical Reactors of Filter-Press Type: Mass Transfer and Flow Visualisation." in *Electrochemical Engineering and Energy*, F. Lapique, A. Storck, and A. A. Wragg, Eds. Plenum Press, New York.
- Sinha, S., B. D. Humphrey, and A. B. Bocarsly. 1984. "Reaction of Nickel Electrode Surfaces with Anionic Metal-Cyanide Complexes: Formation of Precipitated Surfaces." *Inorganic Chemistry* 23:203.
- Streat, M., and D. L. Jacobi. 1995. "Complex Hexacyanoferrates for the Removal of Cesium from Solution." In *Ion Exchange Technology*, A. K. Sengupta, Ed. Technomic, Lancaster, Pennsylvania, p. 193.
- Thomas, H. C. 1944. "Heterogeneous Ion Exchange in a Flowing System." *Journal of the American Chemical Society* 66:1664.

Tusa, E. H., A. Paavola, R. Harjula, and J. Lehto. 1994. "Industrial Scale Removal of Cesium with Hexacyanoferrate Exchanger - Process Realization and Test Run." *Nuclear Technology* 107:279.

U.S. DOE. 1997a. DOE Order 5400.5, Radiation Protection of the Public and Environment. U.S. Department of Energy, Washington, D.C.

U.S. DOE. 1997b. *Empore™ Membrane Separation Technology, Innovative Technology Summary Report*. U. S. Department of Energy, Office of Science and Technology, Decontamination and Decommissioning Focus Area, Washington, D.C.

Appendix A

Development of ESIX Films Selective for Pertechnetate

**Scot Rassat
Pacific Northwest National Laboratory
P.O. Box 999
Richland, WA 99352**

The use of an electroactive material to selectively extract perrhenate ion (ReO_4^-) (surrogate for pertechnetate [TcO_4^-]) in the presence of high nitrate ion (NO_3^-) concentration has been investigated¹. As with the cesium separation process under development, a number of issues need to be resolved to determine the economic feasibility of the electrically switched anion exchange concept: 1) selectivity, 2) stability, and 3) capacity. Recent studies have addressed these issues in part, with a primary emphasis on selectivity. Selectivity of the electroactive material for ReO_4^- was established by examining the cyclic voltammograms and the associated mass loading of the material in solutions containing only NO_3^- , only ReO_4^- , and mixtures of the ions. The electroactive material was deposited as a film on a conducting substrate for these studies.

Typical results of cyclic voltammetry experiments are shown in Figures A1 and A2. The voltammograms show that both the anodic and cathodic peaks shift towards more negative potentials with higher concentrations of ReO_4^- . In Figure A1, selectivity for ReO_4^- is clearly seen by comparing the voltammograms obtained in the mixture and pure ReO_4^- . These two voltammograms essentially overlap, indicating almost complete selectivity for perrhenate over nitrate in the equimolar solution. The series of voltammograms shown in Figure A2 provide additional evidence. Initially, the film was cycled in pure nitrate and then the solution was

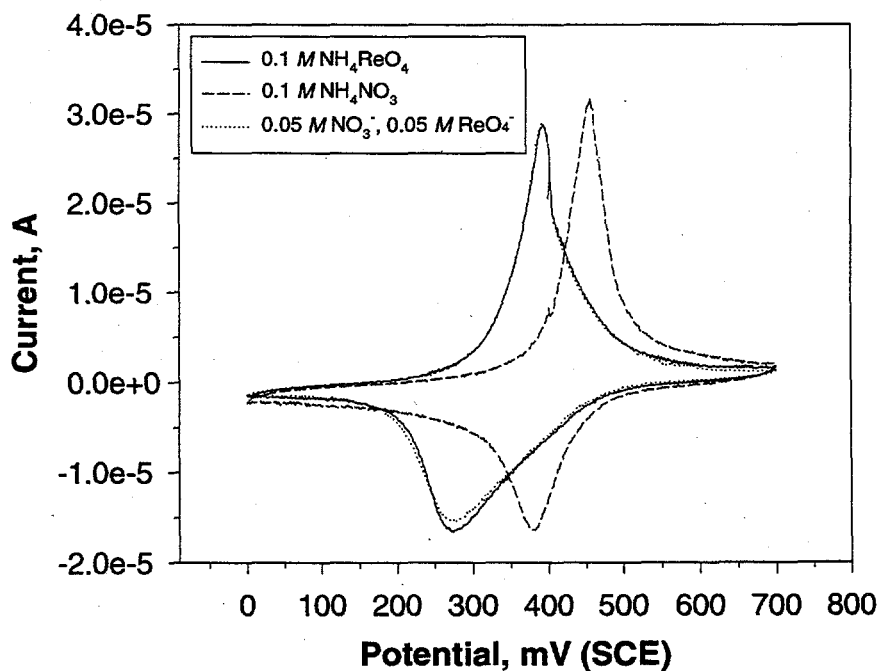


Figure A1. Cyclic Voltammograms of a ReO_4^- Selective Material in Various Solutions

¹ This work supported by Laboratory Directed Research and Development (LDRD) funding under the Pacific Northwest National Laboratory Science Technology for Environmental Processing (STEP) initiative.

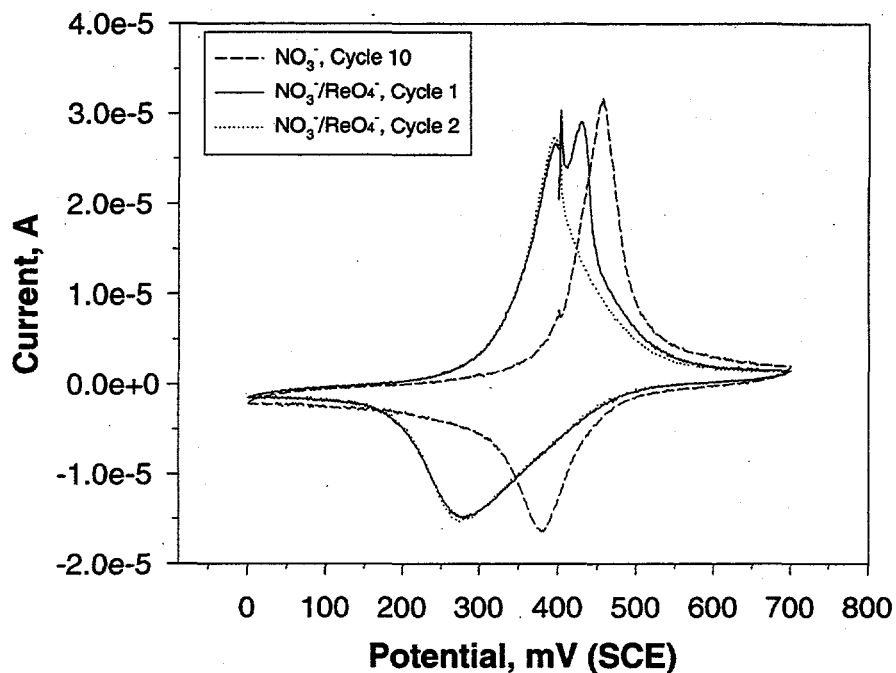


Figure A2. Cyclic Voltammograms Show Displacement of NO_3^- by ReO_4^-

changed to the equimolar mixture. During the first cycle in the mixture, peaks for both NO_3^- and ReO_4^- are observed in the voltammogram. During the second cycle in the mixture, only peaks associated with perrhenate are detected. In order to confirm and attempt to quantify the selectivity, the cyclic voltammograms were examined in conjunction with mass loading data.

Typical mass loading or Quartz Crystal Microbalance (QCM) results are shown in Figure A3. In the QCM technique a quartz crystal electrode is loaded with film, and the frequency at which the electrode oscillates is indicative of the mass loading. An increase of frequency is indicative of mass loss, and a decrease of frequency is associated with a mass increase. The data in Figure A3 are plotted as mass loading (arbitrary scale) as a function of the applied potential for three solutions, and these data correspond to the cyclic voltammograms shown in Figure A1. The QCM data show that in all three solutions (pure NO_3^- , pure ReO_4^- , and an equimolar mix) oxidation of the electroactive material, which corresponds to intercalation of anions, results in a mass increase in the film. The magnitude of the mass change during a cycle in pure nitrate solution is roughly one-fourth the observed mass change per cycle in the pure and mixed ReO_4^- solutions. This mass loading ratio is in good agreement with the ratio of nitrate to perrhenate molecular weights (62.0 g/mole:250.2 g/mole). This again suggests that perrhenate is selectively loaded by the material from a solution mixture.

Additional experiments are needed to quantify the degree of selectivity of the material for ReO_4^- over NO_3^- and to address the issues of film stability and capacity.

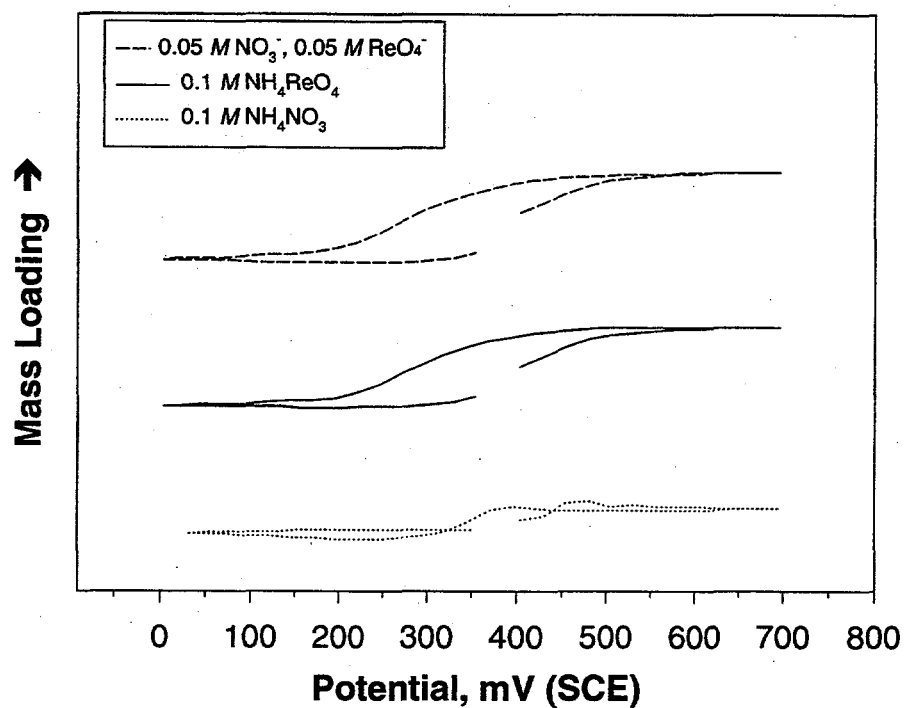


Figure A3. QCM Data Indicate Greater Mass Loading in the Presence of ReO_4^- (Note: the curves for mixed and pure ReO_4^- have been arbitrarily separated vertically for clarity.)

Appendix B

Electrochemically Switched Ion Exchange

Dr. David Genders
Dr. Ram Gopal
The Electrosynthesis Company, Inc.
72 Ward Road
Lancaster, NY 14086-9779

Executive Summary

Previous work at Pacific Northwest National Laboratory on Electrically Switched Ion Exchange (ESIX) has been extended by studying the scale up of the process to a small commercial reactor, the MP cell from ElectroCell AB. The cell has been modified to include a Ni foam (dimensions 100 mm x 100 mm x 6.3 mm, volume 63 cm³) and good quality Na₂NiFe(CN)₆ films have been uniformly deposited. The resulting reactor has been tested using streams with various concentrations of Cs⁺ and using once-through flow. Its initial performance is good but this then decays. In order to understand the reasons, the reactor has been modelled and the model has been shown to fit the experimental data well.

The behavior of the reactor can be understood in terms of a model which includes the role of mass transfer and the deactivation of the Na₂NiFe(CN)₆ film as the Na⁺ cations within the layer are replaced by Cs⁺. The model stresses the role of mass transport in determining the minimum path length, L_{crit}, of the solution through the foam necessary to make possible the desired extent of removal of Cs⁺ from solution. The deactivation of the film by ion exchange is a secondary factor. The deactivation may be considered to shorten the column and therefore to increase the value of c_{out}/c_{in} with time. The performance of the foam therefore depends on the length of the foam, the mass transfer coefficient, the specific surface area of the foam and the fractional deactivation of the film.

It is concluded that the reactor performance could be improved further by increasing the length of the foam and increasing the specific surface area of the active structure; this could be achieved using materials such as Ni Tysar^R, Ni wool or a bed of fine Ni particles.

Our experiments confirm ESIX process is capable of effective scale-up and that it could contribute to the clean up of streams containing radioactive cesium isotopes.

1. Introduction

The experimental program has been designed to extend the work carried out at Pacific Northwest National Laboratory on Electrically Switched Ion Exchange (ESIX) for the removal of Cs⁺ from a variety of waste streams. The objective was to investigate the process using a larger Ni foam within a commercial electrolytic cell.

The approach has been to convert the surface film to its fully reduced Na₂NiFe(CN)₆ form and then to remove the Cs⁺ from the feed by ion exchange without the application of a current or potential (ie. the coated foam is on open circuit). The layer is then regenerated into the Na⁺ form by oxidation using a constant current. The experiments have been carried out in a commercial MP cell (manufactured by ElectroCell AB) which allows the use of a Ni Foam with the dimensions, 100 mm x 100 mm x 6.3 mm. This is of sufficient volume to permit once-through flow of the Cs⁺ solutions, at least at low flow rates. The removal of the Cs⁺ from the film by anodic oxidation using a constant current has also been investigated. The experiments have been carried out as a function of Cs⁺ concentration, feed flow rate and the ratio of Na⁺:Cs⁺ in the feed.

The results may be fitted to a simple model that takes into account mass transfer of Cs⁺ to the surface as well as loading and consequent deactivation of the film by Cs⁺. The model confirms the critical role of mass transport in the ESIX process. For once-through operation, a long contact length between foam and solution is essential and flow-by (vertical flow) operation is essential. If the process is operated in a batch recycle mode, the flow could be in either direction but operation in the vertical mode results in a higher mean linear flow velocity, hence more efficient mass transport conditions and rate of removal.

2. Modeling the Cs⁺ Removal in a Foam Column – Selection of Practical Parameters

Firstly, it should be recognized that the terms “flow by” and “flow through” are only correctly applicable to experiments when current is flowing through the Ni foam; the terms describe whether the directions of solution flow and current flow are perpendicular or parallel respectively. On open circuit, it is perhaps more appropriate to use the terms vertical and cross flow, see figure 1(a).

If, initially, it is assumed that the removal of Cs⁺ at the surface of the Na₂NiFe(CN)₆ film is mass transport controlled (ie. the fastest possible rate of removal) and that the foam may be modelled as a plug flow reactor, the Cs⁺ concentration at the outlet is given by

$$\frac{c_{\text{out}}}{c_{\text{in}}} = \exp\left(-\frac{k_m A_e V_e}{Q_v}\right) \quad (1)$$

irrespective of the direction of the flow. Here, c_{in} and c_{out} are the concentrations at the inlet and outlet respectively, k_m the mass transfer coefficient, A_e the specific surface area of the foam, V_e the volume of the foam and Q_v the volumetric flow rate of the solution.

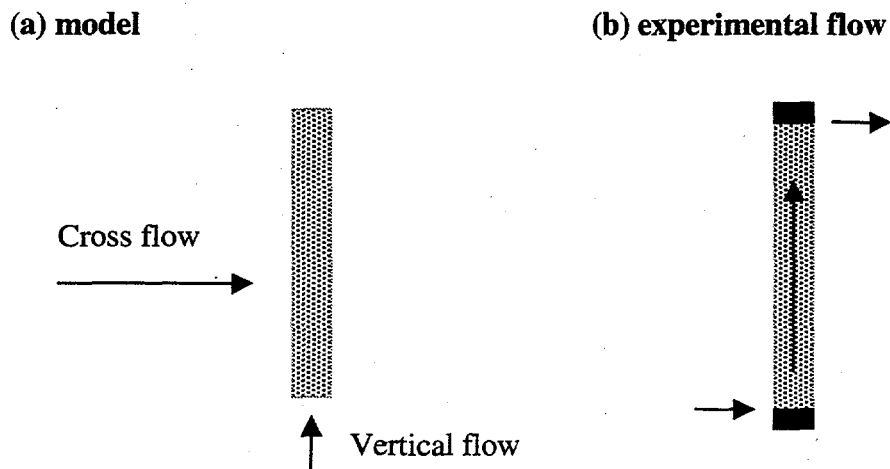


Figure 1 Comparison of (a) the ideal flow through a foam bed on open circuit with (b) the flow achieved in a commercial electrolysis cell, the MP cell, modified to contain a Ni foam with dimensions, 100 mm x 100 mm x 6.3 mm.

The foam will, however, show different performance with the two flow directions since k_m is a function of mean linear flow velocity (v) which, unlike the volumetric flow rate, depends on the direction of flow. This is illustrated in table 1 for one of the foams used in this study (80 ppi and a porosity of 80%) and a volumetric flow rate of $5 \text{ cm}^3 \text{ min}^{-1}$. The values of $k_m A_e$ were calculated using the equation

$$k_m A_e = 1.89 \times 10^{-2} v^{0.7} \quad (2)$$

taken from Pletcher et al (J. Applied Electrochem. 24 (1994) 95) table 2, although this does necessitate a long extrapolation between the rather different flow rates used in the two sets of experiments. Such calculations are very approximate but clearly show the different volumes of foam required with the two flow regimes. With vertical flow and for $c_{out}/c_{in} = 0.1$, the volume of foam is comparable to that used in this work (dimensions 100 mm x 100 mm x 6.3 mm, volume 63 cm^3) but with cross flow the foam must be a factor of seven larger. Better agreement between experiment and theory could be obtained by assuming a higher value for $k_m A_e$.

	$v/\text{cm s}^{-1}$	$k_m A_e/\text{s}^{-1}$	V_e/cm^3 for $c_{\text{out}}/c_{\text{in}} = 0.1$	0.01
Crosswise flow	1.04×10^{-3}	1.54×10^{-4}	1240	2480
Vertical flow	1.65×10^{-2}	1.07×10^{-3}	180	360

Table 1 Estimates of $k_m A_e$ and conversions as a function of flow direction.

A number of conclusions may be drawn:

- (i) With a reactor involving a heterogeneous reaction, the conversion of reactant can never be 100% and always depends on the total area of surface available and the mass transport regime. Hence, the term "column break through" implies a decision as to an acceptable level of Cs^+ at the outlet.
- (ii) The specific surface area of the Ni foams are high compared to traditional electrode materials but remain low compared to commercial ion exchange resins.
- (iii) The table shows that the size of the foam required depends strongly on the conversion sought - 99% removal of the Cs^+ requires a foam volume twice that for 90% removal.
- (iv) Also the conversion is independent of the Cs^+ inlet concentration. Hence, operation at very low Cs^+ concentrations will be the same unless other chemical factors intercede. On the other hand, with low Cs^+ concentrations, the $c_{\text{out}}/c_{\text{in}}$ chosen has to reflect the lowest detection limit of the Cs^+ analysis; with 0.2 ppm and the analytical method used in this work, the lowest limit of $c_{\text{out}}/c_{\text{in}}$ is ≈ 0.1 .
- (v) The plug flow reactor equation, equation (1) above, may be rewritten

$$\frac{c_{\text{out}}}{c_{\text{in}}} = \exp - \frac{k_m A_e L}{v} \quad (3)$$

where L is the length of the foam and v the mean linear flow velocity of the solution. It can be seen that for single pass operation, the foam should be as long as possible in order to give the lowest outlet concentration.

- (vi) For a particular cell geometry and size, the performance will be relatively insensitive to the feed flow rate because $k_m A_e/v$ is proportional only to $v^{-0.3}$.

The model so far only recognizes mass transport control. For Cs^+ exchange at a $\text{Na}_2\text{NiFe}(\text{CN})_6$ film covered Ni foam, a more complete model needs to recognize that, as the layer is converted to $\text{Cs}_2\text{NiFe}(\text{CN})_6$, effectively the active surface area will decrease.

The extent of removal of Cs^+ will get worse with time. The period of acceptable performance will depend on the relative values of the foam length and the critical length to achieve the required removal.

The next level of model would calculate the fraction, θ , of the sodium ions within the film exchanged for cesium from the volume of solution treated and the previous performance of the reactor. The instantaneous fractional removal at that time could then be calculated from the equation

$$\frac{c_{\text{out}}}{c_{\text{in}}} = \exp -\theta \frac{k_m A_e V_e}{Q_v} \quad (4)$$

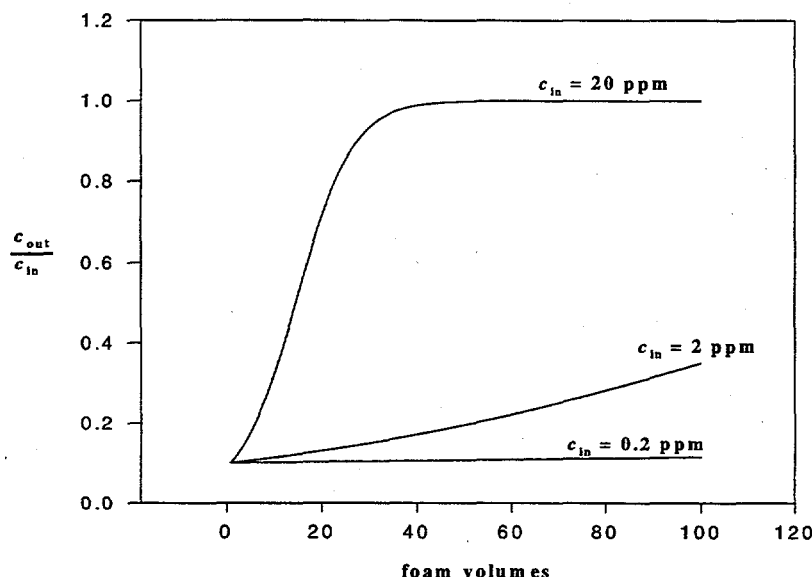


Figure 2 Plots of conversion vs volume of feed, showing the influence of Cs^+ concentration on reactor performance using the model and one set of experimental conditions (see text).

This function may be used to compute a plot of $c_{\text{out}}/c_{\text{in}}$ vs number of foam bed volumes for any inlet concentration and other experimental conditions. Figure 2 shows such theoretical plots for experimental conditions where the volume of foam is 180 cm^3 , $k_m A_e = 1.07 \times 10^{-3} \text{ s}^{-1}$, volumetric flow rate = $0.083 \text{ cm}^3 \text{ s}^{-1}$. The layer of $\text{Na}_2\text{NiFe}(\text{CN})_6$ on the foam is able to exchange 52 mg of Cs^+ . It can be seen that this model predicts no

significant change in the reactor performance during operation lasting 100 foam volumes when the inlet concentration of Cs^+ is 0.2 ppm. The value of $c_{\text{out}}/c_{\text{in}}$ is 0.1 because of the experimental parameters put into the model. In contrast, with an inlet concentration of 20 ppm, the performance is initially the same but decays rapidly because the $\text{Na}_2\text{NiFe}(\text{CN})_6$ layer is rapidly loaded with Cs^+ . The 2 ppm solution shows intermediate behavior.

The model works well because most of the exchange will occur where the solution first meets unloaded $\text{Na}_2\text{NiFe}(\text{CN})_6$ surface. Equations (3) and (4) both show that the concentration of Cs^+ drops off exponentially through the foam and hence the major part of the exchange occurs initially close to the inlet. Then as the film becomes loaded, the reaction zone will move as a front through the foam, the effective length of the foam decreasing with time. It is possible to consider three situations which depend on the relative values of the experimental bed length, L , and the critical active foam length, L_{crit} , necessary to achieve the desired extent of Cs^+ removal.

- (i) For $L < L_{\text{crit}}$, the desired level of Cs^+ removal will not be achieved even at the commencement of an experiment.
- (ii) For $L > L_{\text{crit}}$, the desired level of Cs^+ removal will be achieved for an extended period of time, the period depending mainly on the Cs^+ concentration.
- (iii) For $L \approx L_{\text{crit}}$, the desired level of Cs^+ removal may be achieved for a short period but a decay in performance will soon set in. The performance will depend strongly on the Cs^+ concentration.

The next level of modelling could take into account any kinetics associated with the insertion of Cs^+ into the $\text{Na}_2\text{NiFe}(\text{CN})_6$ layer. Studies with films on two-dimensional electrodes, however, provide no evidence that the kinetics of insertion are ever slow and this additional level of modelling has not been attempted.

The experiments in this program were all carried out in a commercial electrochemical cell, the MP cell manufactured by ElectroCell AB. This allowed the introduction of a foam with dimensions 100 mm x 100 mm x 6.3 mm, volume 63 cm³. The flow, however, is not precisely vertical flow. The flow is sketched in figure 1(b). Because of the ratio of length to width (100 mm to 6.3 mm), the reactor would be expected to behave similarly to a vertical flow reactor of the same dimensions; it is, however, not possible to quantify the deviations from ideal vertical flow. The design and fabrication of a purpose built reactor could remove this uncertainty.

3. Experimental

(a) **Film Preparation:** Porous nickel foams of porosity 60 and 80 ppi were used for all experiments. The electrode dimensions were 100 x 100 x 6.3 mm to fit in an MP flow cell. The film was cleaned initially with deionized water and the film application was done in a large beaker (2-liter) using platinum as counter-electrode. A Luggin probe was used to measure the potential at the foam electrode using Ag/AgCl reference electrode. The cell is shown in Figure 3. The method used to deposit films was a PNNL-proprietary variation of the method of Bocarsly, et al. The electrolyte for film deposition was a solution containing 0.1 M KNO_3 and 0.01 M $\text{K}_3\text{Fe}(\text{CN})_6$. A PAR 273 Potentiostat was used to control the potential at 1.0 V for 360 s. At the end of deposition, the foam was taken out of the bath and rinsed in DI water. A solution of 1 M NaNO_3 was then used with similar arrangement (Pt counter-electrode, luggin probe and Ag/AgCl reference) to run cyclic voltammetric curve. All voltammograms were done at a scan rate of 50 mV s^{-1} between -0.25 and 1.05 V vs. Ag/AgCl. The area under the oxidation and reduction waves was integrated to obtain the film loading or capacity of the film. Chronocoulometric experiments were also performed to determine the film capacity. Current decay at potentials 0.8 V and 0.2 V (vs. Ag/AgCl) for 30 s each was used to measure film capacities. The areas under the current decay curves at 0.8 and 0.2 V were integrated to calculate the film capacity. The same procedure was followed to measure the electrochemical characteristics of all the films prepared.

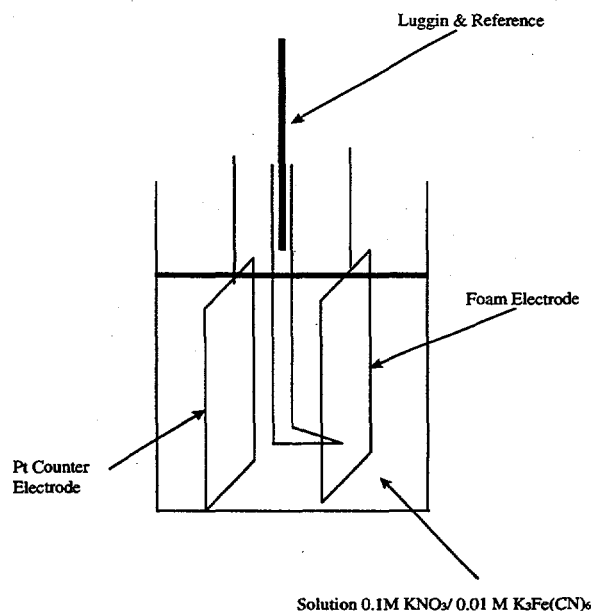


Figure 3. Beaker cell for film Deposition & CV Experiments

(b) *MP flow cell set up and cell operation*: The cell was set up in the way shown schematically in figures 4, 5 and 6. Feed solutions were prepared by dissolving CsNO_3 in DI water to the desired final Cs concentrations (20, 2 and 0.2 ppm). For studies on the effect of ionic strengths, NaNO_3 was used as the electrolyte to obtain Na^+/Cs^+ molar ratio of up to 10^5 . A Masterflex pump was used to control liquid flow through the cell at the desired rate (8 to 24 ml/min). Effluent samples were collected at different intervals for cesium analysis. Samples were analyzed by atomic absorption emission method using proper matrix for the background (see analytical procedure below).

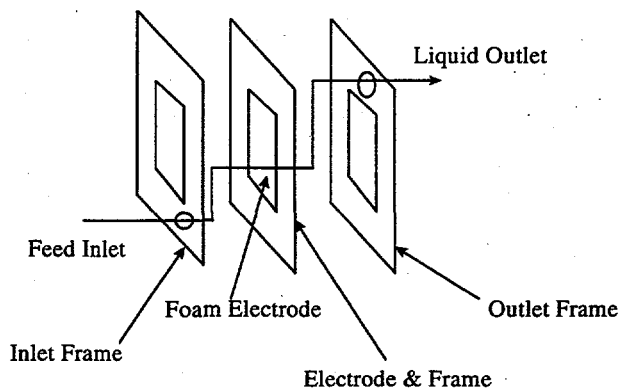
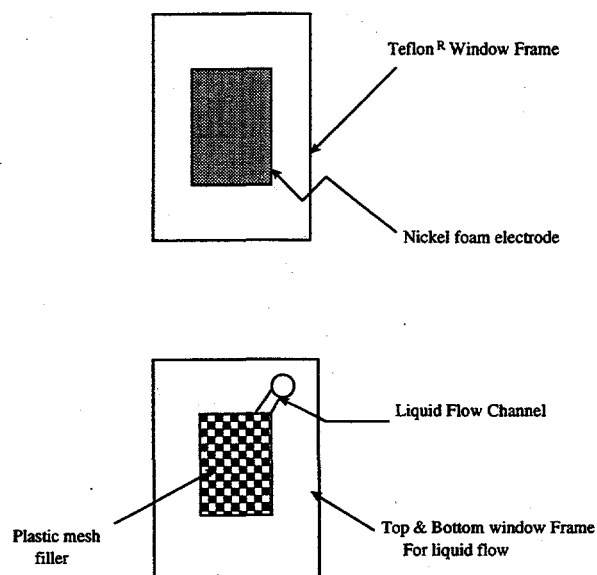


Figure 4 *Electrode and frame arrangement within the cell.*



Viton gaskets placed between the frames with good seals around the foam electrode.

Figure 5: *Cell frames and plastic mesh spacers.*

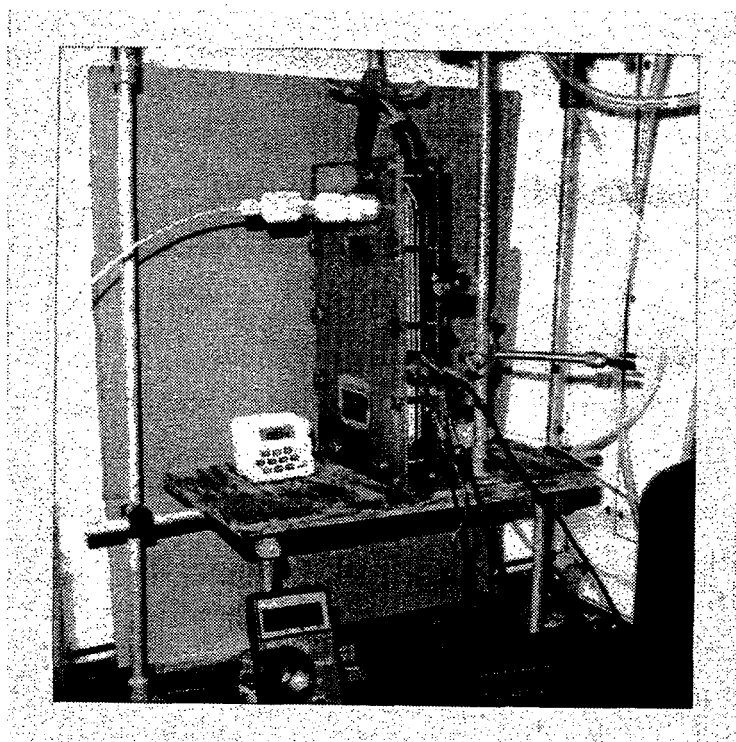


Figure 6: MP cell experimental set up.

(c) **Procedure for in-situ regeneration of the film:** A method was developed for the regeneration of film in-situ. A solution of 0.1 M NaNO_3 was passed through the cell at a flow rate while maintaining a constant current (5 mA). Passage of about 300 cm^3 of 0.1 M NaNO_3 solution for about 2 - 3 hours was sufficient to elute 70 - 75 % of the cesium exchanged on the film. The cell was completely drained and the solution to determine the amount of cesium eluted. The cell was also rinsed with DI water before further experiments using the regenerated film. During elution, very small amounts of colloidal solids were washed with the eluting solution. These were too small to analyze and may be due to the partial removal of the film or from corrosion of nickel during regeneration. This phenomenon may be attributed to the particular regeneration conditions used in these experiments since other experimental work at PNNL has shown no corrosion. Continued use of the electrode over a number of cycles shows some capacity loss. Cyclic voltammetry of films regenerated in-situ showed similar characteristics to the original film.

(d) **Atomic Absorption Emission Analytical Procedure for Cs^+ :** Cesium analysis was performed using the atomic absorption emission method. Using sodium or potassium salts in the matrix increases the sensitivity for cesium detection by emission. All standards for analysis were therefore made in 0.1 or 1 M NaNO_3 depending on the matrix used in the MP cell flow experiments. Standards (0.1 to 1 ppm Cs) were prepared in 0.1 M NaNO_3 matrix. An example of the calibration curve for the standards is given in

Figure 7. Acetylene/air (ratio of 2:4) was used for the flame and wavelength of 852.1nm for cesium detection. A red filter to absorb any radiation below 650nm was also used throughout the analysis. A Perkin-Elmer 3110 was used for analysis. Samples collected from different experiments were diluted to appropriate concentration to make up the final mixture to 0.1 M NaNO₃. The concentration of cesium was then obtained using the calibration curve for cesium from the emission measured for the sample. The lower limit of detection for cesium under these conditions was < 20 ppb. A background solution of 0.1 M NaNO₃ was used to zero the emission background for both the sample analysis and standard calibration.

Cs concentration calibration for AA Run # 28 Sep 5 97

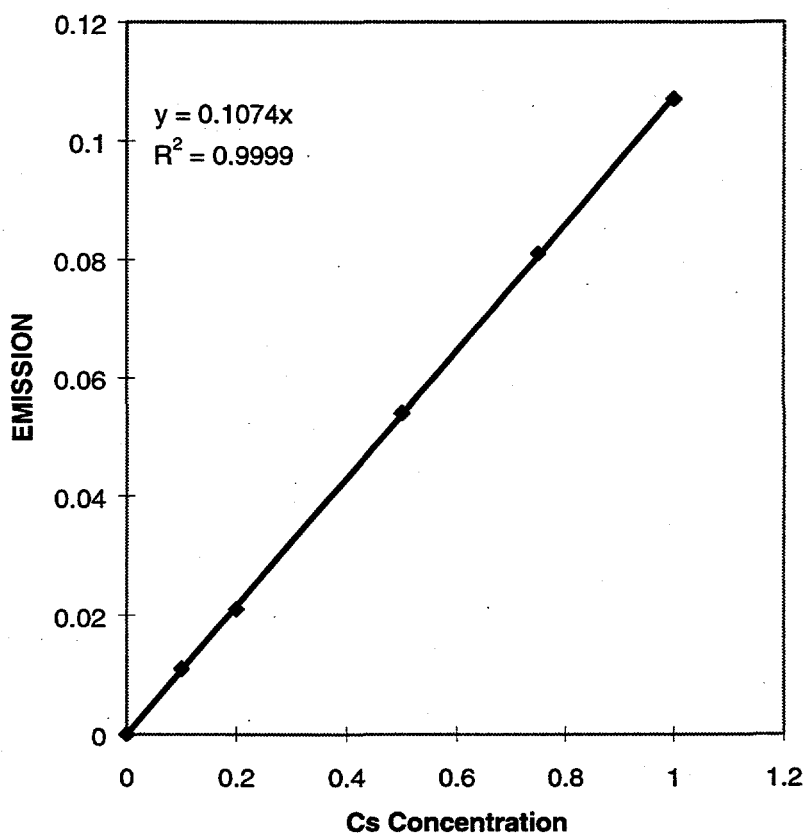


Figure 7: Calibration curve for Emission Spectroscopy

4. Results

4.1 Characterization of the Coated Ni Foams

The 60 and 80 ppi Ni foams were coated with a film of $\text{Na}_2\text{NiFe}(\text{CN})_6$ using a standard procedure similar to that developed in the laboratories of PNNL. The only difference was that the Ni foam was acid washed prior to the film formation. This increased the charge associated with oxidation/reduction of the film and the ion exchange capacity of the film. All freshly prepared coated electrodes (in the Na^+ form) were first characterized using both cyclic voltammetry and a double potential step method. The results were very reproducible and only typical data are reported here.

Figure 8 shows a typical cyclic voltammogram of the $\text{Na}_2\text{NiFe}(\text{CN})_6$ film on 60 ppi Ni foam in 1M NaNO_3 recorded at 50 mV s^{-1} . Well defined oxidation and reduction peaks are clearly observed although both peaks are drawn out compared to those reported

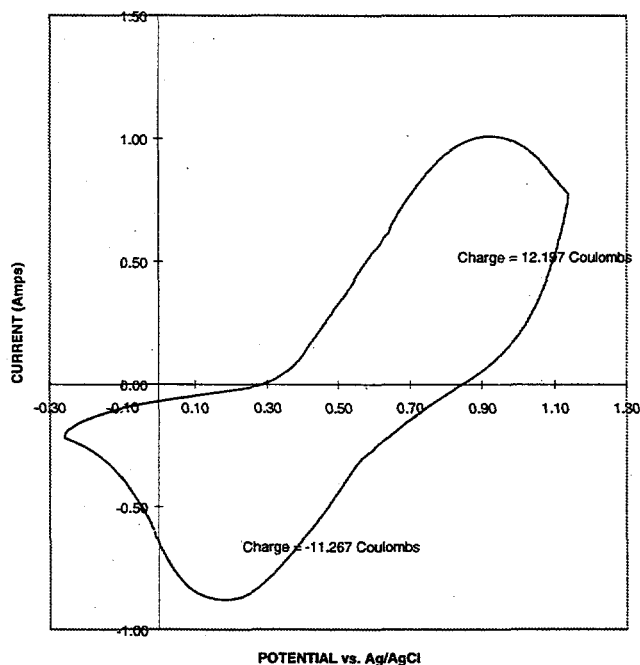


Figure 8: Typical cyclic voltammogram of the $\text{Na}_2\text{NiFe}(\text{CN})_6$ film on 60 ppi Ni foam in 1M NaNO_3 recorded at 50 mV s^{-1}

previously on two dimensional electrodes. This is to be expected, however, in an experiment where the currents approach 1 A; it is inevitable that there is significant uncorrected IR drop despite the use of a three electrode cell. The charges associated with the oxidation and reduction processes are ≈ 12.2 C and ≈ 11.3 C respectively. This is not a significant difference because over the wider potential range employed, there may be contribution from other reactions, for example, oxygen evolution. The average charge corresponds to a charge density of 2 mC cm^{-2} (electrode volume 63.5 cm^3 , specific surface area $60 \text{ cm}^2 \text{ cm}^{-3}$) or a capacity density of $2 \times 10^{-8} \text{ moles cm}^{-2}$. This is a similar charge density to those obtained on two-dimensional electrodes. It was concluded that the coating procedure for the foams was satisfactory.

Figure 9 reports the analogous chronoamperometric response when the same film was subjected to potential steps to + 800 mV and then 0 mV in 1 M NaNO_3 . Again, the precise form of the response should not be interpreted because of uncorrected IR drop. It is, however, confirmed that the rate of Cs^+ loading and discharge are both high, with currents above 1 A being achieved. It can also be seen that the charge balance is again good and that the charge cycled in the potential steps is similar to those in the cyclic voltammetry.

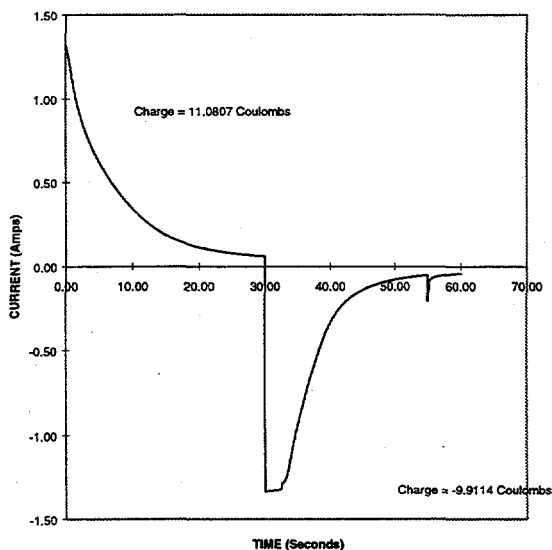


Figure 9: Chronoamperometric response

These experiments with the foams confirm that the movement of ions into and out of the film is rapid and there is no reason to invoke any control by the kinetics of ion movement in the film. Table 2 summarizes some data for the films showing the advantage of acid washing the Ni foam before the $\text{Na}_2\text{NiFe}(\text{CN})_6$ film is formed.

In many experiments, cyclic voltammograms and potential step experiments were repeated during and/or after the use of the films for Cs^+ removal. No significant changes to the responses were observed although it should be noted that the fractional exchange of Na^+ by Cs^+ within the films was generally rather low in these experiments. In no experiments was the exchange driven near to completion before its voltammetry was examined.

Grade Ni foam	$A_s/\text{cm}^2 \text{ cm}^{-3}$	Water washed		Acid washed	
		Charge/C	Capacity/mg Cs^+	Charge/C	Capacity/mg Cs^+
60 ppi	60	5.4	7.4	13.0	17.8
80 ppi	75	7.0	9.6	12.1	16.6

Table 2 Charges and capacities of $\text{Na}_2\text{NiFe}(\text{CN})_6$ films on Ni foams after two different pretreatments. Specific surface areas taken from *J. Applied Electrochem.* 19 (1989) 43.

4.2 The Removal of Cs^+ by $\text{Na}_2\text{NiFe}(\text{CN})_6$ coated Ni Foams on Open Circuit

Figures 10 and 11 report the experimental results from an experiment carried out with a 60 ppi Ni foam (dimensions 100 mm x 100 mm x 6.3 mm, volume 63 cm^3) coated with a $\text{Na}_2\text{NiFe}(\text{CN})_6$ layer with a Cs^+ capacity equivalent to 17.9 mg. The inlet concentration was 2.4 ppm Cs^+ and the flow rate 0.1 $\text{cm}^3 \text{ s}^{-1}$. Figure 10 shows the variation of $c_{\text{out}}/c_{\text{in}}$ with the volume of the inlet stream while figure 11 shows the consequent build up of Cs^+ cation in the film.

Model calculations would suggest that in these experiments, the maximum removal of Cs^+ with the fresh $\text{Na}_2\text{NiFe}(\text{CN})_6$ layer would be $\approx 90\%$. The MP cell dimensions determined the foam size used. It would have been advantageous to have been able to vary the foam length since the experiments are all carried out in the situation where $L \approx L_{\text{crit}}$ and the data would look markedly different if, for example, the foam had been twice as long, ie. 200 mm, without changing other parameters.

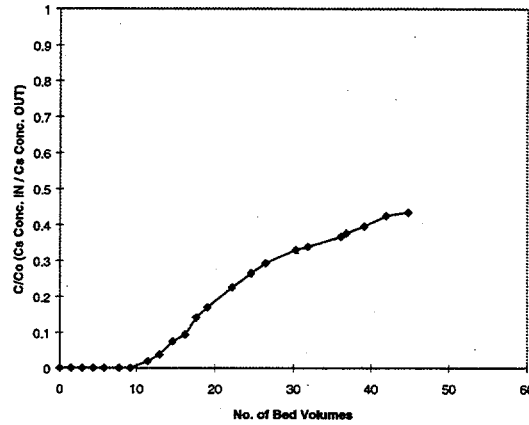


Figure 10: Cesium Concentration as a function of volume passed; Cs concentration 2.4ppm; film capacity 17.9 mg of Cs.

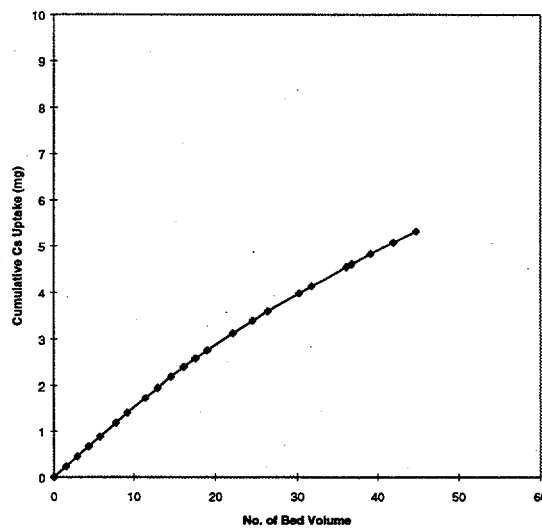


Figure 11: Cesium Uptake as a function of volume passed; Cs concentration 2.4ppm; film capacity 17.9 mg of Cs.

The experimental data shows that initially the foam does rather better than predicted in the model calculations (although because of uncertainty in the lowest detection limit for the analysis, we would caution interpretation of $c_{out}/c_{in} = 0$). After 16 bed volumes of solution, the value of $c_{out}/c_{in} = 0.1$; at this point 13% of the bed has been transformed to the Cs^+ form and some decay in performance might indeed be expected. The slope of the plot of cumulative Cs^+ uptake versus solution volume begins to decrease but cumulative Cs^+ uptake continues. By the termination of the experiment after a volume of solution equivalent to 45 bed volumes, the cumulative Cs^+ uptake has reached 29% and there is a significant decay in the performance of the foam. The value of c_{out}/c_{in} has increased to ≈ 0.4 . We regard this as a reasonable fit with the theory (see section 2) and we believe that the performance of the foam is largely determined by mass transfer characteristics. The only approaches to significantly improving the performance would be to increase the bed length or its specific surface area.

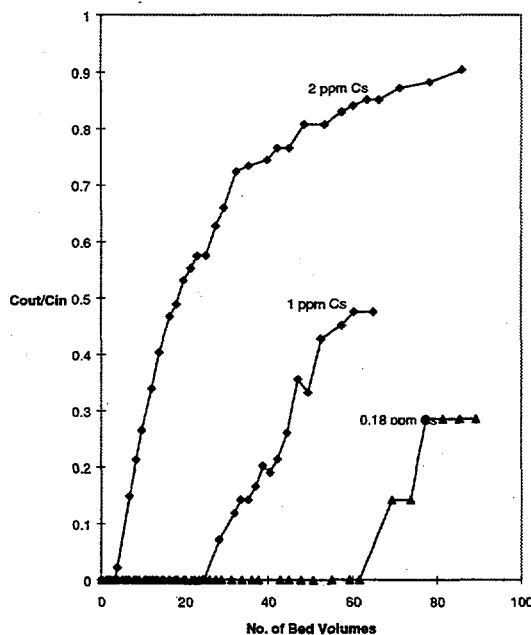


Figure 12: Cesium Concentration as a function of volume passed; Cs concentrations 2, 1, 0.18ppm

Figure 12 shows plots of c_{out}/c_{in} versus volume of Cs^+ solution for three Cs^+ concentrations while table 3 summarizes the data for four concentrations. All these experiments were carried out using foams (dimensions 100 mm x 100 mm x 6.3 mm, volume 63 cm³) with similar loadings of $Na_2NiFe(CN)_6$ (equivalent to 12 – 17 mg Cs^+) as determined voltammetrically. Again a value of $c_{out}/c_{in} = 0.1$ was chosen as the definition of "break through" and values of $c_{out}/c_{in} = 0$ should be thought of as the detection limit for the Cs^+ . In all cases, break through occurred when approximately 10 % of the cations in the layer had been exchanged and this again results from the fact the foam length is only just sufficient initially to achieve $c_{out}/c_{in} = 0.1$. The foam continues to exchange Cs^+ after break through but the observed c_{out}/c_{in} increases rapidly; typically the exchange reached 20 – 30% before experiment were discontinued. It can be seen that in this situation, the performance is very dependent on Cs^+ concentration and the foam performance appears

C_{in}/ppm	Bed volumes to $c_{out}/c_{in} = 0.1$	Fractional loading of layer by Cs^+ at $c_{out}/c_{in} = 0.1$
2.0	6	0.08
1.35	17	0.10
1.03	27	0.12
0.18	65	0.06

Table 3 Performance of the 60 ppi Ni foam (dimensions 100 mm x 100 mm x 6.3 mm, volume 63 cm³) with loadings of $Na_2NiFe(CN)_6$ (equivalent to 12 – 17 mg Cs^+). Flow rates 8 – 12 foam volumes/hour.

ppi	Foam Cs capacity/mg	Bed volumes to $c_{out}/c_{in} = 0.1$	Fractional loading of layer by Cs^+ at $c_{out}/c_{in} = 0.1$
60	11.6	90	0.09
	13.8	110	0.10
	13.8	100	0.12
80	4.4	38	0.09
	16.7	100	0.07
	16.7	80	0.09
	16.7	120	0.10
	16.7	80	0.10
	16.7	80	0.09

Table 4 Performance of the Ni foam (dimensions 100 mm x 100 mm x 6.3 mm, volume 63 cm³). Flow rates 8 – 12 foam volumes/hour.

to improve substantially as the concentration is decreased. The general form of the data resembles that predicted by the model and shown in figure 2.

A large number of experiments have been carried out with a Cs^+ concentration of 0.2 ppm and the data are summarized in table 4. Generally, the experiments have been carried out in similar conditions and are reported here to emphasize the reproducibility of the experimental data. It is, however, clear that a large change in loading by $Na_2NiFe(CN)_6$ does influence the performance; in the experiment with a thin film equivalent to only 4.4 mg of Cs^+ break through occurs at a much lower solution volume although at a similar value of fractional ion exchange.

The data does not distinguish the performance of 60 ppi and 80 ppi foam. This is not surprising since the specific surface areas are not markedly different, 60 and 75 cm² cm⁻³. It is to be expected that a large increase in the specific surface area would improve the performance and materials such as Ni Tysar^R, Ni wools and beds of small Ni particles would be worth investigating. Also, experiments with the solution flow rate varied between 8 and 23 foam volumes/hour showed no significant trends. It was predicted in

the discussion of the model that a large change in flow rate would be necessary to cause marked changes to the data.

The final parameter investigated was the concentration of Na^+ in the inlet stream. Data from an experiment where the inlet stream contained 0.2 ppm Cs^+ and 200 ppm Na^+ are reported in figures 13 and 14. In figure 13, it can be seen that $c_{\text{out}}/c_{\text{in}}$ becomes > 0.1 after ≈ 85 foam volumes and this falls within the range found for solutions containing only Cs^+ (see table 4). Similarly, figure 14 confirms that the ion exchange of Na^+ by Cs^+ within the $\text{Na}_2\text{NiFe}(\text{CN})_6$ layer does not seem to have been changed by the presence of Na^+ in solution. In a further experiment where the Na^+ concentration in the inlet stream was even higher, 20000 ppm, the experimental results were unexpected. The plot of $c_{\text{out}}/c_{\text{in}}$ vs solution volume is shown in figure 15. It can be seen that the coated foam initially performs very badly with $c_{\text{out}}/c_{\text{in}} > 0.3$. The rate of removal of Cs^+ then improves before a perhaps normal fall off in performance is observed after 80 – 100 bed volumes. This result was reproduced in a second experiment but we presently have no explanation. Such behavior is not predicted by the model (which would not suggest any influence of Na^+ concentration) and is neither a mass transport nor a ion exchange capacity effect. It could, for example, arise through the high level of Na^+ ion effecting the structure/swelling of the $\text{Na}_2\text{NiFe}(\text{CN})_6$ layer.

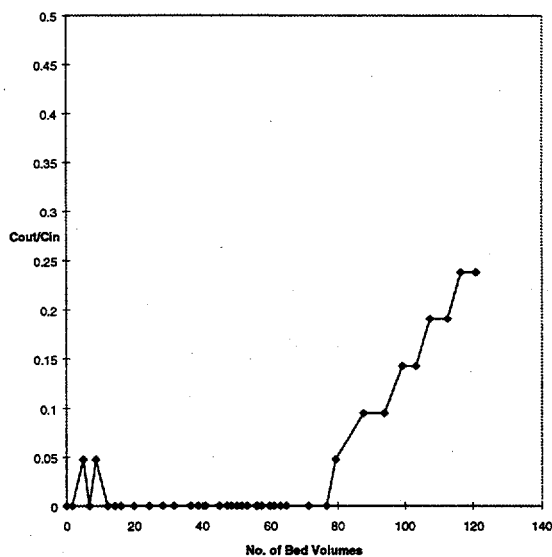


Figure 13: Cesium Concentration as a function of volume passed; Cs concentration 0.2ppm, Sodium concentration 200ppm

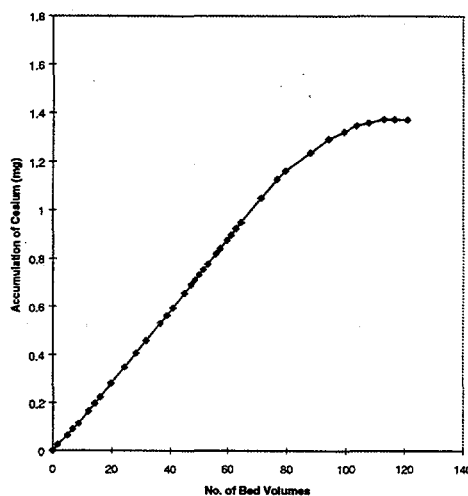


Figure 14: Cesium Uptake as a function of volume passed; Cs concentration 0.2ppm, Sodium concentration 200ppm

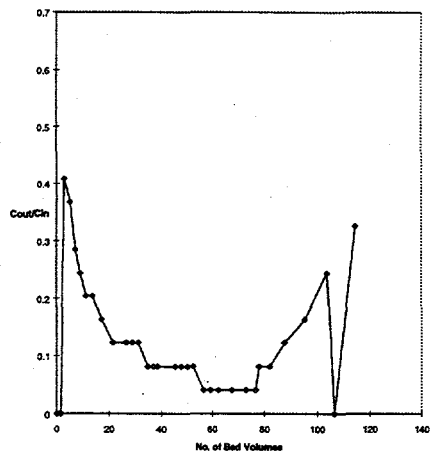
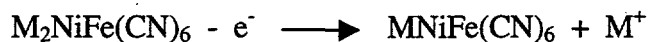


Figure 15: Cesium Concentration as a function of volume passed; Cs concentration 0.2ppm, Sodium concentration 20,000ppm

4.3 The Recovery of Cs⁺ from the Na_{2-x}Cs_xNiFe(CN)₆ Layer

The removal of the Cs⁺ from the film on the Ni foam by anodic oxidation has been studied. The electrode reaction



will clearly lead to removal of a cation from the film and under some circumstances it will be Cs⁺ which will be ejected. Since the thermodynamics of binding of the Cs⁺ within the layer are more favorable than those for Na⁺, removal of the Cs⁺ will only occur where, locally, within the layer, the fraction of Cs⁺ is high. As noted earlier, this will be the case close to the inlet to the foam and through the foam as more complete exchange is carried out during loading. During removal of the Cs⁺, a further problem could be envisaged – the Cs⁺ could exchange back on to the film further down the foam towards the exit.

Four experiments were carried out where a Ni foam (dimensions 100 mm x 100 mm x 6.3 mm, volume 63 cm³) with a Na₂NiFe(CN)₆ layer (Cs⁺ capacity equivalent to 10 – 12 mg) was loaded with to an extent of 15 – 20 % with Cs⁺ using a solution containing 0.2 ppm Cs⁺. The Cs⁺ loaded foam was then oxidized using a constant current of 5 mA while passing a solution of 0.1 M Na NO₃ (300 cm³) through the foam with a flow rate of 1 cm³ s⁻¹. The eluent was ≈ 3 ppm in Cs⁺ and the total recoveries of Cs⁺ were between 60 and 80 %.

These experiments were all carried out at with a current of 5 mA, a very low current density. The voltammetric response would suggest that it would be possible to discharge most of the Cs⁺ at a much higher rate, thus giving a higher Cs⁺ concentration in the eluent and a higher concentration factor. The low current was employed in these preliminary experiments to avoid possible competing electrode reactions such as oxygen evolution.

5. Conclusions

It has been confirmed that the selective removal of Cs⁺ from aqueous effluent is possible using a Ni foam coated with a Na₂NiFe(CN)₆ layer. The coated Ni foams appear to have very similar characteristics and voltammetric properties to a Na₂NiFe(CN)₆ films on small, two dimensional electrodes.

A reactor built by modifying an MP cell to include a Ni foam (dimensions 100 mm x 100 mm x 6.3 mm, volume 63 cm³) has been tested. It is shown that the performance of the foam, operated on open circuit, depends strongly on the Cs⁺ concentration. The film loading, solution flow rate and grade of Ni foam have also been

varied but influence the performance less strongly. Preliminary experiments also confirm that the Cs^+ may be removed from the film by anodic oxidation.

The behavior of the reactor can be understood in terms of a model which includes the role of mass transfer and the deactivation of the $\text{Na}_2\text{NiFe}(\text{CN})_6$ film as the Na^+ cations within the layer are replaced by Cs^+ . The model stresses the role of mass transport in determining the minimum path length, L_{crit} , of the solution through the foam necessary to make possible the desired extent of removal of Cs^+ from solution. The deactivation of the film by ion exchange is a secondary factor. The deactivation may be considered to shorten the column and therefore to increase the value of $c_{\text{out}}/c_{\text{in}}$ with time. The performance of the foam therefore depends on the length of the foam, the mass transfer coefficient, the specific surface area of the foam and the fractional deactivation of the film.

All the experiments in this report were carried out in a reactor where the length of the foam was only just sufficient to permit an outlet concentration as low as $0.1c_{\text{in}}$ (ie. $L \approx L_{\text{crit}}$). Hence, the performance decayed rather rapidly as the layer deactivated; for example, with a solution containing 0.2 ppm Cs^+ , $c_{\text{out}}/c_{\text{in}} > 0.1$ after ≈ 100 foam volumes when only 10% of the bed had deactivated. There would be a substantial advantage in doubling the foam length when it would be expected that $c_{\text{out}}/c_{\text{in}} = 0.1$ would not be reached until ≈ 1500 foam volumes when $> 50\%$ of the bed would be deactivated. There is also an advantage in investigating Ni materials with a higher specific surface area; possible materials include Ni Tysar^R, Ni wool or a bed of fine Ni particles.

Appendix C

Electrochemically Switched Ion Exchange

**Dr. Dan Schwartz
Scott Haight
University of Washington
Department of Chemical Engineering
Box 351750
Seattle, WA 98195-1750**

Introduction

Hexacyanoferrate films on electrodes can be cycled between the oxidized (Fe^{III}) and reduced (Fe^{II}) forms by modulating the potential of the electrode substrate. Cycling can be carried out about 2000 times on a flat plate electrode before 20% of the activity (capacity) is lost. Because the capacity of thin films is relatively low (compared to a packed bed ion exchanger), it is desirable to maintain as high a capacity as possible for as long as possible. Therefore, films were examined *in situ* with use of Raman spectroscopy during potential cycling in an attempt to identify modes of degradation.

In addition, development of a process based on ESIX technology will require use of high surface area electrodes. Associated with large electrodes are the problems of current and potential control that must be accounted for in the engineering design of the electrochemical reactor. An issue with electroactive films is whether redox reactions occur homogeneously or in islands on the electrode. Homogeneous redox reactions are desirable for predictable kinetics and process control and for efficient use of the electrode area.

Experimental

Raman spectra were acquired using the 647.1 nm line of a krypton ion laser (Laser Ionics). The 647.1 nm line is a sensitive probe of the oxidation state of the film and gives minimal film degradation because it lies outside the absorption window of the material. Plasma emissions from the laser were removed with a narrow bandpass filter (Omega Optical). The laser was focused using an f/10 spherical lens. Scattered light was collected at 90° from the incident beam by an f/1.2 Nikon camera lens. The elastically scattered portion of the light was attenuated by an OD6 holographic notch filter (Kaiser Optical) prior to entering the spectrograph through a 100 μm entrance slit. A 270 cm, f/4 imaging spectrograph (Spex Industries model 270M) equipped with 600 and 1800 gr/mm gratings dispersed the inelastically scattered light onto a liquid nitrogen cooled two-dimensional CCD array (Princeton Instruments model LN/CCD-1024E). The spectroscopic and electrochemical instrumentation was controlled by a Macintosh Centris 650 computer running LabView v.2.2.1 over a GPIB interface. Spectra were acquired *in situ* from a 500- μm -diameter Ni disk electrode that was coated with a film and immersed in the sodium nitrate electrolyte. Additional details regarding the spectroelectrochemical instrumentation have been reported previously (Haight and Schwartz 1995).

Film Characterization Using Raman Spectroscopy

The results indicate that Raman spectroscopy is a sensitive probe of the oxidation state of the film. This technique is a good diagnostic tool for *in situ* investigations of the behavior of metal hexacyanoferrate films during redox reactions and should give information about mechanisms of film deactivation or loss. When a literature film is fully reduced with an applied potential of -111 mV, two low wavenumber cyanide stretching modes are evident at 2103 cm^{-1} and 2151 cm^{-1} , corresponding to the ferrocyanide oxidation state (Figure C-1). As the applied potential is made more anodic, the film is observed to become increasingly oxidized. The film is almost completely in the ferricyanide form (peak at 2186 cm^{-1}) at an applied potential of 778 mV as shown in Figure C-1. Ferro- and ferricyanide have been distinguished on potential cycling of films with thicknesses as low as about 100 \AA (10 unit cells thick).

Imaging Raman spectroscopy shows that the thin film redox reactions occur uniformly across the film rather than in isolated regions. Raman images of a $750\text{-}\mu\text{m}$ -long by $30\text{-}\mu\text{m}$ -wide region of film were obtained as oxidation was carried out electrochemically (Figure C-2). Spectral data are displayed as a function of spatial position along the electrode, with signal intensity indicated by a gray scale. Figure C-2 shows that when increasingly anodic potentials were applied to a ferrocyanide film on a nickel wire, the extent of oxidation to ferricyanide also increased, as shown by the increasing intensity of the ferricyanide signal. Furthermore, within the spatial resolution of the technique ($5\text{ }\mu\text{m}$), the formation of ferricyanide occurred uniformly across the film. This is the first time that spatial uniformity of a thin film redox reaction has been demonstrated *in situ*. These results are important for the design of a practical ion separation system and in maintaining as uniform a current distribution as possible at a high surface area electrode.

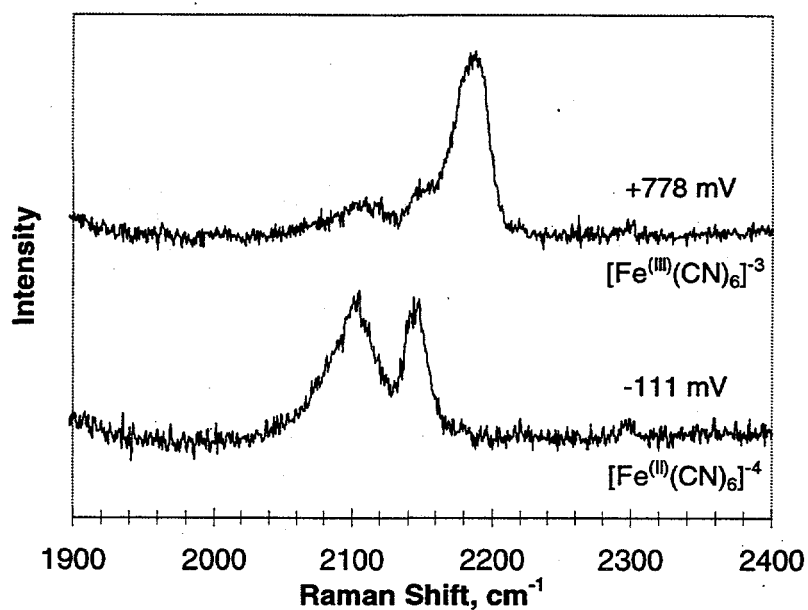


Figure C-1. Raman Spectra of Hexacyanoferrate Films on a Nickel Wire as a Function of Applied Potential

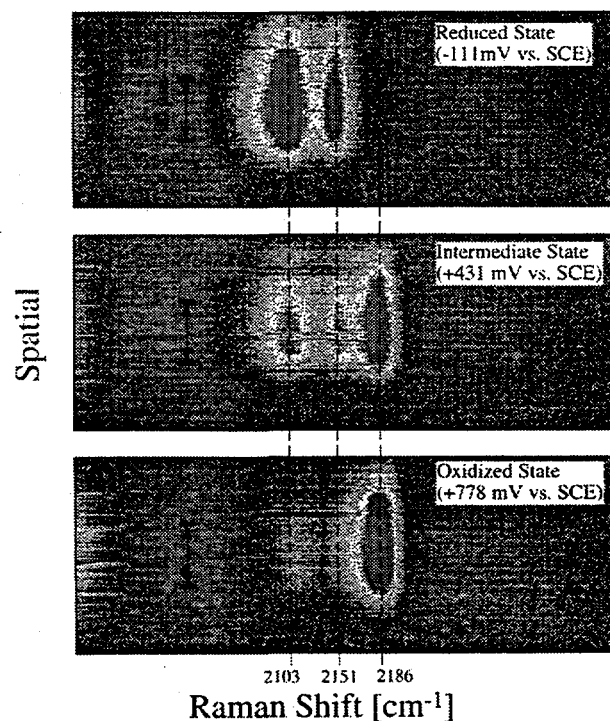


Figure C-2. Imaging Raman Spectra of a Literature Film on a Nickel Wire Showing Spatially Homogeneous Redox Reactions

Appendix D

Electrically Switched Ion Exchange Column Cost Benefit Analysis

**Robert Wilkinson
Parsons Infrastructure and Technology Group, Inc.
1955 Jadwin Avenue
Richland, WA 99352**

Electrically Switched Ion Exchange Column Cost Benefit Analysis

September 24, 1998

Prepared for:

Pacific Northwest National Laboratory
P.O. Box 999
Richland, Washington 99352

Prepared by:

Parsons Infrastructure & Technology Group, Inc.
1955 Jadwin Ave.
Richland, Washington 99352

Table of Contents

1.0	INTRODUCTION	1
1.1	Background.....	1
1.2	Technology Description.....	2
1.3	Technology Status	2
2.0	ELECTRICALLY SWITCHED ION EXCHANGE SYSTEM.....	3
2.1	Configuration.....	3
2.2	Operation	5
3.0	COST	6
3.1	Cost Analysis	6
3.2	Data	6
3.3	Empore™ Technology.....	7
3.4	Electrically Switched Ion Exchange Technology.....	10
4.0	COST COMPARISON AND CONCLUSIONS	14
5.0	REFERENCES.....	17

1.0 INTRODUCTION

1.1 Background

Electrically Switched Ion Exchange (ESIX) is a separation technology that has been developed at the Pacific Northwest National Laboratory (PNNL) as an alternative to conventional ion exchange for removing radionuclides and other metallic ions from aqueous waste streams. This technology has been in development since 1994, and recently has been demonstrated for simulated spent fuel basin waste waters at the U.S. Department of Energy (DOE) Hanford Site, along with development activities for the forest industry. The ESIX technology combines ion exchange and electrochemistry to produce an electroactive film that is regenerable and long lasting. This process minimizes secondary wastes and produces a low-sodium, high cesium concentration waste stream.

In September 1996, Argonne National Laboratories (ANL) provided a Large-Scale Demonstration Project (LSDP) using a 3M technology called Empore™. The LSDP objective was to select and demonstrate potentially beneficial technologies. This demonstration was completed at the ANL-East, Chicago Pile-5 research Reactor (CP-5). The specific work entailed treating radioactive contaminated water, which when treated, met regulatory criteria for the release of wastewater. The guidelines and treatment levels were derived from DOE Order 5400.5 (DOE 1997). The water was contaminated with radioactive isotopes consisting of cesium-137 (Cs -137) and small amounts of cobalt-60 (Co-60).

After completion of the LSDP project, a report was written and issued to the DOE in October 1997. The report, titled *Empore™ Membrane Separation Technology, Innovative Technology Summary Report* (Black, Hoffman, and Kafka, 1997), discussed the benefits of using technologies consisting of Empore™ Membranes, evaporation systems, and mobile ion exchange columns. It also provided extensive detail showing that the Empore™ technology was more cost effective, while allowing for improved waste minimization.

This report compares the ESIX technology with the Empore™ technology, using the same criteria as defined in the *Innovative Technology Summary Report*. To provide this comparison, ESIX system designs are discussed and cost data to perform treatment of 24,000 gal of radioactivity-contaminated liquid are evaluated, as was done for the Empore™ system. The Empore™ system design and costs are the same as detailed in the *Innovative Technology Summary Report*. The ESIX technological capabilities are not discussed in great detail, except where the ESIX technology applies directly to this application. Refer to the *Electrically Switched Cesium Ion Exchange, FY 1998 Annual Report*, PNNL-12002, for details of overall technological data. This report will not discuss in detail the other technologies (mobile ion exchange and evaporation) described within the *Innovative Technology Summary Report* because it has already been shown that Empore™ technology is more applicable than the evaporation and the mobile ion exchange systems.

Although the *Innovative Technology Summary Report* for the Empore™ System discusses the removal of Co-60, it will not be discussed in detail within this report because the ESIX system will require another treatment process (the same as the

Empore™ system required specific cartridges for removal of Co-60). The Cost anticipated for additional equipment used in removing the Co-60 was \$4,000 as detailed in the *Innovative Technology Summary Report*. This equipment would be incorporated into the ESIX system and is listed within the cost detail for the ESIX system to provide a fair comparison against the Empore™ system.

1.2 Technology Description

The ESIX technology was developed by PNNL to provide an alternative to conventional ion exchange for removing radionuclides and other metallic ions from aqueous wastes and wastewaters. The ESIX system provides a pollution prevention technology that significantly reduces secondary waste generation by reusing elution solutions. ESIX, which combines ion exchange and electrochemistry, uses electroactive films that are highly selective and regenerable. During the process, ion uptake and elution can be controlled directly by modulating the electrical potential of an ion exchange film that has been deposited onto a high surface electrode. This high surface electrode is made of nickel foam that has been deposited with ferricyanide $[\text{Fe}(\text{CN})_6^{-3}]$. This deposition gives reproducible films with reversible behavior (i.e., metal ions are loaded and unloaded reversibly by switching the electrode potential).

The ESIX system allows for the removal of radionuclides from aqueous solutions, while minimizing the amount of waste generated. The removal of cesium with ESIX has been demonstrated at bench scale, using simulated waste.

1.3 Technology Status

The ESIX technology is not yet available commercially, although it has been tested and demonstrated previously for removal of cesium from spent fuel basin waste waters, such as found at the Hanford Site K-Basins.

The ESIX system will be manufactured to allow for standard pipe connections and standard electrical hookup requirements. Systems can be produced easily with quick disconnects and electrical receptacle plugs and would be designed as such for the CP-5 scenario. Specific footprint sizes are expected for two standard units and are dependent on radionuclide levels and flow rates.

For the CP-5 scenario the following requirements were used (as provided by the *Innovative Technology Summary Report* for the Empore™ Selective Separations System):

System Requirements

Flow Rate:	0.5 gpm
Total Volume Throughput:	24,000 gal
Radiological Input:	Cs-137 – approximately 0.60 pCi/ml

2.0 ELECTRICALLY SWITCHED ION EXCHANGE SYSTEM

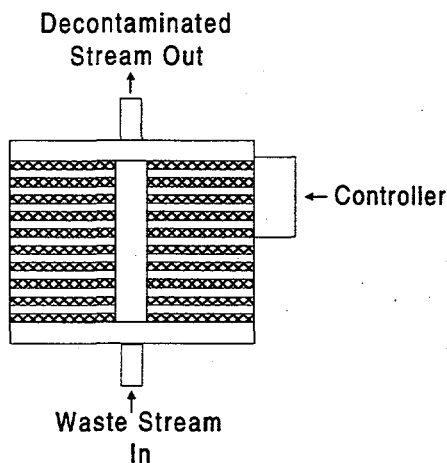
2.1 Configuration

In the ESIX process, an electroactive ion exchange film is deposited onto a high surface area electrode, ion uptake, and elution are controlled directly by modulating the potential of the film. In this specific instance, the electroactive film is hexacyanoferrates, which has high selectivity for cesium in concentrated Na solutions. Loading and unloading of the cesium onto the films or foams is controlled via electric potential. This process allows for a regenerable ion exchange process that minimizes secondary waste generation and produces a low-sodium, cesium-rich waste stream.

The ESIX technology allows cesium to be eluted into the same elution solution over several load cycles, because the unload step or removal of cesium from the cartridges is conducted electrochemically without adding chemicals. This provides a waste stream that is small in volume with very low-sodium and high-cesium concentrations. The only items limiting the concentrations of cesium in the small waste stream are solubility, radiation, and heat generation. Ratios of the volume of generated secondary waste to the volume of processed waste are estimated to be as low as 0.0006 for the ESIX process.

The ESIX system uses cells consisting of high surface area electrodes, derivatized with the electroactive ion exchange material, and wire mesh counter electrodes, separated and sealed with gasket material. This cartridge is fabricated and stacked to allow for the desired flow rates. Two standard unit sizes are anticipated for manufacturing each handling a range of different flow rates. After the units are manufactured, they will be mounted in stacks, placed into cartridge housings, and attached together using standard pipe connections. When the system is anticipated to be used as a portable unit, it would be mounted with quick disconnects to provide for ease of installation and removal. A potentiostat controller on the side of the system would provide the necessary electrical voltage for the electrochemical process. The potentiostat is set up either for hardwiring or a receptacle plug when a portable unit is desired and could be mounted remotely when radiation levels are a factor.

Figure 1. ESIX System

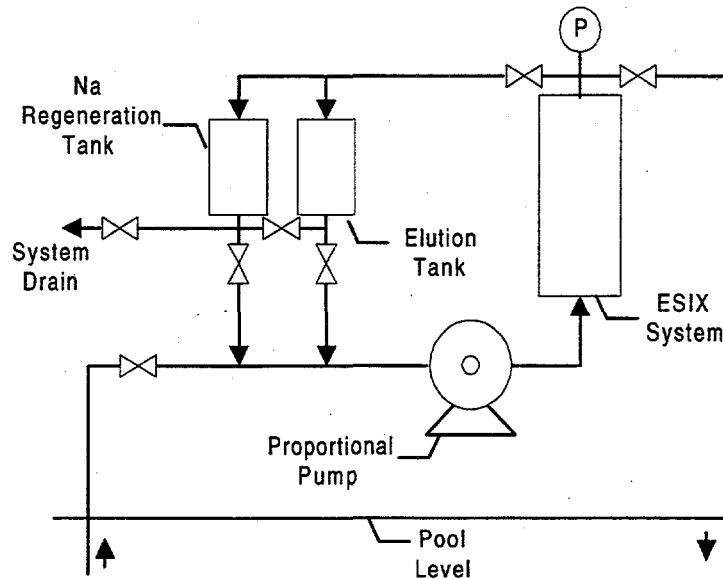


The system layout used for the CP-5 case was based on the 0.5-gpm flow rate used by the Empore™ system and defined within the *Innovative Technology Summary Report*. The unit cartridge size for the system was chosen to be the smaller of the two types available. Twenty units were needed to provide the required bed volume to attain the 0.5-gpm flow rate, as shown in Figure 1. The units would be mounted, stacked in placed within the cartridge housing, and because this application would be used only for a short duration (37 days), quick disconnects would be installed to allow for the ease of removal from the CP-5 reactor basin. On the outside face of the housing, a potentiostat would be mounted to provide the

proper electrical control and wired with a standard 110-V receptacle plug.

The complete system would include a pump, two 10 gal tanks, and an ESIX system including its controller, associated piping, and valves. Facility modifications would include adding piping connections, installing a pump to provide the required flow, adding two small 10-gal tanks that are used for elution solution and sodium (Na) regeneration solution storage, and providing power for the system. Specifically, the intention would be to mount the system with quick disconnects and an electrical receptacle that would allow the CP-5 facility the ability to readily install and remove the system from operation. Since no mention was made in regards to radiological shielding within the *Innovative Technology Summary Report* it is assumed that no shielding is required. However if shielding would be needed it is assumed that temporary shielding would be used due to the small duration of treatment. The final assembly of the ESIX system would weigh approximately 75 lbs and would have a 2-ft- x 2-ft- x 2-ft-high footprint. The only modifications the facility would require would entail the installation of a pump and piping with quick disconnects, and the mounting of the 10-gal storage tanks, as shown in Figure 2.

Figure 2. ESIX System Flow Schematic



Pool water would be drawn from the pool via a small proportional pump, passed through the ESIX system, and passed back to the pool to provide a recirculating action. To facilitate use, the liquid being transferred from the pump to the ESIX system and from the ESIX system to the pool could be routed with flexible hose. The ESIX system would be mounted on grating directly over the pool similar to the Empore™ system. This would allow any leaks generated from pipe connections to fall onto the grating and then back into the pool.

Based on the Cs-137 concentrations (0.60 pCi/ml), flow rates (0.5 gpm), and volume of liquid (24,000 gal) to be processed (as defined in the October 1997, *Innovative*

Technology Summary Report), the ESIX system would require less than two elution cycles. Currently, the ESIX elution solution can be reused up to 10 times (based on cesium concentrations) before it must be replaced. This is contingent upon Cs-137 concentrations and facility-specific dose-rate criteria. However, based on the information provided, it is anticipated that the one batch of elution solution would be able to be used through the entire process of 24,000 gal. This overall elution solution would provide less than 5 gal of liquid waste at the completion of the process. Similarly, at the completion of elution, a Na regeneration would be completed, which would provide less than 5 gal of liquid waste at the completion of the process.

2.2 Operation

System operation would encompass its initial startup to verify proper performance; at this point, any necessary operating corrections would be made. Upon final testing, the ESIX system would be turned on and operated with minimal support. For ESIX, it is anticipated that only a daily surveillance of the system and related equipment would be required.

Samples would be drawn from the system to provide a baseline and confirm proper system operation. This would be completed at an interval as defined by the facility. Table 1 provides the cost data associated with the samples. It should be noted that the amount of samples delineated in the *Innovative Technology Summary Report* actually would be far less for an application if the baseline were only final disposition.

During the treatment process, elution activities would have to occur as concentration in the treated stream increased. When elution becomes necessary, the 10-gal tank would be valved in and the outlet of the ESIX cartridge assembly would be valved out to allow the path of liquid to flow back into the 10-gal tank. The elution solution would be routed through the system and a voltage would be applied to the system to allow for the removal of the Cs-137. The Na would then be valved into the ESIX system, and a voltage would be applied to allow for Na uptake onto the ESIX system. After Na regeneration, the system would be valved back to the original operational configuration and the treatment of the pool would continue.

After treating the entire 24,000 gal, the ESIX system would perform its last elution process to remove/flush the ESIX cartridges of the remaining Cs-137 nuclides. After the treatment is completed, the proportional pump would be shut off and the system would be drained of all liquid. After air drying, the ESIX system would be unplugged and disconnected using the quick disconnects. The openings would be plugged, taped, or bagged, depending on facility requirements, and labeled as internally contaminated. The equipment could then be sent to storage for future use elsewhere or sent directly to burial as low-level waste, depending on the facility requirements. For this application, it was assumed that the equipment would be sent to storage to provide for an accurate comparison to the Empore™ system. The 10-gal elution and Na regeneration tanks would be drained of the elution solution. The solution would then be absorbed and packaged as waste for disposal. The amount of solution would be less than 10 gal of liquid.

During ESIX operation personnel exposure to hazards would be minimal. Specific hazards include noise, electrical, radiological, and chemical, and are similar to those that were experienced during operation of the Empore™ system. The only difference

would be during the draining and packaging of the elution and Na regeneration solution. This would potentially expose personnel to Na, but this is expected to be a minimal risk activity because the personnel performing this activity regularly handle these types of chemicals. The personnel would wear standard protective gear, which is defined as anti-contamination clothing and splash protection.

The radiological waste from ESIX would consist of 4 cu. ft. of absorbed elution and Na regeneration solution. The ESIX system itself would not be able to be decontaminated and released because internal surfaces could not be decontaminated (like the Empore™ system). Based on the footprint sizes of the ESIX system, it was calculated that 12 cu. ft. of low-level waste would be generated. The Empore™ system would generate 147 cu. ft., based on the footprint as defined in the *Innovative Technology Summary Report*. This is not considered in the cost section of this report because the basis used was that the equipment would be sent back to storage for potential future use.

3.0 COST

3.1 Cost Analysis

This cost analysis compares the ESIX technology and the Empore™ technology for a 0.5-gpm filtration system at the CP-5 East Wing pool. The Empore™ system was based on a demonstration performed at ANL CP-5 under controlled conditions. Based on this demonstration, observation of work procedures, and typical duration of work activities, a cost for the Empore™ system was derived and published in the *Innovative Technology Summary Report*. Cost data were attained for the ESIX system, using the requirements, details, and labor rates defined in the *Innovative Technology Summary Report*. Other costs, such as sampling costs were assumed to be the same for both the Empore™ and ESIX systems. For comparison sake, the amount of detail and costs used in this report are similar to those used in the innovative *Innovative Technology Summary Report*. Costs that were omitted were site-specific costs.

3.2 Data

This section presents costs to fabricate, mobilize, operate, demobilize, and dispose of waste. It also contains definitions of cost elements, description of work activities and assumptions, and computations of unit costs that were used in the cost analysis. All information and costs derived for the Empore™ system were taken directly from the *Innovative Technology Summary Report*. Part of the ESIX cost detail and assumptions were based on information used for the Empore™ system. The information was used to allow for an accurate comparison of the two systems.

Each of the technologies cost details were split into fabrication, mobilization and facility modifications, operation, demobilization, and waste disposal costs. Cost information is listed and summarized by those major activities. The Personnel Protective Equipment (PPE) cost per unit of \$46.33 was taken directly from the *Innovative Technology Summary Report*, shown in Table B-1. Both systems would be able to use the same PPE unit cost because of the similarity of the work being performed when requiring the use of PPE.

3.3 Empore™ Technology

The following costs elements and work activity descriptions are summarized from the *Innovative Technology Summary Report*. The costs for the Empore™ system are shown in Table 1.

FABRICATION

Site modification: Modifications to the facility to assemble piping, valves, etc., to construct the Empore™ system. Included is the labor and material to produce a 0.5-gpm system

MOBILIZATION

Lab Analysis of Water: Sampling and analysis performed to determine the type of cartridges required for treatment.

Transport Equipment: Transportation of the Empore™ membrane separation equipment from storage at Argonne National Laboratory to the tank area.

Set up Equipment: Equipment and cartridges are unpacked, surveyed for damage, and prepared for use.

Training of Operators: The operators are familiarized with the Empore™ equipment.

OPERATION

Pre-Operational Check: The system is run to check for leaks and proper performance.

System Operation: The processing of the contaminated water through the cartridge system, taking required samples, changing cartridges as required, and then discharging the treated water into a retention tank for future discharge into the treated sanitary drain system. The technician is present at all times during the weekday (not present at night or weekends). The waste management mechanic is present for sampling events and for changes of the cartridges.

PPE: Personal protective equipment for the innovative technology was worn when samples were collected and when cartridges were replaced. Only two pair of PPEs were used during the demonstration, because the same sets were re-worn for each sample event.

DEMOBILIZATION

Decontaminate Equipment and Prepare for Transport: Empore™ membrane separation technology equipment is surveyed for contamination and packed for transport.

Transport Equipment: Transport back to storage, which involves the same equipment and effort as mobilization.

WASTE DISPOSAL

Waste generated from the decontamination operation and from the disposal of the cartridges and cartridges are included in this activity.

ASSUMPTIONS

The assumptions for projecting the demonstration costs for the Empore™ filtration system to reflect a commercial cost are summarized as follows:

- The demonstration used on radiological and elemental analysis at \$482.70 each and one total carbon and organic analysis at \$429.70 each.
- Transportation costs assumed to include two riggers, one truck with driver, and a fork lift with operator. Rates for equipment from *Innovative Technology Summary Report*.
- Equipment set up crew consists of two waste management mechanics for 6 hours each and an electrical technician for 2 hours.
- The demonstration provided approximately 15 minutes for the required training.
- The demonstration required approximately 2 hours for the pre-operational check.
- System operation labor for the technician will be performed 8 hours per day, 5 days per week. Processing will be done on a continuous basis (24 hours per day) with the exception of the 1.5 hours downtime each day for the sampling and the estimated 16 changes of cartridge sets at 30 minutes each (total of 8 hours). At a rate of 0.5 gpm and with the 1.5-hour-per-day downtime, the duration of processing is 37 days. Cartridges were changed at approximate intervals of 1,500 gal. The demonstration was performed with three different cartridges, but future deployments would only use one type of cartridge, COHEX. Computations by 3M indicate that a single cartridge could have processed the 24,000 gal. The price of \$2,000 is based on a purchase of 10 cartridges.
- Assume that all waste is low-level waste. Each cartridge is approximately 3 in. X 3 in. X 3 in. = 0.0625 cu. ft. For 24,000 gal there would be 33 cartridges used. Volume = 33 X 0.0625 cu. ft. = 2.1 cu. ft. Assume one additional cu. ft. for waste generated by the decontamination for a total of 3.1 cu. ft.

Table 1. Costs for the Empore™ System

Work Breakdown Structure Fabrication (0.5 ppm System)	Labor			Unit Cost Equipment		Total Quantity (TC)	Total UC	Other	Total Cost (TC) note	Comments
	Rate	Hrs	Rate	Rate	Measure					
	0	0	0	0	1					
Material & Labor for system Fab.						1	\$15,000	\$15,000	\$15,000	Site Assembly (Obtained from pg. 12 Innovative Technology Summary Oct. 97)
Mobilization										
Lab Analysis of Water	0	\$0.00	0	\$0.00	\$912	1	\$912		\$912	Determine Cartridge Required
Transport Equipment	2	\$146.90	2	\$32.51	\$0	1	\$359	\$0	\$359	Truck, Forklift, Teamster, Operator & 2 Decon Workers for 2 hours
Set-Up Equipment	6	\$4.92			\$30	1	\$30		\$30	Includes standby of Empore™ \$4.92/hour
Mechanic	12	\$49.67			\$596	1	\$596		\$596	
Electrician	2	\$49.67			\$99	1	\$99		\$99	
Training of Operators (2)	0.5	\$49.67			\$25	1	\$25		\$25	One Time Cost
Operation										
Pre-Operational Check	0	\$0.00	2	\$4.92	\$0	1	\$10		\$10	
Mechanics	2	\$49.67	0	\$0.00	\$0	1	\$99	\$0	\$99	Waste Mngt. Mech. @ \$49.67
Electrician	2	\$49.67	0	\$0.00	\$0	1	\$99	\$0	\$99	
Operator of Empore™	0	\$0.00	0	\$0.00	\$0	0	\$0		\$0	
Technician	296	\$33.60	296	\$4.92	\$0	1	\$11,402	\$0	\$11,402	37 days @ 8 hours/day
Filter Cartridge (2)	0	\$0.00	0	\$0.00	\$279	16	\$279	\$2,000	\$4,464	Two approx. every 1500 gal.
Ion Exchange Cart.	0	\$0.00	0	\$0.00	\$2,000	1	\$2,000	\$2,000	\$2,000	Based on package of ten cartridges
Sampling & Testing	0	\$0.00	0	\$0.00	\$250	74	\$250	\$0	\$18,500	2 samples/day for 37 days
Mechanics	0.5	\$49.67	0	\$0.00	\$0	74	\$25	\$0	\$1,838	
HP Technicians	0.5	\$56.00	0	\$0.00	\$0	74	\$28	\$0	\$2,072	
Change Filters	0	\$0.00	0	\$0.00	\$0	0	\$0	\$0	\$0	16 filter sets
Mechanics	0.5	\$49.67	0	\$0.00	\$0	16	\$25	\$0	\$397	
HP Technicians	0.5	\$56.00	0	\$0.00	\$0	16	\$28	\$0	\$448	
	0	\$0.00	0	\$0.00	\$0	0	\$0	\$0	\$0	
Protective Clothing (PCs)	0	\$0.00	0	\$0.00	\$46	2	\$46		\$93	\$46.33 is based on Table B-1 from Innovative Technology Summary Report Oct. 97
Demobilization										
Decon & Prep for Transport	0	\$0.00	8	\$4.92	\$0	1	\$39	\$0	\$39	Includes standby for Empore™
Mechanics	8	\$49.67	0	\$0.00	\$0	1	\$397	\$0	\$397	
HP Technicians	4	\$56.00	0	\$0.00	\$0	1	\$224	\$0	\$224	
Transport Equipment	2	\$146.90	2	\$32.51	\$359	1	\$359		\$359	Same as Mobilization
Waste Disposal										
Cartridge Disposal					\$53	3.1	\$53		\$164	Low Level Waste Disposal
									Total:	\$59,626

Note: TC=UC*TQ

3.4 Electrically Switched Ion Exchange Technology

The following cost elements and work activity descriptions are derived from ESIX system requirements and from the CP-5 processing requirements and Empore™ cost analysis as described in the *Innovative Technology Summary Report*. The costs for the ESIX system are shown in Table 2.

FABRICATION

Tool Step: One time set up fee charged by the gasket vendor for production of the ESIX system. The costs, which would be sent directly to the manufacturer of the ESIX system and then be passed on to the customer in the final purchase price, are shown separately for clarification.

Facility Modification: Modifications to the facility to assemble piping, valves, etc., to provide system hookups for the ESIX system.

System Component: Fabrication and manufacturing costs associated with each cartridge unit for the ESIX system. In the case of the CP-5 application (0.5-gpm system) 20 units would be made. Also included is the cost for materials and labor associated with power supply, housing, and miscellaneous parts.

ESIX Cartridge Activation: The process to activate the cartridge for the ESIX system.

MOBILIZATION

Lab Analysis of Water: Sampling and analysis would be performed to determine the total number of cartridges required for treatment.

Transport Equipment: Transportation of ESIX system from receipt at Argonne National Laboratory to the pool area.

Set-Up Equipment: System unpackaging, surveying for damage, and preparation for use. The ESIX equipment would be delivered ready to hook up and use.

Training of Operators: Operators would be trained to familiarize them with the ESIX system.

OPERATION

Pre-Operational Check: The system would be run to check for leaks and proper performance.

System Operation: The processing of the contaminated water through the system, taking required samples, performing two elution cycles. As with the Empore™ system, the technician would be present at all times during the weekday (not present at night or weekends). The waste management mechanic would also be present for sampling events.

PPE: PPE for the ESIX system would be worn when samples were collected and during the elution process. Only two pair of PPE are anticipated to be used. The same costs are used as the Empore™ system because the same sets of PPE could be re-worn for each sample event and elution process.

DEMOBILIZATION

Decontaminate Equipment and Prepare for Transport: The ESIX system would be surveyed for contamination and packed for transport.

Transport Equipment: Transportation back to storage. The same equipment and effort as mobilization would be required and are based on the transportation of the equipment for the Empore™ System.

WASTE DISPOSAL

Waste generated from the decontamination operation and packaging of the elution solution.

ASSUMPTIONS

The assumptions for projecting the costs for the ESIX system, using the same requirements for the Empore™ System, are summarized as follows:

- Fabrication of the ESIX system was based on cost estimates provided by manufacturers. When estimates could not be attained for specific items, the most recent purchase cost for that part was used (i.e., Power Supply). The costs for the manufacturing of the ESIX cartridge units are anticipated to be less if the ESIX system is manufactured on a larger scale (more than one at a time).
- The demonstration would use one radiological and elemental analysis @ \$482.70, each, and one total carbon and organic analysis @ \$429.70, each.
- Transportation costs were assumed to include two riggers, one truck with driver, and a fork lift with operator. Rates for equipment are derived from the *Innovative Technology Summary Report*.
- The equipment set-up crew consists of two waste management mechanics for 6 hours each, and an electrical technician for two hours.
- It would take approximately 15 minutes to train and familiarize personnel on proper operations.
- The ESIX system used 2 hours for the pre-operational check, which is the same as the Empore™ System, however less than 2 hours may be required. Until the time needed for the check is verified, two hours will be used in the analysis.
- System operation labor for the technician will be performed 8 hours per day, 5 days per week. Processing will be done on a continuous basis (24 hours per day) with the exception of the 3 hours downtime for 2 elution and Na regeneration processes, and

1.5 hours downtime each day for the sampling. At a rate of 0.5 gpm and with the 1.5 hour per day downtime, the duration for treatment of 24,000 gal is 37 days. The 2 elution and Na regeneration processes are based on Cs-137 concentration levels and flow rates. The amount of Cs-137 that can be collected before elution is required is calculated using historical baseline information used to process cesium from other aqueous liquids.

- After the final elution process, the 5 gal of elution solution would be drained into a container and absorbed with an absorbent material. It is assumed that after this elution solution is absorbed, the absorbent material would be considered to be low-level waste. The Na regeneration solution would also be drained into a container and absorbed with an absorbent material allow it to be classified as low level waste. The absorbed solution from the elution solution and Na regeneration would accumulate to 4 cu. ft., and an additional 1 cu. ft. of waste would be generated during decontamination activities for a total of 5 cu. ft.

Table 2. Costs for the ESIX System

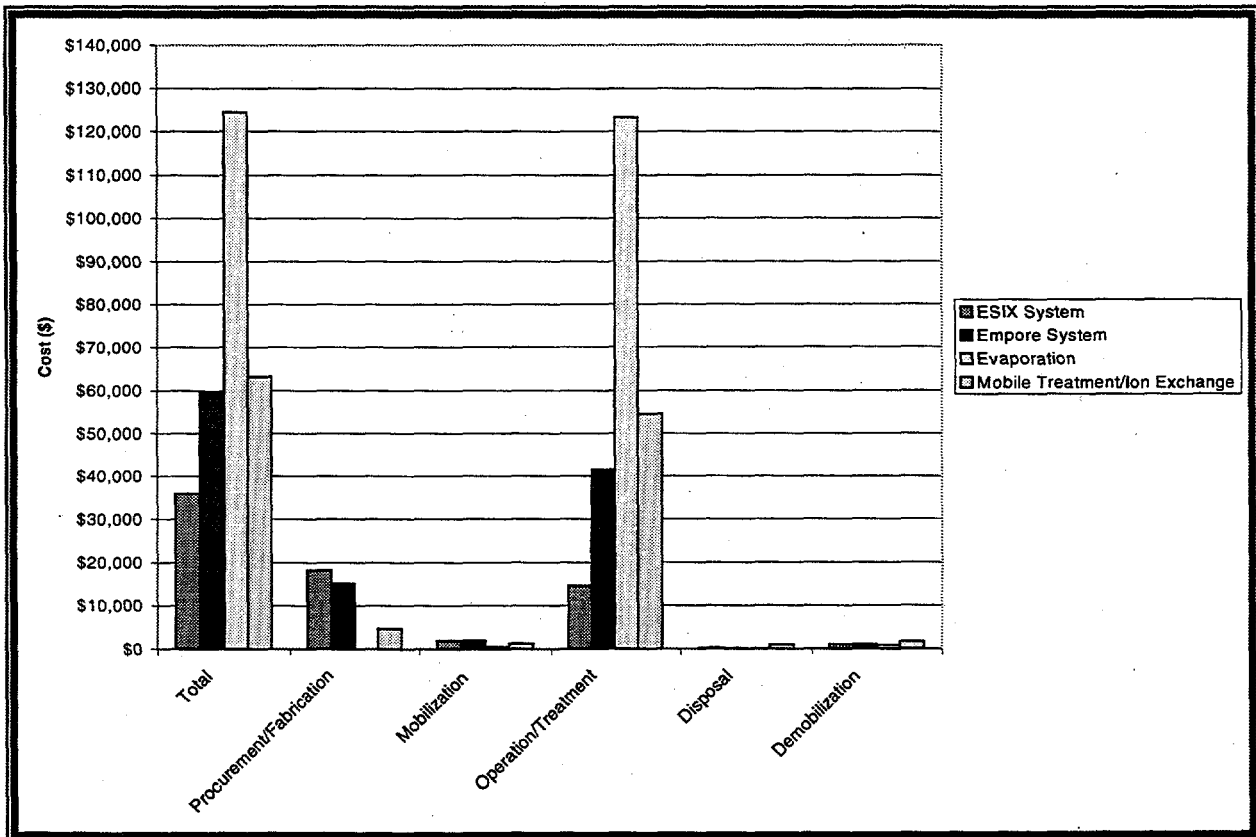
Work Breakdown Structure (WBS) (6-3 gpm System)	Labor		Unit Cost Equipment		Total UC	Other	Total TC	Unit of Measure	Total Cost (TC) note	Comments
	Hrs	Rate	Hrs	Rate						
Tooling Setup					\$50	\$50		1 Each	\$50	This is a charged cost against ESIX by the gasket manufacture for setup time to cut the material. It is a one time fee.
Facility Modification	24	\$49.67	0	\$0.00	\$4,500	\$4,500		1 Each	\$5,692	Based on 3 craft personnel for 3 days and required material (i.e. pipe connections, power supply, pump)
System Component (Filter Stack)					\$83	\$83		20 Each	\$1,654	The TQ for the system components is dependent on flow rates and CSCI concentrations (Specifically 90 BV/hr)
Cobalt-60 cartridge					\$4,000	\$4,000		1 Each	\$4,000	Empore cartridge setup for removal of Cobalt-60. Costs derived from Innovative Technology Summary Report
Power Supply/Control					\$6,000	\$6,000		1 Each	\$6,000	Based on a Boss 60 V, 50 amp, 2.5 Kw potentiostat
Housing and Miscellaneous Parts	0.5	\$49.67			\$375	\$375		1 Each	\$375	Misc. parts including housing and final assembly of overall system
Filter Activation	8	\$49.67			\$397	\$397		1 Each	\$397	One time activation performed by ESIX manufacturer
Subtotal: Facility Work						\$15,759				
Lab Analysis of Water	0	\$0.00	0	\$0.00	\$912	\$912		1 Each	\$912	Determine Cartridge Required
Transport Equipment	2	\$146.90	2	\$32.51	\$0	\$359		1 Trip	\$359	Truck, Forklift, Teamster, Operator & 2 Decon Workers for 2 hours. It is assumed the set up for the equipment will match that of
Set-Up Equipment	12	\$49.67	6	\$4.92		\$30		1 Each	\$30	Empore
Mechanic	2	\$49.67				\$596		1 Each	\$596	
Electrician	2	\$49.67				\$99		1 Each	\$99	
Training of Operators (2)	0.5	\$49.67				\$25		1 Each	\$25	One Time Cost
Sub Total						\$3,021				
Operation										
Pre-Operational Check	0	\$0.00	2	\$0.00	\$0	\$0		1 Each	\$0	No Standby Cost because there is only a one time purchase cost
Mechanics	2	\$49.67	0	\$0.00	\$0	\$99		1 Each	\$99	Waste Mngl. Mech. @ \$49.67
Electrician	2	\$49.67	0	\$0.00	\$0	\$99		1 Each	\$99	
Operation of ESIX	0	\$0.00	0	\$0.00	\$0	\$0		0	\$0	
Technician	296	\$33.60	296	\$0.00	\$0	\$9,946		1 Each	\$9,946	37 days @ 8 hours/day, No Standby Cost because there is only a one time purchase cost
Sampling & Testing	0	\$0.00	0	\$0.00	\$250	\$250		12 Sample	\$3,000	1 sample at the start and end plus two samples per week for 5 weeks
Mechanics	0.5	\$49.67	0	\$0.00	\$0	\$298		12 Sample	\$3,000	
HP Technicians	0.5	\$56.00	0	\$0.00	\$0	\$28		12 Sample	\$336	
Elution & Regeneration	0	\$0.00	0	\$0.00	\$0	\$0		0	\$0	based on 2 elution and regeneration processes
Mechanics	3	\$49.67	0	\$0.00	\$0	\$149		2 Each	\$298	
HP Technicians	3	\$56.00	0	\$0.00	\$0	\$168		2 Each	\$336	
						\$0			\$0	
Protective Clothing (PC's)	0	\$0.00	0	\$0.00	\$46	\$46		2 Each	\$93	\$46.33 is based on Table B-1 from Innovative Technology Summary Report Oct. 97. It is assumed that with less entries there will not be any need for additional PPE.
Sub Total						\$14,505				
Decon & Prep for Transport										
Mechanics	8	\$0.00	8	\$0.00	\$0	\$39		1 Each	\$39	No Standby Cost because there is only a one time purchase cost
HP Technicians	4	\$56.00	0	\$0.00	\$0	\$224		1 Each	\$224	
Transport Equipment	2	\$146.90	2	\$32.51	\$0	\$359		1 Each	\$359	Same as Mobilization
Sub Total						\$1,018				
Waste Disposal										
Elution process solution					\$53	\$53		5 Fl ³	\$265	Low Level Waste Disposal of elution ans Na regeneration solution and decon rags
Sub Total						\$265				
Total:										\$35,978

Note: TC=UC*TC

4.0 COST COMPARISON AND CONCLUSIONS

Figure 3. Cost Comparison

Figure 3 shows the cost comparison between the ESIX, Empore™, evaporator, and mobile ion exchange systems. The costs for the operation of the evaporator and mobile treatment systems were taken directly from the *Innovative Technology Summary Report*. As shown, the ESIX system is cost competitive with the Empore™ system for processing the wastewater. ESIX is projected to save approximately 40% over the Empore™ system, 43% over the mobile ion exchange system, and 71% over the evaporation



system.

This estimate assumed, just as the *Innovative Technology Summary Report*, that the treated effluent would be discharged to a nearby drain. The estimate does not include the costs for obtaining the discharge permit.

Table 3 lists performance areas and compares the two systems for application at the CP-5 facility.

Table 3. Comparison of ESIX and Empore™

Performance Areas	ESIX	Empore™
Cost for CP-5 Pool Treatment	\$35,978	\$59,626
Waste Generation	Total of 5 cu. ft. of low-level waste, 4 cu. ft. of absorbed elution solution and 1 cu. ft. of decontamination material.	Total of 3.1 cu. ft. of low-level waste, 2.1 cu. ft. of absorbed elution solution and 1 cu. ft. of decontamination material
Applicability to CP-5 Pool Treatment	Removes Cs-137 to required treatment levels but has to be coupled with another filtration unit to perform removal of Co-60.	Removes both Cs-137 and Co-60 to required treatment levels.
Mobility	Fully mobile unit. Can be mounted with quick disconnects and electrical receptacle plugs. Facility needs power to supply, pipe connections, and pump to provide required flow.	Fully mobile unit. The system is comprised of multiple cartridge housings that would need to be mounted on a skid system by the facility prior to receiving the cartridges from the vendor.
Commercial Availability	Not yet commercially available. Has been tested on simulated spent fuel basin wastewaters.	Not yet commercially available. Has been field tested.
Production Rates	As flow rates increase, the size of the system increases by stacking units. Currently two types of units are anticipated to be manufactured.	As flow rates increase, cartridges will be added in parallel to give the required flow demand.
Ease of Use	Once in operation, the system is continuous, except for elution. This is completed by manipulation of valves. No increase in exposure to workers occurs throughout the operation of the system.	Once in operation, the system is continuous, except for required cartridge change outs. This is completed by the technician removing the old cartridge and replacing it with a new one.

The procurement costs for a fully functional 0.5 gpm ESIX system is approximately \$12,477 (\$8,477 for ESIX system and \$4,000 for Co-60 system), while Empore™ costs are approximately \$15,772 (\$9,308 cartridge housing installation and \$6,464 cartridge costs). The cost for the ESIX system includes material procurement and assembly (Costs for utility hookup are not included). This was the case because the unit is a fully enclosed and mobile unit. The procurement costs for the Empore™ system consists of the cartridge housing purchase and installation, along with the required cartridges to complete treatment activities. The costs listed herein do not reflect the \$5,692 cost for 3 days of craft time and miscellaneous parts to provide pipe connections and power. Both systems are fully mobile units.

From the *Innovative Technology Summary Report*, a 50-gpm system on the Empore™ system would add an additional \$10,000 worth of cartridge housing hardware. An additional amount of cartridges would also be required, which was not called out in the *Innovative Technology Summary Report*. It is anticipated that the amount of cartridges needed to attain the increase in flow would be at a minimum four times the number used in the 0.5 gpm system. So the total approximate cost for a 50-gpm Empore™ system

would be \$45,164. An ESIX system at the same 50 gpm would cost \$28,840 (including C0-60 removal system). The cost of each system is highly contingent upon the concentration levels of cesium and would increase or decrease depending on cesium concentrations. The prices listed herein are based on cesium concentration levels as experienced at the CP-5 facility.

As indicated in Table 3, the ESIX system is cost effective and reduces worker exposure, while providing a wider range of flow potential. In this specific application the ESIX System produces slightly more waste than the Empore™ system. However, as concentrations of cesium increase and the volume of liquid processed increases, it is anticipated that the ESIX system would produce less waste because of its ability to reuse the elution solution. The Empore™ system is more flexible in the respect that it can be fabricated to allow for removal of more than just cesium from waste streams. Empore™ systems would likely be more cost effective when waste streams contain multiple types of radionuclides requiring removal. However the ESIX system, when used specifically for cesium removal, provides a more flexible and cost-competitive system, while reducing worker exposure and secondary waste generation.

5.0 REFERENCES

- DOE. 1997. *Radiation Protection of the Public and Environment*. U.S. Department of Energy Order 5400.5, Washington, D.C.
- Black D., K. M. Hoffman, T. M. Kafka. 1997. *Empore™ Membrane Separation Technology, Innovative Technology Summary Report*. U. S. Department of Energy, Office of Science and Technology Decontamination and Decommissioning Focus Area, Washington, D.C.
- Lilga, M. A., R. J. Orth, J. P. -H. Sukamto. 1998. *Electrically Switched Cesium Ion Exchange. FY 1998 Final Report*. PNNL-12002, Pacific Northwest National Laboratory, Richland, Washington
- Lilga, M. A., R. J. Orth, J. P. -H. Sukamto, S. D. Rassat. 1997. *Electrically Switched Cesium Ion Exchange. FY 1997 Annual Report*. PNNL-11766, Pacific Northwest National Laboratory, Richland, Washington.
- Lilga, M. A., R. J. Orth, J. P. -H. Sukamto, S. M. Haight, and D. T. Schwartz. 1997. *Metal Ion Separations Using Electrically Switched Ion Exchange. Separation and Purification Technology 11(1997) 147-158*. Pacific Northwest National Laboratory, Richland, Washington.

Distribution

**No. of
Copies**

**No. of
Copies**

OFFSITE

Mr. A. Wayne Akerson
Parsons Infrastructure and Technology
Group, Inc.
1955 Jadwin Avenue
Richland, WA 99352

Dr. Moses Attrep, Jr.
Los Alamos National Laboratory
P.O. Box 1663, MS J514
Los Alamos, NM 87545

Ms. Debra A. Bostick
Oak Ridge National Laboratory
P.O. Box 2008
Oak Ridge, TN 37831-6201

Professor Daryle Busch
University of Kansas
Department of Chemistry
Lawrence, KS 66045

Professor Greg Choppin
Florida State University
Department of Chemistry
600 West College Avenue
Tallahassee, FL 32306

Dr. J. David Genders
The Electrosynthesis Company, Inc.
72 Ward Road
Lancaster, NY 14086-9779

Dr. Dirk Gombert
Lockheed Martin Idaho Technologies
P.O. Box 1625, Mail Stop 3875
Idaho Falls, ID 83415

Dr. Ram Gopal
The Electrosynthesis Company, Inc.
72 Ward Road
Lancaster, NY 14086-9779

Dr. Jerry L. Harness
U.S. Department of Energy
Oak Ridge Operations Office
P.O. Box 2001, 3-MAIN
Oak Ridge, TN 37831

Mr. John R. Hunter
Parsons Infrastructure and Technology
Group, Inc.
1955 Jadwin Avenue
Richland, WA 99352

Prof. Dennis Kelsh
Gonzaga University
Department of Chemistry
E. 505 Boone Ave.
Spokane, WA 99258-0001

Dr. John H. Kolts
U.S. Department of Energy
Idaho Operations Office
765 Lindsay Blvd., Mailstop 1147
Idaho Falls, ID 83401

Prof. KNona Liddell
Washington State University
Department of Chemical Engineering
Pullman, WA 99164-2710

Mr. John Mathur
U.S. Department of Energy
Office of Science and Technology
EM-53 CL
19901 Germantown Road
Germantown, MD 20874

**No. of
Copies**

Mr. Phil McGinnis
Martin Marietta Energy Systems
4500-N, MS-6273
P.O. Box 2008
Oak Ridge, TN 37831

Mr. Jim McGlynn
Science Applications International Corp.
555 Quince Orchard Road, Suite 500
Gaithersburg, MD 20878

Mr. Bruce Monzyk
Battelle Memorial Institute
505 King Avenue
Columbus, Ohio 43201-2693

Dr. Don Orth
124 Vivion Drive
Aiken, SC 29803

Dr. James Phelan
Sandia National Laboratories
P.O. Box 5800, Mail Stop 0719
Albuquerque, NM 87185-0719

Mr. Steven L. Stein
Battelle Seattle Office
4000 NE 41st Street
Seattle, WA 98105

Dr. Martin Steindler
Argonne National Laboratory
9700 South Cass Avenue
Argonne, IL 60439

Dr. Dee Stevenson
3367 E. Bernada Drive
Salt Lake City, UT 84124

Dr. John Swanson
1318 Cottonwood Dr.
Richland, WA 99352

**No. of
Copies**

Dr. Ian R. Tasker
Waste Policy Institute
Quince Diamond Executive Center
555 Quince Orchard Road
Gaithersburg, MD 20878-1437

Dr. Major Thompson
Savannah River Technology Center
P.O. Box 616
Aiken, SC 29802

Dr. Terry Todd
Lockheed Martin Idaho Technologies
P.O. Box 1625
Idaho Falls, ID 83415-5213

Dr. Paul Usinowicz
Battelle Memorial Institute
505 King Avenue
Columbus, Ohio 43201-2693

Dr. Jack Watson
Oak Ridge National Laboratory
P.O. Box 2008
Oak Ridge, TN 37831-6149

3 Mr. Robert E. Wilkinson
Parsons Infrastructure and Technology
Group, Inc.
1955 Jadwin Avenue
Richland, WA 99352

Dr. J. A. Wright
U.S. Department of Energy
Savannah River Operations Office
P.O. Box A
Aiken, SC 29808

Dr. Ray Wymer
188A Outer Drive
Oak Ridge, TN 37831

ONSITE

**No. of
Copies**

**No. of
Copies**

53 Pacific Northwest National Laboratory

5 DOE Richland Operations Office

T. L. Aldridge K8-50
J. P. Hanson K8-50
C. S. Louie A0-21
R. A. Pressentin K8-50
B. M. Mauss K8-50

B&W Hanford Company

R. L. Hobart L5-65

Duke Engineering & Services, Inc.

D. R. Precechtal X3-85

Lockheed Martin Hanford Company

J. N. Appel A3-03

5 Numatec Hanford Company

D. B. Bechtold T6-07
J. Bourges T6-07
D. L. Herting T6-07
J. R. Jewett T6-07
R. A. Kirkbride H5-27

SGN Eurisys Services Corporation

R. K. Biyani B4-51

E. G. Baker K2-12
W. F. Bonner K9-14
R. A. Brouns K9-04
T. M. Brouns K9-91
J. L. Buelte K2-14
R. T. Hallen K2-12
W. L. Kuhn K8-93
D. E. Kurath P7-28
J. P. LaFemina P7-27
W. E. Lawrence P7-41
M. A. Lilga (25) P8-38
N. J. Lombardo K9-04
W. J. Martin K9-14
S. V. Mattigod K6-81
N. J. Olson K9-46
R. J. Orth K3-75
M. E. Peterson K2-20
S. D. Rassat P7-41
L. J. Sealock K2-20
S. C. Slate K1-50
T. L. Stewart K9-69
J. P. H. Sukamto K8-93
Information Release (7)

